A parametric approach to a probabilistic design of rubble mound slope protection

F.B. Sijbesma

Technische Universiteit Delft

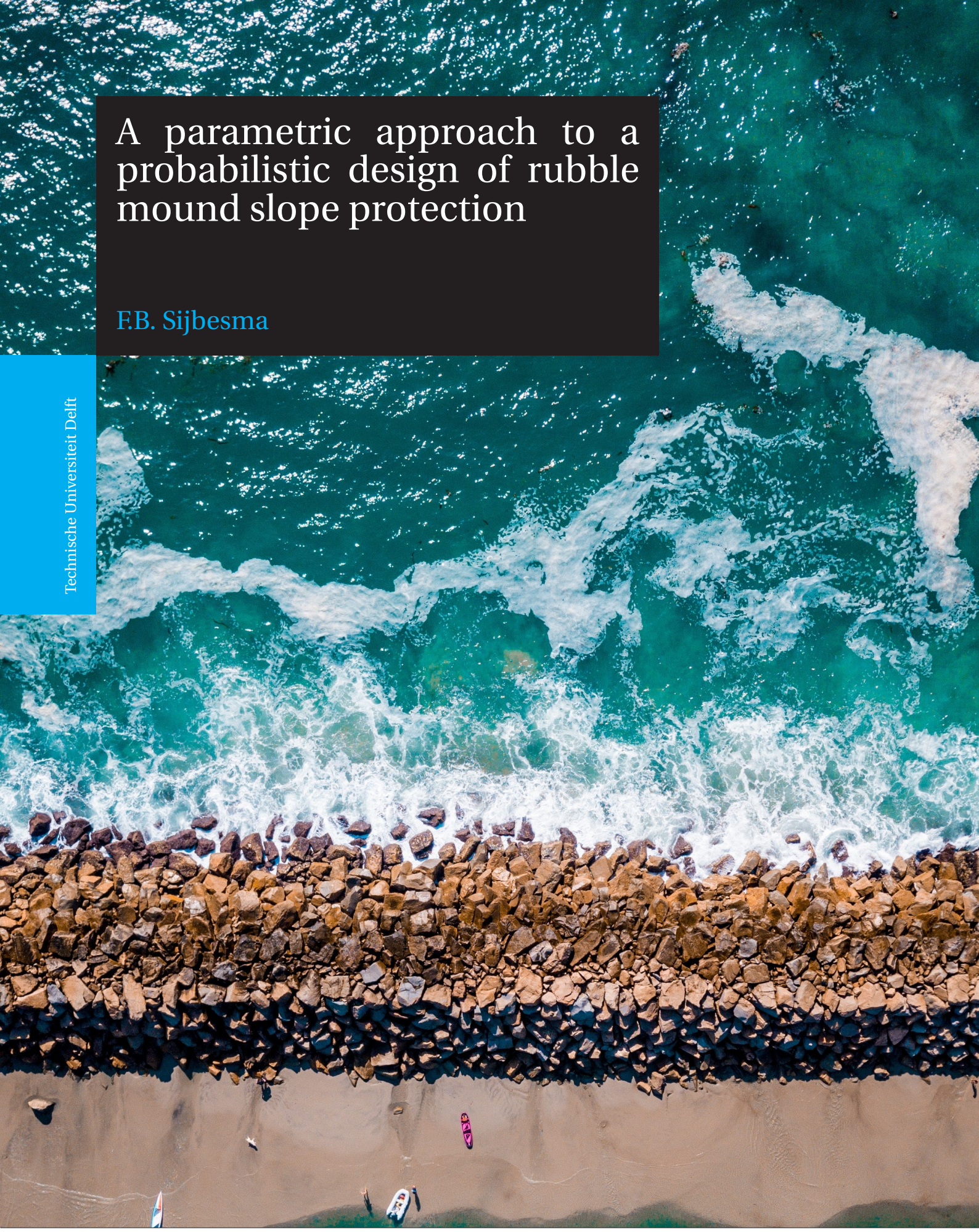

TU Delft Delft University of Technology

Challenge the future

Photo cover image:
Dana Point Harbor, Dana Point, United States.
Source: Zoom Drones, https://unsplash.com/photos/JEP4OCo019Y,
Austin Neill
October 2019

The work in this thesis was conducted and carried out in cooperation with,
Royal HaskoningDHV.

A PARAMETRIC APPROACH TO A PROBABILISTIC DESIGN OF RUBBLE MOUND SLOPE PROTECTION

by

F.B. Sijbesma

For the degree of Master of Science in Civil Engineering at Delft University of Technology

October 24, 2019

DELFT UNIVERSITY OF TECHNOLOGY
DEPARTMENT OF
HYDRAULIC ENGINEERING

THE UNDERSIGNED HEREBY CERTIFY THAT THEY HAVE READ AND RECOMMEND TO THE FACULTY OF CIVIL ENGINEERING AND GEOSCIENCES (CEG) FOR ACCEPTANCE A THESIS ENTITLED

A parametric approach to a probabilistic design of rubble mound slope protection

by

F.B. Sijbesma

in partial fulfillment of the requirements for the degree of

MASTER OF SCIENCE CIVIL ENGINEERING AND GEOSCIENCES (CEG)
HYDRAULIC ENGINEERING

at the Delft University of Technology

Dated: October 24, 2019

Thesis committee:

Chairman:
Prof. dr. ir. S. Aarninkhof
Delft University of Technology
Hydraulic Engineering
Coastal Engineering

Dr. ir. B. Hofland
Delft University of Technology
Hydraulic Engineering
Hydraulic structures and flood risk

Ir. M. Schoemaker
Royal HaskoningDHV
Water Netherlands Rivers and Coasts
Dike analysis, flood risk analysis

Dr. ir. O. Morales Napoles
Delft University of Technology
Hydraulic Engineering
Hydraulic structures and flood risk

PREFACE

This thesis is conducted in partial fulfilment of the requirements for the degree MSc Civil Engineering at the Delft University of Technology. For me this is the last challenge before two and a half years of Hydraulic Engineering can be successfully completed. The work conducted over the past months has been supported and made possible by the people who have guided me throughout the graduation process. I would like to take this opportunity to express my gratitude to them for their effort and help.

First of all, I would like to thank Prof. Stefan Aarninkhof for his guidance in conducting a research. His reflection has taught me to always keep in mind the bigger picture and has demonstrated this by leading the meetings in the right direction.

The design of coastal defence structures is a complex process, in which a mere student can easily loose his way. Bas Hofland's input, guidance and extensive knowledge on this matter has helped me a lot trough out the whole process. He was always willing to take the time to spar and discuss my thesis. Without his input this thesis would not have reached its full potential, for this I'm grateful.

I would like to thank Oswaldo Morales Napoles as well, for his time to attend every meeting and helping me with questions regarding probabilistic design and reliability. He has helped me with the correctness of the probabilistic method implementation into the model, without which would be useless. Also I would like to thank Gina Torres for her time and help.

It goes without saying, that I would like to express my gratitude to my daily supervisor at Royal HaskoningDHV, Maarten Schoemaker. He has welcomed and introduced me to the company and the ongoing equivalent projects. The feedback he has provided and the discussion sessions has helped me make a complete thesis of which I can be proud.

Royal HaskoningDHV has supported and encouraged this thesis from the start. They have allowed me to become part of an internal technical development initiative which has helped me a lot in developing my python capabilities and in understanding the design process better. Furthermore, the company has provided me with a playground of expertise and interested colleagues. Discussions with senior consultants Cock van der Lem and Ronald Stive, have helped me increase the quality and completeness of thesis.

Last but not least, I would like to thank all my friends and family for their unconditional support.

F.B. Sijbesma
Delft, October 24, 2019

Abstract

Around the globe, breakwaters and revetments are designed and built to protect coastal areas, harbours and shores. These hydraulic structures mainly serve to preserve desired conditions of the hinterland such as harbours and inhabited areas. One of the elements of such structures is the rubble mound slope design.

When designing hydraulic structures, engineers follow a structured and predetermined set of design phases, referred to as the design process. Within this process, the preliminary design phase is a highly iterative process, which requires many calculations. From these calculations many different initial designs of the structure are derived. Generally, these possible configurations are compared to the design requirements. An important requirement is the safety of the structure over its lifetime. This can be reasonably accounted for by applying different reliability methods. Within these methods, different elements of uncertainty are considered. In the preliminary and final design stage, depending on the engineer, the quantification of these uncertainties and the safety of a structure during its service lifetime are often based on expert judgement, partial safety factors or are not considered at all. It is generally perceived that a full probabilistic approach gives more insights into the reliability and safety of the design. Thus, three main problems occasionally occur within the preliminary design process:

- The preliminary design phase is is a time-consuming process.
- In the preliminary design phase, a limited amount of possible slope protection configurations can be considered.
- The uncertainties in these configurations are either based on experience or are not considered at all.

Due to the complex nature of this process and the mathematical workload, computer automated designs are becoming more popular. One possible automation method is the parametric design method, which translates different mathematical relations into parameters which can be easily altered. This research aims to develop a model which parametrically determines multiple solutions for a probabilistic design approach of a rubble mound slope protection, which takes into account uncertainty. This leads to an expansion and acceleration of the insight into possible design options in the preliminary design phase.

This research proposes a Python based parametric model within the predetermined design boundaries for rock armour slope protection. The design methods which are included are: the conventional approach, the conventional approach with uncertainty, the FORM approach and the Monte Carlo design method. Three failure mechanisms are considered, overtopping, armour layer stability and toe stability. An optimisation scheme is implemented to provide more insight into the output and to reduce computation time.

The model is applied to a case study, which proposes a preliminary breakwater design. With a conventional deterministic method, this design is built to accept moderate damage to the structure. A comparison with the probabilistic output of the model shows the following:

- Only a short amount of computation time is required for a large range of design solutions.
- Multiple cost optimal solutions are possible with relatively slight difference in costs.
- More reliable designs can be generated.

Furthermore, the cost optimal configurations of the probabilistic approaches show that the structure of the case study is under-dimensioned with respect to the probability of moderate damage. For a more safe structure, the dimensions are different. This results in a slightly higher crest height and larger stone sizes for the toe and armour dimensions.

The optimisation scheme shows promising results in terms of a reduction in computation time and output size. By finding local minima in the deterministic output it is possible to select cost-optimal solutions. However, it also disregards a few cost optimal solutions and should therefore be more thoroughly analysed.

The implementation of both FORM and CMC provides an easy and accessible basis for sensitivity analyses. Methods, such as the omission factor and reliability elasticity coefficient, can be implemented in the use of the model. In this research, the omission factors show that the optimisation parameters do not necessarily need to be randomly distributed. Consequently, this diminishes the computation load. The reliability elasticity factors show that the crest width and unit sizes inflict the largest rate of change in the overall reliability. Moreover, the probability of the toe stability has the most significant influence on the reliability of the model.

Overall, the model proposes a good start towards a parametric design model for rubble mound structures with an integrated probabilistic design method. It allows the engineer to diverge faster and wider at the start of the preliminary design phase, providing a large output of possible design configurations. This analysis shows that it can generate many configurations in a short amount of time, relative to the time that is currently required, given conventional design tools. This model incorporates probabilistic design methods, which enable engineers to quantify the structural safety and to incorporate more uncertainties, which makes the whole design more reliable. By carefully building upon this proposed model, the applicability could be elaborately extended.

Contents

List of Figures

List of Tables

1

INTRODUCTION

1.1. BACKGROUND

This research touches multiple fields of the engineering practice; parametric engineering, probabilistic design and rubble mound slope protection design. This chapter gives a brief introduction on the background of these aspects.

Nowadays, worldwide breakwaters and revetments are designed and built to protect coastal areas, harbours and shores. These hydraulic structures mainly serve to preserve desired conditions of the hinterland. For instance, harbours want to have as little downtime as possible due to transmitted wave action. These structures may be built with rubble mound slope designs.

1.1.1. DESIGN PROCESS OF RUBBLE MOUND SLOPE PROTECTION

Realising the aforementioned structure from problem to completion is a time-consuming, iterative and complicated process. Therefore, engineers follow a structured and predetermined set of design steps. This design phasing has been translated to a scheme, proposed by The Rock Manual, which explains the different phases (CIRIA/CUR, 2007b). Note that this is a generalisation and merely and example of the design phasing used in practise. However, this scheme is considered an accurate representation of the practical design process, for instance followed by Royal HaskoningDHV and is therefore explained further. The consequent phases are as follows:

1. Project definition
2. Conceptual design / Feasibility study
3. Preliminary Design
4. Final design
5. Detailed design

In the above phases, the construction and operation phase have been left out, since from the work of an engineer mainly involves the preceding phases.

Every project is initiated due to the lack of or the need for protection from hydraulic induced loads. Therefore, in the project definition phase states clear design objectives, restrictions and requirements. Henceforth, an engineer has a clear understanding of the required engineering solution to meet the identified need (CIRIA/CUR, 2007a). In the concept phase, the engineer does a feasibility study on the technical, economic, social and environmental aspects of the project. Furthermore, informational requirements are considered, e.g. which physical conditions. Once this phase is successfully executed, all ingredients are gathered to proceed to the next stage. The preliminary design phase aims to develop a number of alternative configurations. Moreover, different assessments such as an environmental impact and economic assessments are carried

out, but the focus mainly lies upon the technical feasibility (CIRIA/CUR, 2007a). This is an iterative and interactive process in which many different parties are involved, in order to eventually agree on several possible configurations. The final design involves determining a set of configurations for which the system in which the final shape of the components is fixed (Verhagen and Van den Bos, 2018). In this stage, further physical and technical data can be required and acquired through model tests on the configurations. From the preceding design phase the detailed design is drawn and further elaborated upon with final drawings and specifications to be set for construction.

The preliminary and the final design phase reacquire many and iterative calculations, which is time costly. The highly iterative process requires engineers to continuously repeat their calculations based on their previous findings and consequent alterations. Generally, these calculations are done with computational aid, however, this is not an integrated or automated design. Therefore, this repetitive process takes a lot of time and work. Consequently, the design process can be enhanced and computation time can be reduced, by integrating these calculations in the use of new technologies.

During the aforementioned phases, many configurations are realised. Initially, structural dimensions such as the widths, slope angles and materials are quantified. Furthermore, multiple different factors are considered, such as whole-life costs, risks and the complexity of operation and maintenance. Conventionally, expert judgement determines which dimensions and structural elements are likely to satisfy the requirements of the structure. Not all possible configurations within the scope of the requirements an be realised and analysed, simply due to time- and cost-management. This iterative process indicates a convergence from a particular initial configuration towards a couple of optimised configurations. In fact much more possible optimal options could be realised. Unfortunately, this is momentarily not possible within the time and cost frame. This possibly indicates the need for automation of this process. With new and fast emerging technologies, competitive pressure increases. This emphasises the need to incorporate computational power.

1.1.2. PARAMETRIC DESIGN

As previously indicated, the need for computer automated designs for projects is becoming more popular, due to the use of computational power, instead of conducting in calculations by hand. An automation method, amongst many others, is the parametric design method. Parametric design follows from the derivation of the (mathematical) relations used in different designs. Subsequently, it translates these relations into parameters which can be more easily altered and used as input variables. A preliminary or final design can be manipulated and modified by altering the parameters and their dependencies. In this way, a a more integrated design is achieved and more knowledge on the impact of various parameters is gained (Schnabel, 2012).

A parametric design approach, should give a more flexible, integrated and efficient design process, because hand calculations can be preformed computationally. Different approaches to a design problem can be more easily and quickly reviewed. Thus, a solution can be reached by converging more quickly from a wider range of design solutions. On the other hand, the pitfalls of parametric engineering should also be carefully observed. Even though parametric engineering strives for a more integrated approach to the problem, it might induce the opposite. For instance, an engineer may not be able to distinguish or identify the engineering process and formulas of a highly advanced model. This could lead to knowledge deterioration.

A complex aspect of parametric design is the trade-off between insight and calculation time. Insight defines the level of detail and amount of different solutions. Preferably, one would want to see as much solutions as possible to gain more insight into the different design possibilities. On the other hand, however, this is a computationally heavy option and the difference between solutions might not be significant. Therefore, optimisation procedures are often applied to automated or parametric designs. The solutions then converge to a predetermined optimum or minimum. This option has the advantage of less computational time, since non-significant solutions can be disregarded. On the other hand, it has the disadvantage that design choices and other options are not clearly reviewed and might be overlooked. It might become unclear what steps are taken and how (Schnabel, 2012). Also, the solution might not be the optimum, due to computational decision errors or assumptions. Therefore, this trade-off system should be carefully considered when automating engineering practices. Thus, optimisation is an intrinsic aspect of parametric engineering.

1.1.3. PROBABILISTIC APPLICATION

When one designs a slope protection structure, an important requirement is safety. The engineer will want to be sure that it will withstand the anticipated loads during a certain lifetime (Verhagen and Van den Bos, 2018). This can be reasonably accounted for by applying reliability methods. Within these methods, different elements of uncertainty are considered, e.g. statistical uncertainty of environmental data.

In the preliminary and final design phase, the quantification of uncertainties and the safety of a structure during its service life time, are often based on expert judgement or partial safety factors. Unfortunately, this approach does not consider the actual probability of failure and uncertainties of the physical and mathematical relations of the input variables. Therefore, these configurations might be over- or under-dimensioned (Verhagen and Van den Bos, 2018). Furthermore, accounting for model, physical and statistical uncertainties will diminish the overall uncertainties in the final costs of the designs, an thus making it more reliable.

There are several methods to calculate the reliability of a structure or to incorporate uncertainties and the probability of failure. According to (Jonkman et al., 2015) this is subdivided into five method groups:

- **Level 0**: Full deterministic approach.
- **Level I**: Semi-probabilistic approach, which accounts for uncertainty with the partial safety factors.
- **Level II**: Methods which incorporate approximation analyses.
- **Level III**: Numerical approach
- **Level IV**: Risk-based design methods, where consequences of failure are considered and where the risk is used to measure the reliability (Jonkman et al., 2015)

The level II or III probabilistic design approaches consider the effect of uncertainties and probabilities of failure in more detail. The level II approach includes the uncertainties on different parameters by expressing them by a mean, standard deviation value and distribution. Also, correlation coefficients are applied between stochastic variables. In the level III approach, the uncertainties of variables are modelled by their joint distribution functions. The probability of failure is exactly determined by numerical integration. This method is adapted in the Spanish ROM, which has made a Monte Carlo analysis obligatory (Puertos del Estado and Ministerio de Fomento, 3002). Each of these levels has a different approach and different limitations to their outcomes. Generally, it is perceived that a full probabilistic approach (level II and III) gives more insights in the reliability and the variable impact.

Like the design process, these probabilistic approaches are complicated and time-costly. Since this is implemented in the preliminary or final design phase, it becomes part of the iterative process. Thus, the integration of these methods is even more time and labour-costly. The added value and complexity of these methods emphasise the need for new technologies and automation.

1.2. PROBLEM DEFINITION

From the section above, three main recurring problems can be identified.

- The preliminary design phase is is a time-consuming process.
- In the preliminary design phase, a limited amount of possible slope protection configurations can be considered.
- The uncertainties in these configurations are either based on experience or are not considered at all.

These problems are all connected to the issue that, with emerging technologies, the design process is lacking behind on the potential optimisation in effectiveness and accuracy. Royal HaskoningDHV has already made a step in the right direction. However, much can still be done to enhance the conventional way of engineering. A problem statement is derived from the aforementioned problems:

> ***"The preliminary design phase is time-consuming and therefore a limited amount of design configurations can be realised. Furthermore, the included uncertainties are often based on expert judgement and not quantified."***

1.3. RESEARCH OBJECTIVE & QUESTIONS

This research should give a quicker understanding of the effect of a full probabilistic analysis on multiple solutions of a rubble mound slope protection as opposed to a parametric deterministic approach. Simultaneously it should give more insight in the sensitivities of different parameters on the cost optimal solution and probability of failure. Furthermore, it should consider the relation between different failure modes and the distribution of the probabilities of failure. This should be applicable to national and international designs. This is translated in the following research objective:

> ***"Develop a model which parametrically determines multiple configurations of a rubble mound slope protection also integrating a probabilistic design method to account for multiple different uncertainties."***

The following research questions are extracted from the research objective:

1. Is it feasible to create a parametric design-tool, which simultaneously incorporates a probabilistic approach, for the preliminary design of a rubble mound slope protection?
2. What are the advantages of the integration of the probabilistic analysis in the proposed model as opposed to the current design process?
3. What is the practical added value of the model in the design process?

1.4. RESEARCH SCOPE

For this research to be successfully completed, a general scope of the research is made. The following points of attention define the scope:

- Develop a Python based model in which multiple failure mechanisms are incorporated.
- Incorporate a probabilistic calculation method into the model. This must be a Level II and / or III method.
- Include a parametric build-in and an optimisation scheme.
- Case study for model validation purposes.
- Include costs to investigate and quantify the sensitivity analysis of the model.

1.5. RESEARCH METHODOLOGY

To answer the four research questions and contribute to the research objective, a methodology is proposed that entails six steps:

1. Literature study on parametric engineering, reliability and rubble mound slope protection.
2. Set framework for the model. Development of a model coded in Python language to perform parametric and probabilistic calculations, with a cost function. This step mainly involves modelling.
3. Data analysis of the case study applied to the model. Raw data are extracted and analysed for further use.
4. Model validation. The model is validated on the calculation and parametric correctness. The results are compared with the case study results.
5. Conducting a sensitivity analysis in which the effects of different parameters on the optimal solution are determined.

1.6. THESIS OUTLINE

The current chapter is an introductory chapter, which introduces the research subject, problem definition, the research objective and the main research questions, the scope and methodology. This chapter is followed by a theoretical chapter (Chapter 2), which gives some background information on subjects applied in the model, such as the reliability analysis, the failure mechanisms and cost function. The third chapter involves a description of model (Chapter 3). The model framework is explained, which involves design choices, e.g. the choice of failure mechanisms and probabilistic approach level(s). This is followed by the model setup, in which, among other aspects, the model restrictions, in- and outputs are considered. How is this processed, which steps and in which (calculation)flow. In Chapter 4, the case study is explained. Furthermore, a data analysis is made for further use in the reliability analysis. Consequently, an extreme value analysis is documented, which provide inputs for further use. In the subsequent section the model is validated using a case study and recognised programs such as Prob2B and Mathcad. Chapter 5 shows the results and performence of the model for different situations. In the chapter "Sensitivity Analysis" (Chapter 6, the effect of different uncertainty parameters on the costs and reliability of different configurations is investigated. Furthermore, the time-sensitivity of the model is tested. Finally, a discussion regarding this research is conducted, followed by conclusions and recommendations Chapter 7.

2

THEORETICAL BACKGROUND

2.1. SLOPE PROTECTION

Slope protections can be applied in many places and on many different structures. For instance, on the banks of river and canals or on dikes revetments and groynes in coastal areas. Each different location deals with a different situation. These different situations cause different loads, such as storm wave loads or loads caused by flow. The function of slope protections is to withstand these loads; or, in other words, to withstand the energy of moving water. Protections can classified either under bank protections or shore protections. Bank protections can be realised by revetments or rigid structures. Shore protections can be realised by groynes and breakwaters or by revetments and dikes. A slope of such hydraulic structures can be built in different ways with different materials, such as:

- Loose rock or rubble-mound
- Placed blocks or composite mattresses
- Asphalt
- Grass
- Rigid: E.g. Sheet pile walls
- Unconventional materials, e.g. reefs

This research only covers the rubble-mound slope protections. Apart from the variety in materials, there are many different types, shapes and forms of slope protection. The different forms are a result of stability requirements. For instance, some slopes include a berm or are submerged.

2.1.1. CONVENTIONAL RUBBLE-MOUND SLOPE

A rubble-mound slope is generally a part of for instance a dike or a breakwater. To illustrate the components of the slope protection, an example is shown in Figure 2.1.

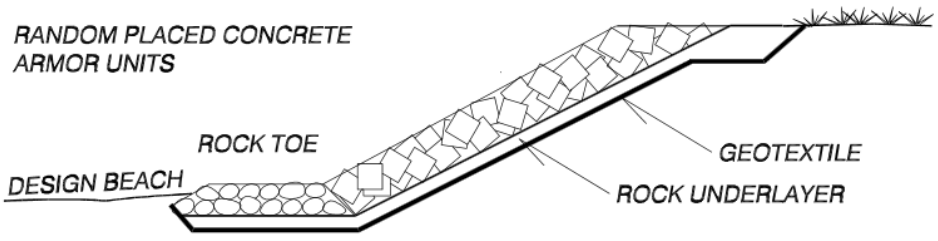

Figure 2.1: An example of a rubble-mound slope (Burcharth and Sørensen, 2006)

The core of the rubble-mound slope protection is either placed on the subsoil, in case of a breakwater or groyne, or is a part of the shore or bank. On top of the core, a filter layer can be placed, or in Figure 2.1 a geotextile. This is followed by an under layer. The top layer is the armour layer, in the example randomly

placed concrete blocks. As shown in the example, a toe is placed to increase the stability of the slope and armour layer.

2.1.2. FAILURE MECHANISMS

Hydraulic constructions such as dikes, revetments and breakwaters, function to protect the hinterland from undesired effects. For instance, port downtime due to wave transmission, hinterland flooding or coastal erosion. Failure to retain the water from flooding, can be caused by several failure mechanisms. An overview of different failure mechanisms is shown in Figure 2.2. The failure of the structure can caused by hydraulic, structural or geotechnical failure:

- Hydraulic failure occurs when water enter the hinterland by overflow or overtopping
- Structural failure occurs when the structure is breached, e.g. damage to the armour layer.
- Geotechnical failure occurs when the structure is breached or when water enters the hinterland as a results of soil failure, caused by slip failure or subsoil settlement.

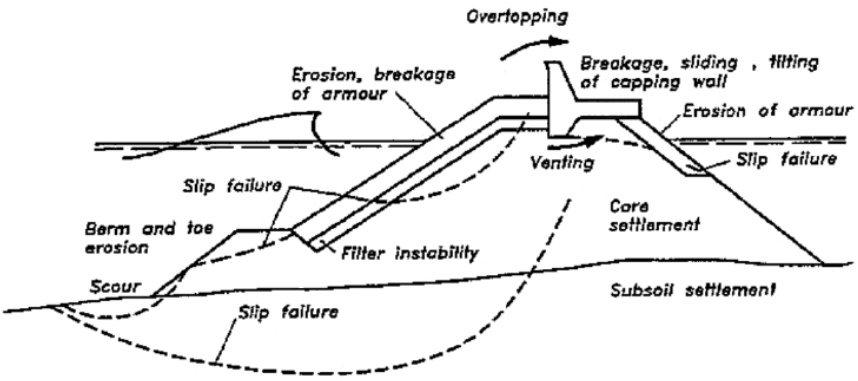

Figure 2.2: An overview of different failure modes of a breakwater (Burchart, 1995)

Figure 2.2 shows that a rubble mound slope structure can fail under many different mechanisms. Moreover, these mechanisms can also occur through different circumstances. This research only considers overtopping, armour layer stability and toe stability, as shown in figs. 2.3 to 2.5 respectively. A further elaboration on these failure mechanisms follows.

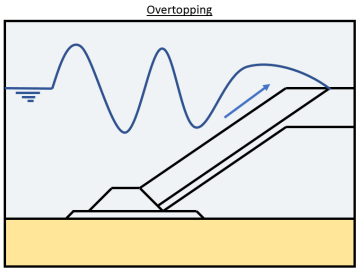

Figure 2.3: Failure Mechanism: Overtopping

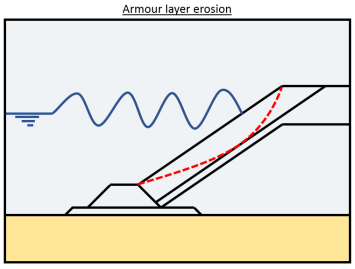

Figure 2.4: Failure Mechanism: Armour layer erosion

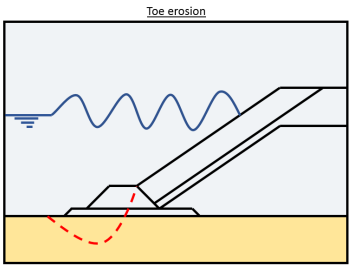

Figure 2.5: Failure Mechanism: Toe erosion

OVERTOPPING

Overtopping is a phenomenon that occurs when waves supersede the crest level of the structure, provided that the water level is below the crest level. These waves run-up on the seaside slope of the structure and spill over the crest, as animated in 2.3. Excess overtopping can lead to erosion of the hinterland. This can lead to a collapse of the upper part of the slope protection.
The overtopping of a structure can be calculated using different methods and approaches, given below:

Methods (van der Meer et al., 2018):

- Empirical methods, mainly formulae
- CLASH European project, Neural Network tool
- Numerical models
- Physical modelling
- Simulating in reality, laboratory to dike

This research only focuses on the empirical methods. Thus, only formulas are considered and implemented. Over the years, a number of different formulae have been empirically determined. Only the most common and recently altered formulae are mentioned.
Empirical formulae:

- EurOtop 2007
- EurOtop 2018
- TAW (2002a)
- Owen's method: Besley (1999)

The above methods for predicting the mean overtopping rate are listed. Moreover, in each design situation a tolerable discharge or overtopping rate is allowed. This is based on the design criteria and allowable failure, damage or hazard type (Allsop et al., 2009). Suggestions for the critical values for the mean overtopping rate per design situations are made by (Allsop et al., 2009), these are listed in Figures B.1 to B.3.

ARMOUR LAYER STABILITY

Rubble mound slope protection erosion is considered to be local erosion, rather than erosion due to longshore sediment transport, which is part of coast morphology (Schiereck and Verhagen, 2012). The local armour layer erosion can then be classified as the instability of one or multiple armour layer units. This does not necessarily lead to total failure of the structure, for instance if just a few units have moved. However, under severe conditions this instability may lead to total failure, possibly leading to breaching and flooding.

Instability of armour layer units can be a consequence of a number of events:

- Displacements of armour units causing underlayer and core to erode.
- Breakage of armour units, due to wave and gravity stresses.
- Deterioration due to temperature, abrasion or chemical reactions.
- A premature failure of the toe berm can cause a failure in the armour layer.
- Seabed scour occurs when the armour layer can experience sliding and eventual failure.
- Lastly, pore pressure build-up either can either lift a proportion of the armour layer or the entire armour layer. As a results the underlayer is exposed to erosion (Burcharth and Hughes, 2006).

As previously noted, this research only considers rock slope protection elements. Thus, the formulae for other rubble mound protection elements, such as concrete blocks and Accropodes, are disregarded.

TOE STABILITY

Toe erosion is conceptually similar to the armour layer erosion. The local toe layer erosion can then be classified as the instability of one or multiple armour layer units. Toe stability failure may lead to armour layer erosion or failure, which can lead to total breaching of the structure. The movement of the toe armour units can be due to a variety of reasons.

- A lowering of the beach level due to erosion can cause the toe material to erode or sink in seabed.
- A similar mechanism can occur if scour holes for around the toe of the structure.
- In shallow waters, forces caused by breaking waves can induce rock or armour unit movements. Excessive movement or force can cause failure.
- Wave induced pressure gradients can cause the finer materials to wash out, finally resulting in instability (Burcharth and Hughes, 2006).

The most commonly used empirical formulae are , Gerding 1993 or Van der Meer 1995 (Gerding, 1993; van der Meulen et al., 1996).

2.2. RELIABILITY ANALYSIS

BASIC CONCEPTS

The basic criterion for structures to perform safely, is the notion that the structural resistance (R) is larger than the load (S) on the structure, as shown in equation 2.1. Reliability is then explained as the ability of a structure to fulfil its requirements, over its lifetime, for which it has been designed (Institution of Civil Engineers (Great Britain), 1988).

$$R > S \tag{2.1}$$

However, the resistance and loads are not deterministic variables but random (or stochastic) variables. This is because loads on a structure experience a certain spatial and temporal variation. Likewise, the strength of the structure is not always the same in all elements. This randomness is indicated with statistical parameters. The means of the load and resistance are indicated as, μ_S and μ_R respectively. Additionally, σ_S and σ_R, are the respective standard deviations, and f_S and f_R, the probability density functions.

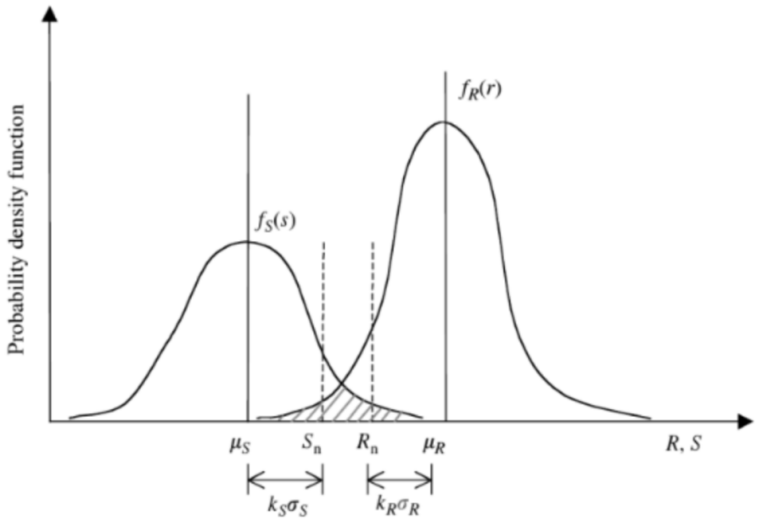

Figure 2.6: Probability density function of resistance and load (Manoj, 2016)

Figure Figure 2.6 shows that the aim of a design is to keep the design resistance R_n greater than the design loads S_n. Or differently put, the probability that a high load (S) occurs and a low resistance (R) occurs at the same time should be kept low (Jonkman et al., 2015). Thus, the probability of failure can be defined, expressed in R and S as shown in equation 2.2.

$$P_f = P[S > R] \tag{2.2}$$

GENERAL DESCRIPTION OF THE LIMIT STATE FUNCTION

The probability of failure can also be indicated by means of the limit state function, or performance function. It can be expressed in accordance with resistance R and load S, show in equation 2.3.

$$Z = R - S \tag{2.3}$$

For if $R < S$ the limit state function will become $Z < 0$, in which case the failure probability can be indicated $P_f = P[Z < 0]$. The limit state simply indicates the difference between the unsafe and safe region with respect to the load and resistance. Since the resistance (R) and load (S) are both stochastic variables, the function Z can be generalised, as shown in equation 2.4

$$Z = g(x) \tag{2.4}$$

This function is defined so that the performance can be indicated as follows:

- $g(x) > 0$: Safe zone

- $g(x) = 0$: Limit state
- $g(x) < 0$: Unsafe zone

In order to calculate the level of reliability, five different methods have been developed. This research uses level II and III methods. These are approximation and numerical approaches respectively.

FORM ANALYSIS

One of the levels of probabilistic approach is the level II approach which uses approximation. In this case the uncertain parameters are modelled by their mean values, standard deviations and correlation coefficients between stochastic variables. This method is considered one of the most reliable computational methods and a good alternative to the Monte Carlo Analysis (Zhao and Ono, 1999). However, it is mathematically more complex.

This method is an analytical approximation method. It searches the most likely failure point (i.e. the design point, or point with the highest probability density) by means of mathematical programming (Zhao and Ono, 1999). It interprets the beta value as being the distance from this design point to the origin of the limit state surface in a standardised normal space. Since the limit state function is linearised in the design point, shown in Figure 2.7, the accuracy of this method decreases in case of a highly non-linear limit state function (Jonkman et al., 2015).

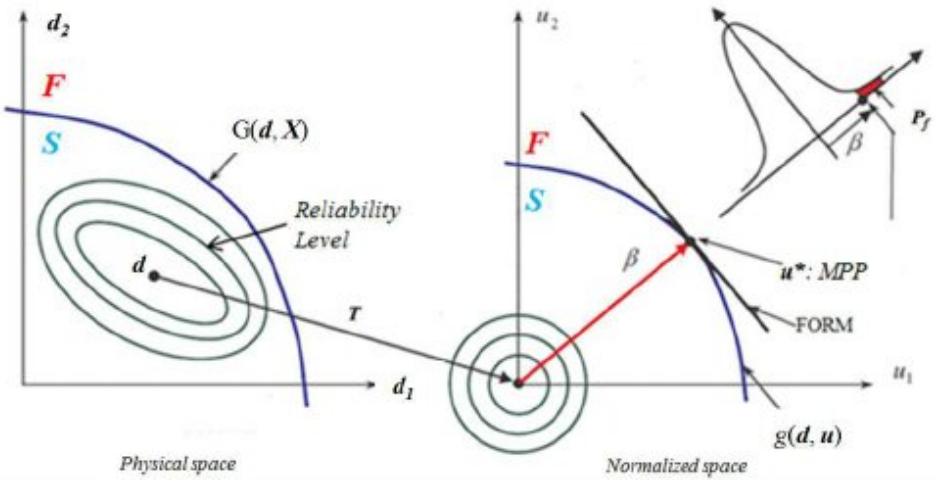

Figure 2.7: Transformation T and the First Order Reliability Method (FORM) (Lopez and Beck, 2012)

The performance or limit state function is given by equation 2.3. Since both R and S are considered random variables, of which their distributions are considered normal, Z can also be considered a normally distributed random variable, as shown in equation B.1.

MONTE CARLO ANALYSIS

The level III approach uses numerical integration, which is commonly done with Monte Carlo simulations. Uncertain quantities are generated by their joint distribution functions, to calculate the probability of failure (Jonkman et al., 2015). The Monte Carlo simulation uses random sampling to see how a system with stochastic components behaves. The method is applied by describing the joint probability distributions of the random variables within a system. The system is implemented into a program as a model in order to simulate N random samples for each basic variable over a certain time frame. The behaviour is analysed and statistical inference is performed to see the whether the model fails or works accordingly. Thus, as probability of failure can be determined.

2.2.1. FAILURE

If a structure does not manage to fulfil its purpose, e.g. due to extreme wave attacks, it means it has failed in some way. Two different most common limit state situations are discussed which describe an amount of failure during an undesired event, such as flooding.

ULS

The Ultimate Limit State (ULS) relates to the complete loss of the original function of a certain part of the structure. The ULS will only be reached in extreme conditions. The rubble mound slope protection can fail due to different failure mechanisms, such as extensive wave overtopping, instability of the primary armour layer or toe erosion. This damage often leads to insufficient protection against wave attacks and can result in breaching.

SLS

The Serviceability Limit State (SLS) relates to operational inconveniences/hindrances. The structure should be able to survive without repair. During normal conditions, operations are hindered if the wave height exceeds the maximum allowed wave height. It should be noted that no or minor repairs are made to the structure. For instance, if wave activity causes overtopping in port basin, leading to downtime, but the structure remains intact.

Whether each of these states is exceeded depends on whether the damage caused exceeds an accepted damage level or target failure. Generally, the chances of reaching the ULS are lower than reaching SLS. The acceptance damage level of the structure can be determined, based on the acceptance of the client, acceptable repairs or lifespan of the structure. It should be noted that besides ULS and SLS other limit states can be considered. However, these are not taken into account in this research. It should be kept in mind that the limit states are related to an undesired event. It differs depending on the nature of the project and the structure.

2.2.2. UNCERTAINTY

The limit state equation is a deterministic model indicating functioning or failure of the structure. Uncertainties are generally related to the input of the limit state equation (Allsop et al., 1999). However, uncertainty can be qualified into three different types; inherent, model and stochastic uncertainty. Below it is explained how they are defined.

INHERENT UNCERTAINTY

This uncertainty still remains even if unlimited data is available. It is generally the uncertainty that is inherent to physical processes. For example, even if wave buoy would measure at a location for an infinite period of time, the wave properties would still remain uncertain in the future. However, probabilistic distributions can be used to approach and quantify this uncertainty.

MODEL UNCERTAINTY

According to (Allsop et al., 1999) this uncertainty can be categorised into two different types:

- The limit state function uncertainty.
- The uncertainty of the distribution of input parameters.

The first uncertainty refers to the schematisation of physical processes. By assuming and leaving out some parts of these processes the model is subjected to some degree of uncertainty. These assumptions introduce an amount of scatter in comparison to the measurements. By using a more refined model with a more accurate description of the physical processes, the uncertainty can be reduced.
The second type of uncertainty is related to the input parameter distribution function. Naturally, an uncertainty is inherent to a theoretical distribution representing the random variables. In fact, a distribution is simply a model related to the input variable.

STATISTICAL UNCERTAINTY

This uncertainty mainly lies in the distribution fitting to limited data. This uncertainty reduces with an increase in data points. For instance, when measuring, an uncertainty lies in the measurements. If more measurements are conducted this uncertainty decreases. Hence, the parameters of the distribution are of a random nature as well. For example, a wave buoy measures a wave-height during a certain period of time. These measurements contain a certain uncertainty. Thus, the measured wave height contains a statistical uncertainty.

MODEL CORRESPONDENCE UNCERTAINTY

This type of uncertainty is not described in the PROVERBS (Allsop et al., 1999). This uncertainty is best placed under inherent uncertainty. It is the uncertainty of implementing a model in-situ. Even if the inherent uncertainties, the model uncertainties and stochastic uncertainties are quantified, the behaviour of a model in the future on-site will still be uncertain. For instance, even an equally sized scale model will not contain all of the correlated physical-process uncertainties and model behaviour uncertainties. Material degradation, sea-level rise, sea-bed ripple effects, vegetation and other natural effects all weigh-in differently.

2.3. EXTREME VALUE ANALYSIS (EVA)

The design of a structure is based on the design lifetime of the structure. Based on the desired life time, the sea-states over a longer period of time must be known, e.g. the sea-states over 100-year period. Unfortunately, sea variable data is not always available for longer periods of time. This means that an estimation of the sea states for a longer period of time is needed, given the available data. In order to properly estimate these values, a good representation of the data should be acquired, regarding statistical terms. An overall fitting of the given data is made to determine a representation of its empirical distribution. Subsequently, this empirical distribution is then fitted to theoretical distributions. Based on a few criteria, the best fit is then chosen to represent the data with a theoretical distribution. However, these distributions may give a poor representation of the tail area (Castillo et al., 2003a; Genest et al., 2011). This means that the extreme events observed in the data are not optimally represented by the theoretical distribution. Nevertheless, methods have been developed to estimate the tail estimations. An EVA provides an approach to estimate the extreme values based on the given data.

To acquire water levels, wave heights and periods for larger return periods, an extreme value analysis is performed. Generally, an EVA can be performed with: (1) The block maxima model and (2) The Peak over Threshold (POT) model, shown in Figures 2.8 and 2.9 respectively (Katz et al., 2002). Each of these approaches has a different take on the classification of extremes. The first approach takes samples of the bulk data over a certain period of time. For instance, this can be every year, every week or every month. It then determines either the maximum or minimum per sample, which is then considered an extreme event. The second approach predetermines a certain value, representing the threshold value. Subsequently, every observation larger than this threshold value is considered an extreme observation.

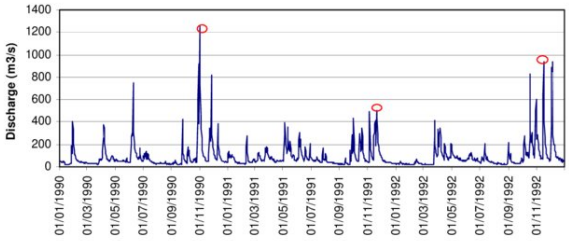

Figure 2.8: Illustration Block Maxima(Prudhomme et al., 2010)

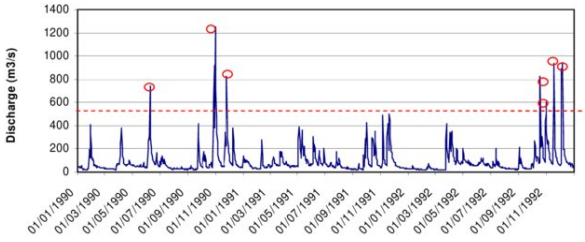

Figure 2.9: Illustration Peak over threshold(Prudhomme et al., 2010)

2.4. PARAMETRIC AND RELATIONAL DESIGN

2.4.1. THE CONCEPT OF PARAMETRIC DESIGN

Parametric design is an ingredient of computer automated design in the field of engineering. It is the integrated management of parametric equations and relations in a design process or calculations. (L.P.L. van der Linden, 2018). It can therefore be said that parametric design is closely related to automated design, but they are not equally the same. One should therefore carefully assess whether the design is of a genuine parametric nature.

The practice of parametric engineering is already widely used in the building engineering disciplines and architectural practices (L.P.L. van der Linden, 2018). However, in hydraulic engineering, parametric and automated designs are not yet widely used or applied. This is mainly due to the many empirical relations which are defined and used in the field of hydraulic engineering. Consequently, design choices are made by experienced engineers, who are often confronted with exceptions on various formulae or situations. Moreover,

the design guidelines are sometimes a bit ambiguously defined, which gives room to multi-interpretable design approaches. This can result in varying solutions, based on different design choices which follow from expertise and experience. As a result, it is challenging to develop automated and integrated designs for various hydraulic structures or projects, since the designs are ultimately unique. This is especially difficult when attempting to parametrically define different empirical relations and boundaries in order to automate and integrate calculations.

APPLICATION TO RUBBLE MOUND SLOPE PROTECTION

In the engineering field of rubble mound slope protection designs, several applications of parametric studies have been conducted. Some of these studies aim to gain more insight in the effect of different parameters on the design, formulae or efficiency of the solution, such as (Pezzutto et al., 2012) or (Booshi and Ketabdari, 2016). Other design approaches are aimed at generating an optimised solution or sensitivity analysis to different design criteria, such as the studies of (Galiatsatou et al., 2018) or (Castillo et al., 2003b). These researches mainly involve a specific engineering case or specific parameters. These researches mostly seek the effect of parameters on an implied optimum. The parametric equations and relations are intertwined with the physical model tests and results. Despite the undeniable fact that model tests are of vital importance in the engineering field, one can only conduct a small number of tests and must surrender to the fact that these often implicate scaling factors. By using computational power more design possibilities can be generated.

W. de Haan stated that due to the unique character of breakwaters, it is difficult to use computer designed breakwaters. This is the main reason why developments of Computer Aided Design (CAD) are hardly applied in the engineering practice of breakwater design (Medina, 1992). Nevertheless, he conducted a research on the possibilities of a deterministic computer-aided optimum design of rock rubble-mound breakwater cross-sections. Similar researches were conducted by Nielsen and Burcharth (1983) and by Le Mehaute and Wang (1985). He developed a computer package called RUMBA, which computes the optimum rubble-mound breakwater by minimising the costs (maintenance and construction). However, this package does not consider all the relevant parameters and is also relatively outdated.

(A. Vittal Hegde and Bhat, 1998) developed an algorithm for computer aided optimum design of rubble mound breakwaters. The optimum design is based on the lowest total cost, exiting of maintenance, construction and wastage costs. It only contributes to non-overtopping rubble-mound breakwater using a deterministic approach. Initially, it designs a large number of breakwater sections, which all suffice to the pre-chosen design life. It then chooses the optimum section, as this is the one with the lowest total costs. (De Smet, 2015) describes a similar tool (CE-CLOUD) in his thesis, based on Microsoft Excel. However, this tool designs multiple configurations and therewith the costs separately. The purpose of this tool is to design two types of breakwaters for deeper seas: caisson and rubble-mound breakwaters. Once multiple options have been designed, the engineer can make a better decide which breakwater types he wants to apply. Deltares has also developed a tool to design and test hydraulic structures. It has been developed in the 1980's and has been updated ever since (Deltares, 2018). This tool is only available for professional use and is thus not commercialised. Therefore, little information regarding this tool is available for research.

2.5. COST FUNCTION

An optimisation criterion can be based on the least cost function. What these costs entail is different for each project and must be specified beforehand. The cost function depends on the limit state, for instance if the structure totally fails or if only some repairs are needed. Many different aspects can be included in the total cost function. Below a few of these aspects are shown (Burcharth et al., 2018):

- Initial costs (building costs)
- Cost of repair for minor/major damage
- Cost of failure
- Downtime costs
- Maintenance costs
- Decommissioning costs

The costs for the repair of major or minor damage can be coupled with the probability of these damages occurring (Burcharth and Sørensen, 2006). Furthermore, the real rate of interest (r) is coupled with the service life (T_L) of the structure. Occasionally, or when it is known, the benefits per year (b) can also be included in the total cost function.

3

MODEL DESCRIPTION

3.1. MODEL FRAMEWORK

3.1.1. DESIGN PROCES & METHODS

DESIGN PROCESS

In the chapter 1 the full design process is introduced. This research is target the preliminary design phase to be implemented in. Furthermore, for a probabilistic calculation to be implemented in the design process, initially a deterministic design is required. Subsequently, the reliability of this design can be determined with the probabilistic design method. The probability of failure which follows from this method is compared to the requirements, i.e. target reliability. Everts (2016) has made a simplified visualisation of this design process, shown below:

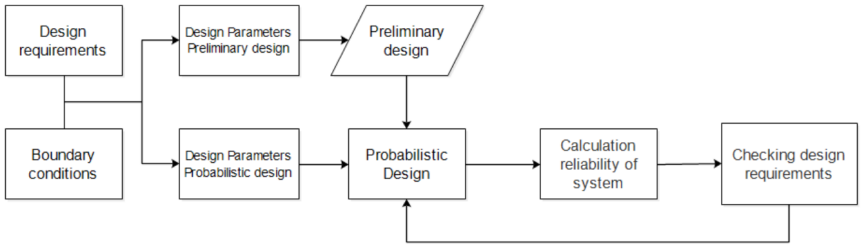

Figure 3.1: Simplified probabilistic design process in the preliminary design phase (Everts, 2016)

To further specify this diagram, the sequential steps which are undertaken are further explained as shown below:

1. Boundary conditions are the environmental conditions which can be hydraulic boundary conditions such as the wave height and period or the geotechnical boundary conditions such as the density and material of the seabed.

2. The design requirements are all of the aspects and fulfilment the structure is able to meet. Its basically setting structural acceptance terms. These are, for instance, the limit state or acceptable probability of failure.

3. The preliminary design is a first estimate, and a deterministic design. Hence, the use of deterministic input variables and the conventional method without uncertainty, the "mean value approach".

4. Subsequently, a probabilistic design can be made with a probabilistic method, such as FORM or CMC. Evidently, in this stage the probabilistic design parameters are used, such as parameter distributions and standard deviations.

5. Whence the reliability of the configuration is determined, the output can be compared with the design requirements, which have initially been set. If they agree with one another the configuration can be considered acceptable, if not it is disregarded and the inputs are altered to generate a new configuration.

In fig. C.1 a more thorough and extensive overview is shown.

METHODS

This research considers the following design methods:

1. Conventional method - Deterministic method without considering uncertainty
2. Conventional method - Deterministic method considering uncertainty
3. Probabilistic method - FORM analysis
4. Probabilistic method - CMC analysis

Method 1: In the Overtopping manual, this is referred to as the "mean value approach" (Verhagen and Van den Bos, 2018). This approach does not include any uncertainty. It simply selects the design wave height based on the target probability of failure and the design life time (Verhagen et al., 2009).

Method 2: Sometimes referred to as the "Design or assessment approach" (Verhagen and Van den Bos, 2018). This approach accounts for the uncertainty of different empirical models by section of "safer" values for the empirical fit coefficients. Commonly, the 5% exceedance value is used, or the value for the 5% confidence boundary, i.e. $\mu - 1.64\sigma$ (Verhagen et al., 2009; Verhagen and Van den Bos, 2018).

Method 3 & 4: Explanations are discussed in Sections 2.2 and 2.2.

3.1.2. STRUCTURAL DESIGN

In section 2.1 a few examples of slope protections and revetments have been introduced. This research will only focus on rubble-mound slope protection structures. Below, a few other design choices are displayed, with regards to a rubble-mound slope protection:

- High crested structures
- No berms
- No crown or wave wall
- No smooth or soft covers
- Steep slopes
- Relatively steep slopes

"High crested structures" refers to a structure which allows no or marginal overtopping. Consequently, overtopping occurs during extreme wave conditions (CIRIA/CUR, 2007b). In case no crown wall or crest element is taken into account, access along the top of the slope is limited (in case of a breakwater application). Rubble-mound structures exclude the use of smooth covers. These structures generally have more steep slopes. The slope angle can vary between 1:1.5 and 1:3.0, with a physical maximum of 1:4/3 (van der Meer et al., 2018).

3.1.3. FAILURE MECHANISMS & LIMIT STATES

In section 2.1.2, an overview of different failure mechanisms was given. Three of these failure mechanisms have been selected to incorporate in this research. They have been chosen because they are considered to be most significant. The failure mechanisms overtopping, armour layer erosion and toe erosion are elaborated upon in the following subsections. Their corresponding limit state functions are also explained. **NOTE:** the limit state functions in this section are all deterministically defined. The uncertainty of these equations are explained in Section 3.1.10.

OVERTOPPING

For the overtopping equations, the equation from the Overtopping Manual 2018 has been adopted, provided by eqs. (3.1) and (3.2)(van der Meer et al., 2018). **NOTE:** since eventually probabilistic analysis is conducted, the mean value approach is adopted.

$$\frac{q}{\sqrt{g \cdot H_{m0}^3}} = \frac{0.023}{\sqrt{\tan\alpha}} \gamma_b \cdot \xi_{m-1,0} \cdot \exp\left[-\left(2.7 \frac{R_c}{\xi_{m-1,0} \cdot H_{m0} \cdot \gamma_b \cdot \gamma_f \cdot \gamma_\beta \cdot \gamma_v} \right)^{1.3} \right] \tag{3.1}$$

with a maximum of,

$$\frac{q}{\sqrt{g \cdot H_{m0}^3}} = 0.09 \cdot \exp\left[-\left(1.5 \frac{R_c}{\xi_{m-1,0} \cdot H_{m0} \cdot \gamma_b \cdot \gamma_f \cdot \gamma_\beta \cdot \gamma_v} \right)^{1.3} \right] \tag{3.2}$$

In eqs. (3.1) and (3.2), γ_f, γ_b, γ_v and γ_β are all overtopping influence factors depending on the roughness, berm, seawall and obliqueness respectively. As discussed in section 3.1.2, some design restrictions are considered, meaning that some of these influence factors are not considered in this research. No berm or crown wall is considered, which indicates that both γ_b and γ_v are equal to 1.0. The slope roughness γ_f is dependent on which armour and what permeability is considered. This doesn't contain a lot of design freedom and is fairly constant depending on the types of armour and permeability, thus a mildly rigid variable (CIRIA/CUR, 2007b). γ_β considers the angle of wave attack.

The breaker parameter or the Iribarren number is denoted by $\xi_{m-1,0}$. This dimensionless parameter encloses the relations between the wave height, slope angle, wave period and wave length. It gives the discrimination between different types of breaking waves. This research considered both plunging and surging wave types. The breaker parameter combines the slope angle and steepness of the waves. Therefore, the foreshores must also be considered, specifically shallow or very shallow foreshores, which induce higher breaker parameters. Since eqs. (3.1) and (3.2) are only valid for $\xi_{m-1,0} \cong 5$, a different equation is proposed in (CIRIA/CUR, 2007b) for shallow to very shallow foreshores with $\xi_{m-1,0} > 7$. This equation is shown in C.1. (CIRIA/CUR, 2007b) also proposes a solution for breaker parameters which lie between the boundaries, $5 < \xi_{m-1,0} > 7$. Interpolating between eqs. (3.1) and (3.2) and C.1 should be exercised.

Armoured crest berms are also included. A simple slope with a narrow crest berm, which is smaller than 3 times the nominal diameters of the rock. However, a reduction in overtopping can be induced by creating a wider berm, so more energy is dissipated (van der Meer et al., 2018). Initially, the overtopping at the front of the crest should be determined. Thereafter, Equation (3.3) can be used to calculate the reduction factor.

$$Cr = 3.06 \cdot exp\left(-1.5 \frac{B}{H_{m0}} \right) \quad \text{, with max Cr} = 1 \tag{3.3}$$

LIMIT STATE FUNCTIONS OVERTOPPING

With regard to the overtopping failure mechanism, the structure fails when the amount of overtopping is larger than the admissible overtopping. The amount of overtopping is calculated by means of the previously discussed equations and that follows from the hydraulic boundary conditions and geometries. The admissible amount of overtopping is predetermined and matches the design preferences. By constructing a limit state function, the admissible amount of overtopping can be seen as the resistance and the amount of calculated overtopping the load. The limit state function for overtopping can then be shown by eq. (3.4).

$$Z_{overtopping} = q_{adm} - q \tag{3.4}$$

To give an example of a complete limit state function considering eq. (3.1), the following limit state function(eq. (C.2)) is fully written out, for the sake of completeness. The limit state function for eqs. (3.2) and (C.1) are constructed in a similar manner.

ARMOUR LAYER EROSION

Similar to overtopping, armour layer stability also includes the wave breaker type. In this research, only includes plunging and surging waves. Furthermore, in shallow water, the number of broken waves increases.

Thus the wave spectrum may be different. Since different equations govern, it is also important to consider whether the structure is in deep or shallow water.

For the armour layer stability, equations the equations from the (CIRIA/CUR, 2007b) have been adopted. For deep water the equations are provided by eqs. (3.5) and (3.6) and for shallow water by eqs. (3.8) and (3.9).
Deep water, Van der Meer 1988:

$$\frac{H_s}{\Delta d_{n50}} = c_{pl,d} \cdot P^{0.18} \cdot \left(\frac{S_d}{\sqrt{N}}\right)^{0.2} \cdot \xi_s^{-0.5} \quad \text{(Plunging breakers)} \tag{3.5}$$

$$\frac{H_s}{\Delta d_{n50}} = c_{s,d} \cdot P^{-0.13} \cdot \left(\frac{S_d}{\sqrt{N}}\right)^{0.2} \cdot \xi_s^{P} \cdot \sqrt{\cot\alpha} \quad \text{(Surging breakers)} \tag{3.6}$$

with,

$$\xi_s = \frac{\tan\alpha}{\sqrt{\frac{2\pi \cdot H_s}{g \cdot T_{m0,2}^2}}} \quad \text{and} \quad \xi_{cr} = \left[\frac{c_{pl,d}}{c_{s,d}} P^{0.31} \sqrt{\tan\alpha}\right]^{\frac{1}{P+0.5}} \tag{3.7}$$

For shallow water the following equations are adopted, Van Gent et al 2004:

$$\frac{H_s}{\Delta d_{n50}} = c_{pl,s} \cdot P^{0.18} \cdot \left(\frac{S_d}{\sqrt{N}}\right)^{0.2} \left(\frac{H_s}{H_{2\%}}\right) \cdot \xi_{s-1,0}^{-0.5} \quad \text{(Plunging breakers)} \tag{3.8}$$

$$\frac{H_s}{\Delta d_{n50}} = c_{s,s} \cdot P^{-0.13} \cdot \left(\frac{S_d}{\sqrt{N}}\right)^{0.2} \left(\frac{H_s}{H_{2\%}}\right) \cdot \xi_{s-1,0}^{P} \cdot \sqrt{\cot\alpha} \quad \text{(Surging breakers)} \tag{3.9}$$

with,

$$\xi_{s-1,0} = \frac{\tan\alpha}{\sqrt{\frac{2\pi \cdot H_s}{g \cdot T_{m0,2}^2}}} \quad \text{and} \quad \xi_{cr} = \left[\frac{c_{pl,s}}{c_{s,s}} P^{0.31} \sqrt{\tan\alpha}\right]^{\frac{1}{P+0.5}} \tag{3.10}$$

Where the following parameters represent:

H_s	= significant wave height [m]
$H_{2\%}$	= wave height exceeded by 2 per cent of the incident waves at the toe [m]
Δ	= relative density [-], given by $\frac{\rho_S}{\rho_W} - 1$
ξ_s & $\xi_{s-1,0}$	= breaker parameter or Iribarren number [-]
d_{n50}	= nominal median rock diameter [m]
$c_{pl,d}, c_{s,d}, c_{pl,s}$&$c_{s,s}$	= constants [-]
P	= notional permeability coefficient [-]
S_d	= Damage level [-], given by A/d_{n50}^2 with A the eroded area
N	= Number of waves [-]
α	= angle of the slope [°]

The type of breaking waves is determined by the breaker parameter and the critical breaker parameter. If $\xi_s < \xi_{cr}$, then plunging waves occur. If this is vice versa, surging waves occur.

In order to determine the design restrictions, it is important to understand the validity range of both the formulae for deep water and for shallow water. A complete overview of the design restrictions is provided

in figs. C.2 and C.3. A few points of interest are explained. Primarily, the slope angle for deep water formula is only validated for slopes between 1 : 1.5 & 1 : 6 and for shallow water only between 1 : 2 to 1 : 4. However, this research only considers steep slopes, since rubble mound slopes are solely considers. Thus, slopes milder than 1 : 3 are redundant. The deep water formulae is validated for breaker parameters $0.7 < \xi_m < 7$ and for shallow water between $1.3 < \xi_{s-1,0} < 6.5$. Furthermore, the deep water equations have a restriction regarding the notional permeability, since this is only validated between 0.1 - 0.6. This range is sufficient for an impermeable core, since the notional permeability is 0.1 in most cases. The stability number is only validated for deep water between 1.0 - 4.0 and for shallow water between 0.5 - 4.5.

LIMIT STATE FUNCTIONS ARMOUR LAYER EROSION

The armour layer fails when an undesired amount of armour layer units are displaced during certain conditions. This may be due to the fact that the armour units are under-dimensioned. The chosen armour layer units should be larger or equal to the required armour layer units, for the limit state function to be acceptable. By constructing a limit state function, the design armour layer unit can be seen as the resistance and the calculated required armour layer unit size the load. The armour layer unit size is expressed by the nominal median rock diameter. The limit state function for armour layer erosion can then be shown by eq. (3.11).

$$Z_{armour} = d_{n50,design} - d_{n50,required} \tag{3.11}$$

To give an example of a complete limit state function considering eq. (3.5), the following limit state function(eq. (C.3)) is fully written out, for the sake of completeness. The limit state function for eqs. (3.2) and (C.1) are constructed in a similar manner.

TOE EROSION

For the toe stability equation the equation by van der Meer (1998) is adopted (CIRIA/CUR, 2007b). These equations are provided by eq. (3.12).

$$\frac{H_s}{\Delta d_{n50}} = \left(2 + 6.2 \cdot \left(\frac{h_t}{h}\right)^{2.7}\right) \cdot N_{OD}^{0.15} \quad \text{for} \quad 0.4 < \frac{h_t}{h} < 0.9 \tag{3.12}$$

Where the following parameters represent:

H_s = significant wave height [m]
Δ = relative density [-], given by $\frac{\rho_S}{\rho_W} - 1$
d_{n50} = nominal median rock diameter [m]
N_{OD} = Damage number [-]
h_t = the depth of the toe below the water level[m]
h = water level [m]

Like any other empirical formula, this formula also has its restrictions wit its regard to its applicability. It has been derived by cases with a depth limit wave attack. Therefore, it would not be applicable for structures in very large water depths (h > 20 – 25 m). The equation is therefore, valid for depth-limited situations only. Furthermore, a toe with a high toe level, thus ht/h < 4, almost represents a berm and should therefore be approached as one.

LIMIT STATE FUNCTION TOE EROSION

The toe erosion limit state is very similar to the armour layer limit state. The toe fails when an undesired amount of toe layer units are displaced during certain conditions. This may be due to under-dimensioning. The chosen rock units should be larger or equal to the required rock units for it not to fail. By constructing a limit state function the design rock unit can be seen as the resistance and the calculated required rock unit size the load. The toe layer unit size is expressed by the nominal median rock diameter. The limit state function for toe erosion can then be shown by eq. (3.13).

$$Z_{toe} = d_{n50,design} - d_{n50,required} \tag{3.13}$$

To give an example of a complete limit state function considering eq. (3.13), the following limit state function(eq. (C.4)) is fully written out, for the sake of completeness.

3.1.4. RELIABILITY ANALYSIS

DISTRIBUTIONS

Some variables are randomly distributed. The input of the stochastic distribution is freely alterable. However, not all distributions are available. Most distributions require only a mean and standard deviation input but some, such as the Weibull distribution, also require an epsilon value input. The ones which are included, are the following:

- Deterministic
- Beta
- Gamma
- Gumbel
- Lognormal
- Normal
- Shiftedexponential
- Shiftedrayleigh
- Uniform
- Weibull

RELIABILITY LEVEL ANALYSES

This research only considers the Crude Monte Carlo and FORM II analyses. For these probabilistic calculations to be implemented in the model a Python module called PyRe is used. This is an open source module from GitHub. PyRe (Python Reliability) is a python module for structural reliability analysis. Its flexibility makes it applicable to a large number of problems. Along with core reliability analysis functionality, PyRe includes methods for summarising output. This module only supports First-Order Reliability Methods, Crude Monte Carlo Simulation and Importance Sampling.

3.1.5. PROBABILITY OF FAILURE

TOTAL PROBABILITY OF FAILURE

In this research, the system of failure is considered to be in series. This means that the failure of the top event, i.e. structural failure of the slope structure, happens when at least one of the underlying events fails. The series system is depicted with an or-gate, shown in Figure 3.2.

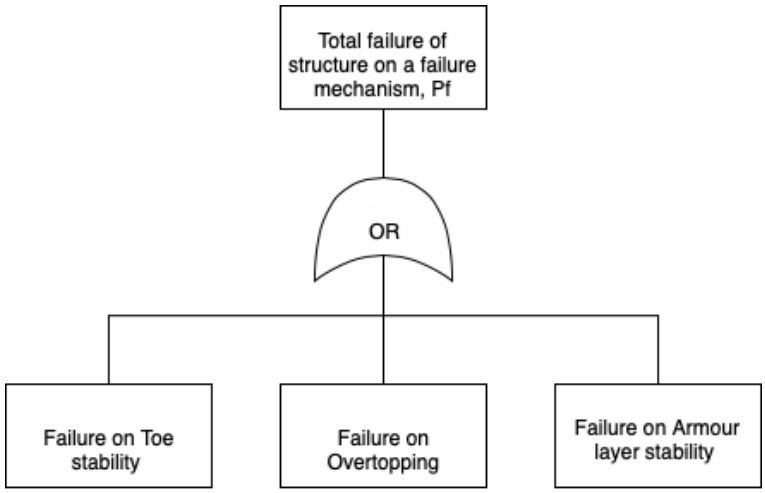

Figure 3.2: Fault tree total probability of failure of system

Furthermore, within a series system, a lower bound is assumed to avoid over-dimensioning. Hence, the underlying events are fully dependent. The total probability of failure is then determined by the maximum probability of failure of the underlying events, as shown in eq. (3.14).

$$P_{f,system} = max\{P_i\} \tag{3.14}$$

TARGET RELIABILITY

In the design process, to test if the total probability of failure is acceptable, it is compared with an acceptable probability of failure during a life time, as per eq. (3.15).

$$p_{f,T_L} = 1 - e^{-T_L/R} \tag{3.15}$$

The values for a lifetime failure probability are dependent on the use of the structure and the limit state. Typically, these values range between 5 - 20% for structural failure, for a typical life time of 20 to 50 years (Verhagen et al., 2009). Subsequently, the corresponding return period of a storm can be determined with eq. (3.16).

$$R = \frac{T_L}{-ln-(1-p_{f,T_L})} \tag{3.16}$$

3.1.6. GEOMETRIES AND INPUT

The rubble mound slope protection design can be subdivided into multiple elements. After which the geometry and volume of these elements can be defined. This is useful to know for further cost analysis and potential optimisation techniques. This model subdivides the geometries calculations into five different elements: The armour layer, underlayer, core, toe and geotextile. Since an exact determination of the geometries is not part of the scope of this research, a simple approximation per element is made. An overview of the elements is shown in Figure 3.3. A more thorough description and calculation of the volumes of each of the elements is given in Appendix C.

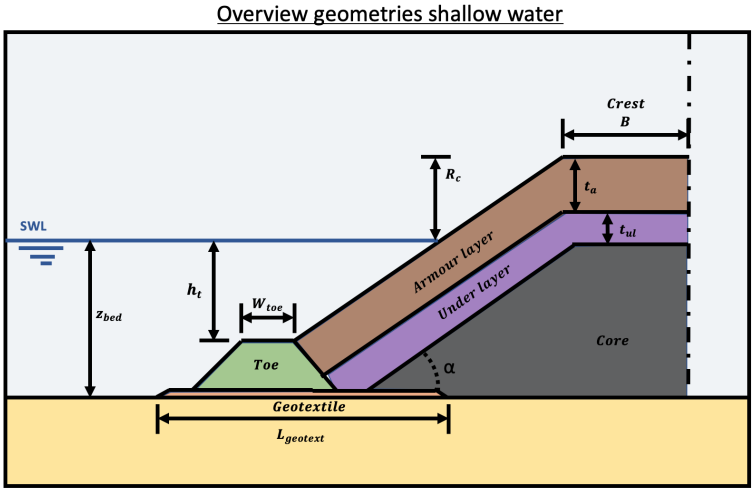

Figure 3.3: An overview of the geometries of the hydraulic sturcture in shallow water

3.1.7. COST FUNCTION AND INPUT

As stated in Section 2.5, many different types of costs can be adapted in the cost function. However, not all costs make a significant impact on the total costs and not all unit rates are always known. This thesis only considers the construction and maintenance costs. With regard to construction costs, only material or volumetric costs are considered but not labour or machine costs. Maintenance costs are expressed in a percentage of damage to the initial costs. This percentage is based on the number of displaced armour units. The number of displaced armour units is specified by the allowable damage level, thus the predetermined limit state. (Burcharth et al., 2018) proposed four types of limit state; Initial, Serviceability, Repairable, Ultimate.

Damage level	S (rock)[1]	Estimated D	Repair policy
Initial	2 - 3	2%	No repair
Serviceability (minor damage)	3 - 8	5%	Repair armour
Repairable (major damage)	5 - 12	15%	Repair amour + filter 1
Ultimate (failure)	8 - 17	30%	Repair amour + filter 1 + (filter 2)

Table 3.1: Classification of damage and estimated D, with D is the relative number of displaced units (Burcharth and Liu, 1995)

FORMULATION OF CONSTRUCTION COSTS

The construction costs are determined by means of the volume per element and the unit rates of the material. The unit rates of the material is different for each client, project or location. Therefore, they can be modified accordingly. However, they are given in euros per cubic metre [euro/m³]. The formulation of the construction cost per element is shown in Equation (3.17).

$$C_{C_n} = V_n \cdot UR_n \tag{3.17}$$

with, n representing the individual elements per structure, UR_n the unit rate per elemenet and V_n the corresponding volume.

FORMULATION OF REPAIR COSTS

The repair costs are simply a percentage of the construction costs. This percentage is determined by the damage percentage factor D, given in Table 3.1. The formulation of the repair cost per element is shown in Equation (3.18).

$$C_{R_n} = C_{C_n} \cdot D \tag{3.18}$$

with, C_{I_n} the construction costs per element and D the estimated percentage of damage. However, for different limit states the repair policy differs. Four different situations can be defined, following the limit states of Table 3.1.

D = 2%

For the initial damage level the repair policy is "no repair". Thus, for this limit state the repair costs are disregarded, even though a value for D is given.

D = 5%

The repair costs of minor damage in the serviceability limit state, is expressed by the following equation:

$$C_{R_1} = (1+K)DC_{C,armour}R \tag{3.19}$$

Where $C_{I,armour}$, represents the construction construction costs of the armour layer. The factor which represents the mobilisation costs is expressed by $K = 0.3$ and the factor which represent the high cost of repair is $R = 3$ (Burcharth et al., 2018). These values are changeable according to the preferences of the engineer, user or customer.

D = 15%

The repair costs of major damage in the repair limit state, is expressed by the following equation:

$$C_{R_2} = (C_{C,armour} + C_{C,underlayer} + KC_{C,armour})DR \tag{3.20}$$

D = 30%

The repair costs of failure damage in the ultimate limit state, is expressed by the following equation:

$$C_{R_3} = ((C_{C,armour} + C_{C,underlayer} + C_{C,core} + KC_{I,armour})DR \tag{3.21}$$

[1] Damage numbers are extracted from Verhagen, H., d' Angremond, K., and van Roode, F. (2009).Breakwaters and closure dams (Verhagen et al., 2009)

FORMULATION OF TOTAL COSTS

The total costs are then the sum of the construction and the repair costs of the life time of the structure. The formulation of construction cost per element is shown in Equation (3.22).

$$C(T) = \sum_{t=1} C_{C_n}(T) + \sum_{t=1}^{T_L} \{C_{R_n}(T) \cdot P_{f_n}(t)\} \frac{1}{(1+r)^t} \tag{3.22}$$

Where,

T_L = Service lifetime
r = real rate of interest
P_f = probability of failure per element in a year

3.1.8. PARAMETRIC ANALYSIS

The design choices regarding the parametric analysis are in the optimisation variables and optimal solution definition. The optimisation variables as mentioned in Sections 3.1.9 and 3.1.9 are the following:

- Nominal median rock diameter (Toe and Armour)
- Toe level
- Slope angle
- Crest freeboard
- Crest width

In the design phase, these parameters dominate the design freedom, since they have a wide design range. To parametrically approach these variables in the model, they are given an upper boundary, lower boundary and step size. This generates a range of options for each variable. Subsequently, a combination matrix can be made of all possible options, possibly competent with the design criteria of the structure. **NOTE**: the design freedom, given by the upper and lower boundaries must be carefully determined by expert judgement. Furthermore, the smaller the step size, the more options. However, a logical step size should be chosen, since the smaller step size will also result in more calculation time.

Previously, it was discussed that parametric engineering also includes a certain optimisation scheme. This is to prevent the model from blowing up. The amount of possible options needs to be minimised based on a predetermined optimal solution. This research considers two optimisation criteria, which eliminates an amount of possibilities. Namely, the allowable probability of failure and the least cost. A certain target life time is predetermined and corresponds to a target probability of failure. If an option does not meet these demands, it is considered futile.

3.1.9. INPUT VARIABLES AND PARAMETER DEPENDENCIES

In this section, the various input parameters, which are extracted from the previously determined equations, are examined and categorised. Each parameter has a different effect on the system and results. Some are stochastic variables and other deterministic. These parameters are meant to function as the input freedom of the proposed model. This is visualised in Figure 3.4.

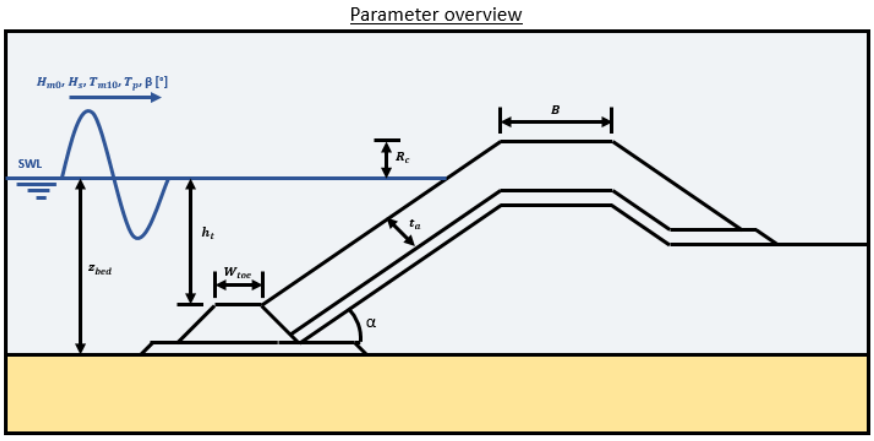

Figure 3.4: An overview of the input parameters

Furthermore, some of these parameters are freely alterable by the user of the model and some of these parameters are set as default values. Below, it is explained which of the variables are free to alter and which are default. Moreover, some of the freely alterable parameters are only alterable to a certain degree. For instance, the mean values and standard deviations are freely alterable, but the distribution is set as a default.

HYDRAULIC BOUNDARY CONDITIONS

The hydraulic boundary conditions are the environmental representative variables such as wave heights, wave periods and water levels. An overview of the variables which are considered are shown in Table 3.2.

Variable	Symbol	Unit	Distribution	Mean (μ)	Std.dv.(σ)
Spectral wave height	H_{m0}	[m]	variable	variable	variable
Significant wave height	H_s	[m]	variable	variable CWD	variable
Wave height exceeded by 2 per cent of the incident waves at toe	$H_{2\%}$	[m]	variable	variable $R_{2\%} \cdot H_s$ CWD	variable
Peak wave period	T_p	[s]	variable	variable	variable
Mean wave period	T_m	[s]	variable	variable	variable
Mean spectral wave period	$T_{m-1,0}$	[s]	variable	variable	variable
Mean zero-crossing period	T_{m02}	[s]	variable	variable	variable
Direction	β	[]	Lognormal	variable	variable
Water level	SWL	[m]	normal	variable	0.1
Bed level	z_{bed}	[m]	deterministic	variable	0.05

Table 3.2: Hydraulic boundary conditions

The significant wave height and the wave height exceeded by 2% of the incident waves at toe, can be determined by a composite Weibull translation function, a simple translation factor $R_{2\%}$ or they can be manually entered. Furthermore, the wave height mean values, standard deviations and distributions can be freely altered. Like the wave heights the periods input fields are all fully alterable. The wave direction is given a default lognormal distribution. The water level and bed level both have a variable mean, a default value for the distribution and standard deviation. **NOTE**: Some of these variables are stochastically distributed. The variety of distributions which are included in the framework are specified in Section 3.1.4.

OPTIMISATION DESIGN VARIABLES

The optimisation design variables are principally the geometric variables. They determine the size and shape of the structure. An overview of the variables which are considered are shown in Section 3.1.9.

Variable	Symbol	Unit	Distribution	Mean (μ)	Std.dv.(σ)
Crest freeboard	R_c	[m]	normal	parametric	0.03
Crest width	B	[m]	normal	parametric	0.10
Slope angle	α	[-]	normal	parametric	0.15
Toe level	h_toe	[m]	normal	parametric	0.03
Nominal median rock diameter toe	$d_{n50,toe}$	[m]	normal	select	0.03
Nominal median rock diameter armour	$d_{n50,armour}$	[m]	normal	select	0.03

Table 3.3: Geometric variables

As shown in the table above, the mean values of the parameters are given a parametric input approach. This means that the user should specify a lower bound, upper bound and step size for the given parameters. The standard deviation and ditributions are default values. Further specfications regarding parametric distribution are discussed in Section 3.1.8.

The nominal median rock diameters are based on the standard classes of rock grading (CIRIA/CUR, 2007c). The standard deviation is estimated to be in the order of 5%, which gives a default standard deviation of 0.03. The selection of stone sizes can be manually altered since in some occasions not all stone sizes are available or on the other hand some may even be more desirable.

NON OPTIMISATION DESIGN VARIABLES

The amount of allowable overtopping is dependent on the limit state, the function of the structure and the designer's goal. Thus, it should be freely alterable as well as its mean and standard deviation. However, the input thereof is a delicate choice and should be reviewed by expert judgement.

The rock density is dependent on the rock grading selection. However, rock density usually lies in the order of $2650 kg/m^3$. This can differ between different sites, locations and projects. Also, within a site the rock density may not always be the same and the standard deviations should be altered accordingly, but a default value of $50 kg/m^3$ is proposed.

Variable	Symbol	Unit	Distribution	Mean (μ)	Std.dv.(σ)
Mean overtopping rate	q	$[m^3/s]$	normal	variable	variable
Rock density	ρ_s	$[kg/m^3]$	normal	variable	variable
Damage level armour	S	[-]	deterministic	automatic	-
Damage level toe	N_{od}	[-]	deterministic	automatic	-

Table 3.4: Restrictional variables

The distributions of all these values are set as default variables and given a normal distribution. However, it should be said that in case of an overtopping value of 1 l/s/m is given as a mean value and a rather large standard deviation, i.e. 0.5 l/s/m, a negative value can be drawn from the normal distribution function. This gives an error in the probabilistic approximation which follows. The damage levels for the toe and the armour are both implemented in the model and dependent on the limit state and the slope of the design. Therefore, these values are automatically determined and non-alterable. How these are defined is shown in Table 3.1.

RANDOM MODEL PARAMETERS

The random model parameters are all other parameters considered in the incorporated equations of the considered failure mechanisms. Some are deterministically fixed, such as the influence factors of seawall and berm. This is because these are not alterable, since the framework of this research does not consider a seawall or berm. An overview of the variables which are considered are shown in Section 3.1.9.

Variable	Symbol	Unit	Distribution	Mean (μ)	Std.dv.(σ)
Notional permeability coefficient	P	[-]	normal	variable	0.05
Storm duration	T_{storm}	[hrs]	normal	variable	variable
Roughness factor seaward slope	γ_f	[-]	normal	variable	0.03
Influence factor sea wall	γ_v	[-]	deterministic	1.0	-
Influence factor berm	γ_b	[-]	deterministic	1.0	-

Table 3.5: Random model parameters

The notional permeability is a variable with a default standard deviation and a variable mean value. Notably, this value is dependent on the type of core. The storm duration is case dependent and thus variable in the mean and standard deviation. The roughness factor of the seaward slope is dependent on the type of slope material and thus given a variable mean and a default standard deviation. The other two influence factors are both deterministic and default, since both a seawall and a berm are not within the scope of this research.

FIXED OR NON-OPTIMISATION VARIABLES

The fixed variables are water density ρ_w and the gravitational velocity g. These are both deterministically distributed with values of $1025[kg/m^3]$ and $9.81[m/s^2]$ respectively. Even though the water density can be different for different locations, for simplicity reasons in this research a fixed value is used.

PROBABILISTIC INPUT

The probabilistic input includes the variables and information needed for the calculation of the probability of failure of the structure. This includes the probability method, the target life time, number of storms, return period, target probability of failure and limit state.

To start with, only the FORM II and Crude Monte Carlo calculations are included. Either can be chosen and the model should run accordingly. The target life time is the service life time in years. This is the desired number of years the structure should hold. The target probability of failure is calculated accordingly. The limit state is defined for four possible situations: Initial damage, Serviceability limit state, Repairable limit state and the Ultimate failure limit state.

COSTS AND UNIT RATES INPUT

In these input fields, the user is required to assign a value to the unit rates of the following elements, as function of euro/m^3/m:

- Armour layer
- Under layer
- Toe layer
- Core
- Geotextile [$euro/m^2/m$]

Furthermore, it is required to specify the type of core; A quarry rock, sand fill or an in-situ sand core.
A few other parameters have been given a default offset value, but are variable, being the following:

- The mobilisation costs factor, $K = 0.3$
- The high cost of repair factor, $R = 3$
- The real rate of interest, rr

3.1.10. UNCERTAINTY IMPLEMENTATION

Section 2.2.2 discussed the theory behind different types of uncertainty. However, the implementation and the approach on this phenomenon in this model is yet to be explained.

INHERENT UNCERTAINTY

The uncertainty type can be best approached and quantified by the application of probability distributions. Examples of these distributions are given in Section 3.1.4. These models can describe the probability of occurrence of a particular parameter to some degree.

MODEL UNCERTAINTY

As explained in Section 2.2.2, this uncertainty can be scaled under the limit state function uncertainty and the uncertainty of the distribution of input parameters.

The first model uncertainty relates to the uncertainty in the representation of the limit state function in relation to actual physical processes. Some of these limit state functions have compared their model to measured data. Some of these models have even included the uncertainty of fits to the scattered data, by defining a standard deviation to the empirical fitting coefficients. In Table 3.6, this is shown for the limit state functions used in this model.

Empirical fitting coefficient	Distribution	Mean value	Std. Dev. Value
Overtopping			
A_{ov}	Normal	0.023	0.003
B_{ov}	Normal	2.7	0.20
C_{ov}	Normal	0.09	0.0135
D_{ov}	Normal	1.5	0.15
E_{ov}	Normal	-0.79	0.29
Armour layer stability			
$c_{s,s}$	Normal	1.3	0.15
$c_{pl,s}$	Normal	8.4	0.7
$c_{s,d}$	Normal	1.0	0.08
$c_{pl,d}$	Normal	6.2	0.4
Toe stability			
γ_{toe}	Normal	1.0	0.04

Table 3.6: Model uncertainty parameters

The values for the overtopping equations have been derived from the Overtopping Manual 2018 (van der Meer et al., 2018). The variables for the armour layer stability uncertainty are specific for the Van der Meer formula (1988) (CIRIA/CUR, 2007b). The reliability of the toe stability limit state function is extracted from the Van der Meer (1998) formula for toe stability. The uncertainty of this model is 16%(Muttray, 2013). Since it is unknown to which empirical fitting factor this uncertainty should be applied, an extra parameter is introduced and applied on the stability number of the toe stability limit state function.

STATISTICAL UNCERTAINTY

This uncertainty applies to the prediction of the wave climate and the lack and uncertainty of measurements. In this model only the wave-height prediction uncertainty is incorporated. This can be due to measurements, visual observations, etc. (Burcharth et al., 2018) describes this as X_{Hs} and (Verhagen and Van den Bos, 2018) describe this as $gamma_m$. For which the mean values are 1.0 and the standard deviations $\sigma_{X_{Hs}} = 0.1$ and $\sigma_{\gamma_m} = 0.05 - 0.15$, respectively. Both approximations lie around 0.1. This standard deviation is used in the model.

MODEL CORRESPONDENCE UNCERTAINTY

This type of uncertainty is basically an extra uncertainty on the limit state model. Thus, a parameter is added to the load component in the limit state function. This has been defined separately for each failure mechanism. The mean values of these parameters remain 1.0. However, the standard deviations include different effects, such as scaling, natural variability, climate change, ageing of structure, material properties, etc. (Schüttrumpf et al., 2008). In Table 3.7 an overview is given of the default values of this uncertainty.

Empirical fitting coefficient	Unit	Distribution	Mean value	Std. Dev. Value
Overtopping	$\gamma_{overtop}$	Lognormal	1	0.05 - 0.15
Armour layer stability	γ_{armour}	Lognormal	1	0.05 - 0.15
Toe stability	$\gamma_{toestab}$	Lognormal	1	0.05 - 0.15

Table 3.7: Model correspondence uncertainty parameters

To give an example of a complete limit state function with all the uncertainties combined considering eq. (3.1), the following limit state function(eq. (C.2)) is rewritten in eq. (3.23) is fully written out.

$$Z_{overtopping,mcu} = q_{adm} - \left(\sqrt{g \cdot \left(X_{H_s} H_{m0}\right)^3} \cdot \frac{A_{ov}}{\sqrt{\tan\alpha}} \gamma_b \cdot \xi_{m-1,0} \cdot \exp\left[-\left(B_{ov} \frac{R_c}{\xi_{m-1,0} \cdot \left(X_{H_s} H_{m0}\right) \cdot \gamma_b \cdot \gamma_f \cdot \gamma_\beta \cdot \gamma_v} \right)^{1.3} \right] \right) \cdot \gamma_{overtop} \tag{3.23}$$

3.2. OPTIMISATION

A full parametric approach displays all of the possible solutions as a result of the initial input. This is a time consuming procedure and the initial inputs only capture a predetermined range of options. In order to reduce the computation time and to increase the possibility of more economical options an optimisation scheme can be introduced. This can either be done manually by altering the input variables and narrowing them down as far as possible or it can be done computationally by an optimisation algorithm with predetermined optimisation criteria. This section proposes such an algorithm.

OPTIMISATION CRITERIA

Before initialising an optimisation, the criteria to which a solution is optimised must be determined. Below two criteria are selected and discussed which are considered within this optimisation proposal.

Minimisation of computation time

The computation time is one of the most important criteria for the use of such a model. In Section 6.4, the computation time of a single option for different settings is discussed. For a large number of options this can amount to hours of computation time. Hence, the computation time is dependent on the number of options and the probabilistic calculation settings. Thus, to optimise a set of settings need to be chosen as well as more selected amount of options, consequently diminishing the amount of options.

Minimisation of costs

The minimisation of the total cost of each solution is regarded as one of the key influencing components in choice of design and therefore worth minimising. In the previous chapter, the sensitivities and influence of different parameters to the total cost is investigated. This information can be used to determine which parameters are worth altering within an optimisation algorithm.

OPTIMISATION FRAMEWORK

Local vs. Global optimisation

In mathematical optimisation techniques, many different algorithms have been developed to reach a certain desired outcome. This outcome is mainly a problem of maximising or minimising a certain function by continuously altering the inputs until the outcome of such a function has reached the desired value. Generally, an optimisation technique attempts to find the best possible value of an objective in the predetermined domain.

The minimisation or maximisation of an objective function. This can either be done by determining the local minimum (or maximum) or the global minimum (or maximum), depending on the objective. The local minimum is defined as such, that within a predetermined region around a value of the objective function all of the other values are either greater or equally to the value of that specific element. Thus, the local minimum is either at least as good as or better than its nearby elements whereas the global minimum is at least as good as or better than every element in the entire domain. To illustrate the difference, see Figure 3.5.

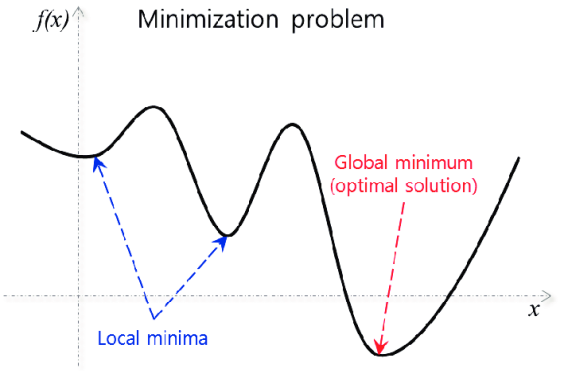

Figure 3.5: Local vs Global optimisation (Jeon et al., 2017)

A global optimisation function generally returns a single best value within the domain. However, as shown in the figure below, the local minimisation can return multiple values. As stated before, the objective of a

parametric design tool is not to return a single optimal design. It is to show multiple possible solutions for the given input. Thus, the principle of local optimisation is a more suitable approach for this research. In this way, other outcomes, apart from the best value, are not neglected.

A local optimisation technique is usually performed on an objective function, designed to find the "best" values based variable inputs. However, the model in this research already finds multiple solutions, not based on solely a single function. Therefore, a different approach is followed from usual optimisation algorithms, such as an iterative or a random search algorithm. The approach defines the local minima within the range of the deterministic output, i.e. all of the possible deterministically determined options. This is the domain for the optimisation technique. The local minima are based on the lowest cost within the proximity of each value. The order of this proximity is defined by the smallest amounts of steps per parametric variable, i. Subsequently, this is divided as the algorithm looks to both sides of a value n, thus $n-order, n, n+order$. The order is defined as follows:

$$order_i = \frac{UpperBound_i - LowerBound_i}{StepSize_i} \cdot 0.5 \tag{3.24}$$

As a result, only the minimum cost solutions for similar solutions remain. Thus, the amount of options is diminished and selected based on minimum costs. Even though the local optima are determined on minimum costs, this approach mainly benefits the minimisation in computation time. In the next step, this output is used as in input for the probabilistic method. The whole process is summarised in Figure 3.6.

Figure 3.6: Optimisation scheme

Ultimately, a minimised output is extracted from the optimisation scheme. The idea behind this scheme is that, the minimisation the deterministic output eventually results in less computation time in the probabilistic calculations.

3.3. MODEL SETUP

A general view of the structure of the model is shown in Figure 3.7.

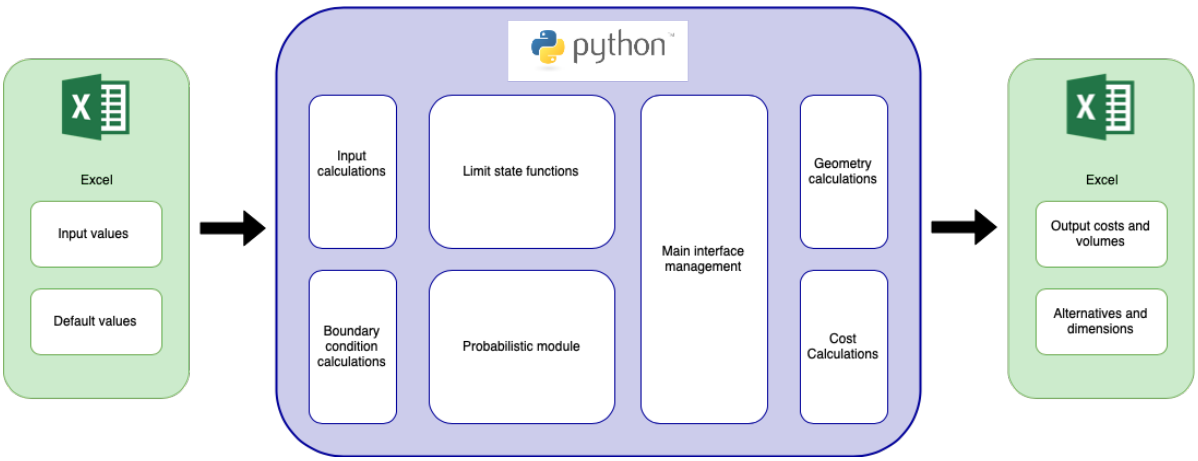

Figure 3.7: An overview general layout of model

Initially, the engineer enters the input variables in an Excel file. The file is a simple General User Interface (GUI). Furthermore, in this GUI also default values are presented, for clarity considerations. Subsequently, the file is imported and read by the Python script. The Python script then calculates the limit state functions, the boundary conditions and translates the inputs. Depending on the inputs, a probabilistic calculation is performed either with Monte Carlo or with FORM. In order to generate alternatives, a different section of the script is dedicated to the parametric analysis and partial optimisations, which are explained in the main interface management. Ultimately, the Python script calculates the volumes and geometries of the different alternatives and carries on with the costs per alternative.

Like the GUI, also the output of the alternatives is stored in Excel, for a clear and accessable overview. All dimensions, costs, materials and variables are shown as well.

The model code is fully written in PyCharm, which is an integrated development environment (IDE) and which uses programming language Python. The Python directories are marked as a source root directories. These roots contain the actual source files and resources. PyCharm uses the source roots as the starting point for resolving imports.

4

CASE & VALIDATION

4.1. AREA OF STUDY: PROJECT RUFISQUE

The case is from a project in Rufisque, Senegal (see Figure 4.1), executed by Royal HaskoningDHV. The project addresses the breakwater reference design for the ferry berth. The proposed design is a basic design with the purpose of showing the main dimensions of the breakwater(s), upon which the tenders can base their bid. The breakwater reference design includes two alternative breakwater options. They are both rubble mound breakwaters. One has a rock core and the other one a sand core in the form of geo-containers.

Figure 4.1: Location of Rufisque ferry berth (source: Google Earth)

The main function of the breakwaters is to provide a sufficiently sheltered area for vessels at the ferry berth. The breakwater does not connect berths or other facilities to the shore and does not need to be accessible for pedestrians or cars. The breakwater layout as well as the approximated breakwater locations as proposed are shown in appendix D. The southern and northern breakwater length is approximately 340 m and 170 m respectively. The following is noted on this layout:

- The southern breakwater 'uses' the rocky outcrops 1 and 2 and is assumed to connect to the shore (land tip) from rocky outcrop 1 in a straight line (dashed line).
- In view of the predominant wave direction from SW (to NW), it is questionable whether the northern (lee) breakwater will be very effective in sheltering the ferry berth area.

4.1.1. DATA DESCRIPTION

BATHYMETRY / TOPOGRAPHY

The overall bathymetry (depth soundings) near Rufisque is shown in appendix D It also shows some lines (PL1 to PL8) along which depth profiles have been established.

Southern breakwater
A zoomed-in overview along the southern breakwater is shown in appendix D, corresponding to line PL6.

Northern breakwater
An overview along the northern breakwater is shown in appendix D. The depths along line PL1 are taken as basis, although the breakwater is located at a distance of about 85m from this line.

WATER LEVELS

The following water levels are taken from the project info (with ZH = 'Zéro hydrographique':

- High water level: +1.80mZH
- Mean sea level: +1.0mZH
- Low water level: +0.20mZH

Unfortunately, it is not known what the high and low water level consist of; whether it includes tidal levels, seasonal (pressure) variations, storm surges, sea level rise, etc.

WIND AND WAVE CONDITIONS

The offshore wind and wave conditions have been acquired from the National Oceanic and Atmospheric Administration (NOAA) organisation. The considered data point as shown in Figure D.1. The data had been collected from 02 February 2005 until 31 December 2014, with a time series of three hourly 2D wave spectra. The distance from offshore data point to the nearshore output point is approximately 500 meters and the depth is at approximately 250 meters. Per spectrum and time series, the wave energy can be computed as a function of the frequency and direction. The number of peaks and the amount of energy on a corresponding frequency band determine the number of wave climates. Within such a spectrum, these climates can be situated on different frequency and directional bandwidths. In this case, a preliminary study is done by COSEC (Conseil Sénégalais des Chargeurs) and Royal HaskoningDHV, on the characterisation of the wave and wind climate around Rufisque and Senegal. Wind waves of local origin can appear when the winds are strong. They could be significant during the period of the trade winds from the North-East, that is to say from November to February. But overall, they are waves of low height and short period. This study only considers the long swells. With the wind waves not being considered critical to the solution, they have concluded that wave climate at the coast of Senegal, including the coast at Rufisque, is swell dominated. In order to acquire more insight into these conclusions, Figure 4.2a is computed. In this figure, the data points of the wave periods are plotted against the data points of the wave height.

As shown in this particular wave study two different wave climates are present. As described above, the swell waves and wind waves are separated by the steepness line of approximately 0.0125. It is noticeable that in this case the wind waves have a small wave height and a small wave period. They are therefore negligible for this case. The wave climate is dominated by two main directions. North-West swells and South-West swells. This can be seen in Figures 4.3 and 4.4.

Figure 4.2b shows the amount of observations from the complete data set corresponding to the wave direction. This provides more information regarding the wave climates in each direction, to determine the (mode) dominant wave direction, for a further extreme value analysis. To conclude, two dominant directions determine the wave climate at Rufisque, North-Western and South-Western waves.

North-Western swells
All year round, there are swells from the North Atlantic. These waves are predominant and according to previous studies would have the following characteristics:

- Wavelength in deep water of about 300 m.

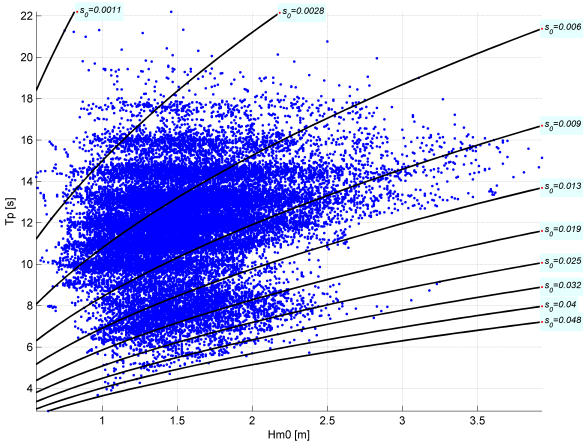

(a) Wave height H_s versus Wave period T_p graph with steepness s lines

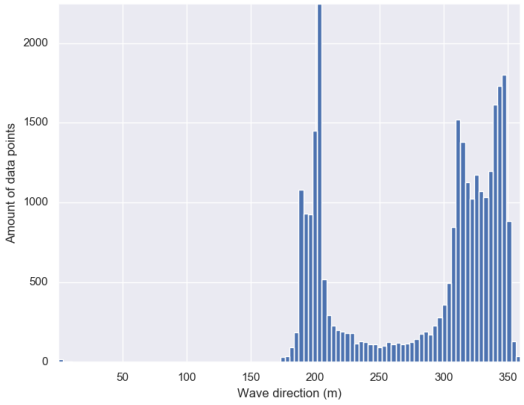

(b) This figure shows the histograms of wave direction.

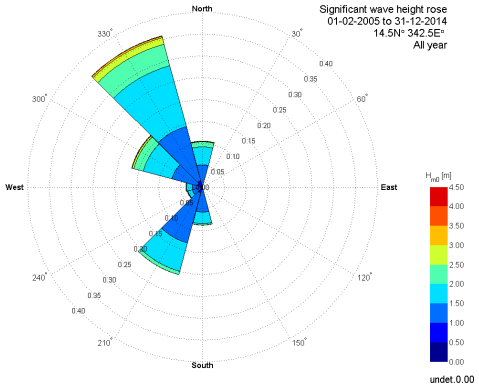

Figure 4.3: Rose of the wave height H_s all year round

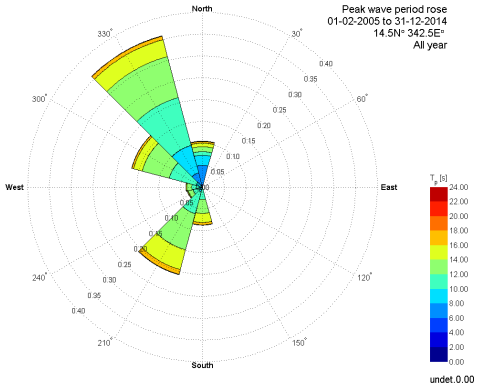

Figure 4.4: Rose of the wave period H_s all year round

- Average wave height of 1 m.
- Average period of 14 s (range 12 - 15 s).
- Maximum wave height of 4 m.

On the North coast of Senegal, these swells arrive strongly. They weaken on the South coast, following a series of diffractions around different points of the peninsula of Cape Verde (Almadies, tip of Fann, Cap Manuel). These diffractions cause a series of change in propagation direction: the swells that cross the Bay of Gorée have a North-South direction.

South-Western swells

Swells from the South Atlantic only occur from July to October. These swells revolve around the peninsula of Cape Verde to take a direction from South to South-West. Their amplitude is not greater than that of West-North-West swells, but they are less damped east of the Cape Verde peninsula. These Northwest and Southwestern swells are the only ones whose height is considered sufficient to exert a significant action on the coast. However, there are also exceptional and very energetic West swells, generally between October and November, which would be generated by cyclones in the Caribbean Sea. The majority of swells that reach the coast of Rufisque have a direction between 175 ° North and 275 ° North. This is cause by two factors: Firstly, the site is naturally protected against swells from North-East and North-West. Secondly the concentration effect is caused by refraction in the direction on all offshore swells. The two larger peaks around 200 and 300 degrees are waves coming from South-West and North-West respectively.

4.2. EXTREME VALUE ANALYSIS

Conducting an Extreme Value Analysis (EVA) can be done by obtaining extreme values through sampling and fitting a marginal distribution to these samples. Two methods are commonly used to obtain these samples; Peak over Threshold and Block maxima method. An explanation regarding the EVA methods and fitting criteria are explained in Section 2.3. **Note**: the EVA results which are henceforth discussed and documented are acquired from Royal HaskoningDHV.

As discussed and shown in Section 4.1, the waves arrive at the coast of Rufisque between the directions 175 ° North and 275 ° North. The wave climate is swell dominated. Even though fewer data points are observed between 200 ° North and 250 ° North, it does not necessarily mean that this segment is negligible with regard to extreme values. Therefore, the range of incoming wave directions should be considered in the EVA. An EVA cannot be conducted on the entire time series as a whole, considering directional and seasonal influences. Thus, an EVA is made in directional segments of 22.5 °, within the range of 168 ° to 303.8 °. Thus, six segments are presented. Within each segment 3 combinations of spectral wave height (H_{m0}) and peak wave period (T_p) have been selected. Each combination is a 1 in 1100 year condition for the sector under consideration. The selected conditions represent the following conditions:

- Highest waves (with lower periods).
- Longest waves, thus highest wave periods (with lower wave heights).
- Largest wave steepness, i.e. wave height divided by wave length.

The considered variables are not independent and should not be regarded as such in the EVA. In a bivariate extreme value analysis, the dependence between the variables is secured. This is done by joint observations; the two variables are simultaneously considered. Moreover, only one of the variables can be regarded as extreme. The other variable should be the value in correspondence with the significant other maximum. Thus, only one of the variables can represent the results of a certain return period. Therefore, it is important to determine which value is chosen to represent the results of a certain return period. This is the extreme variable. This is project and situation dependent. In this case, slope protection structures are considered. Thus a larger wave height is of more significance and is considered to be more influential to the structures design than the wave period.

The altered data set does not represent the full time series any longer, since the data have been split in directional sectors. Considering this, the block maxima approach or annual/monthly maxima approach is not applicable any longer. Therefore, the POT approach would make a more reliable option. Furthermore, a difference in reaction and correspondence to environmental change is found in different variables. For instance, wind reacts much more instantly to cyclones than waves. Consequently, delays in the time series can be expected between different variables. In order to avoid such complications, a POT approach would be the better option than a block maxima approach.

4.2.1. SAMPLING EXTREME EVENTS

As previously discussed, only the wave height is regarded as an extreme variable within this multivariate system. In order to successfully conduct the EVA, firstly sampling is done to create the extreme data set. A POT analysis is made on the wave height. Lastly, the threshold value(s) is(are) determined per theorem discussed in Section 2.3. The POT has been performed in such a way that a sample of 10 (extreme) storms per year on average is obtained. In order to achieve this average, the duration of an event or storm has been set to 2 days. For the significant wave height of swell waves, the choice of threshold is 1.41 meters, which together with the 'physical' threshold, leads to a sample of 99 extreme observations.

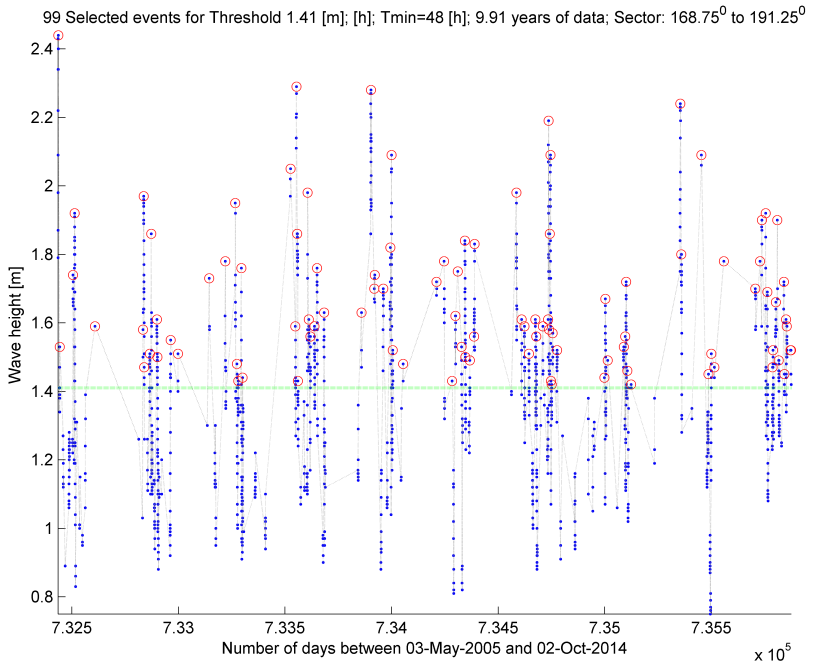

Figure 4.5: POT analysis for significant wave height Extreme observations sample. The red points comprise the extreme observations sample.

4.2.2. FITTING TO MARGINAL DISTRIBUTION

A marginal distribution to each variable on the extreme data set is fitted. Different fitting methods are used for each extreme data set. These methods are used to determine the shape factors of the distribution corresponding to the extreme data set. In Table D.1, the methods corresponding to each data set are shown. The following methods are used to fit the a marginal distribution to the wave height per directional data set.

- Maximum likelihood method (ML)
- Method of Moments (MOM)
- Maximum product of spacing estimation (MPS)

A more thorough explanation of these methods and the results is given in Appendix D.2.1. Subsequently, the goodness of fit is tested for each of the marginal distributions which are determined with one of the methods above. The goodness of fit is determined with the following error measurements:

- Residual Quantile plot (RSQ)
- Root mean square Error (RMSE)

4.2.3. EXTRAPOLATION OF DATA TO LARGER RETURN PERIODS:

The wave height is best fitted and represented by either a Weibull or a Generalized Pareto distribution function. The distributions are extrapolated to larger return periods for the variable wave height. The return periods are extrapolated to a maximum of a 1000 years. For an example of see Figure 4.6.

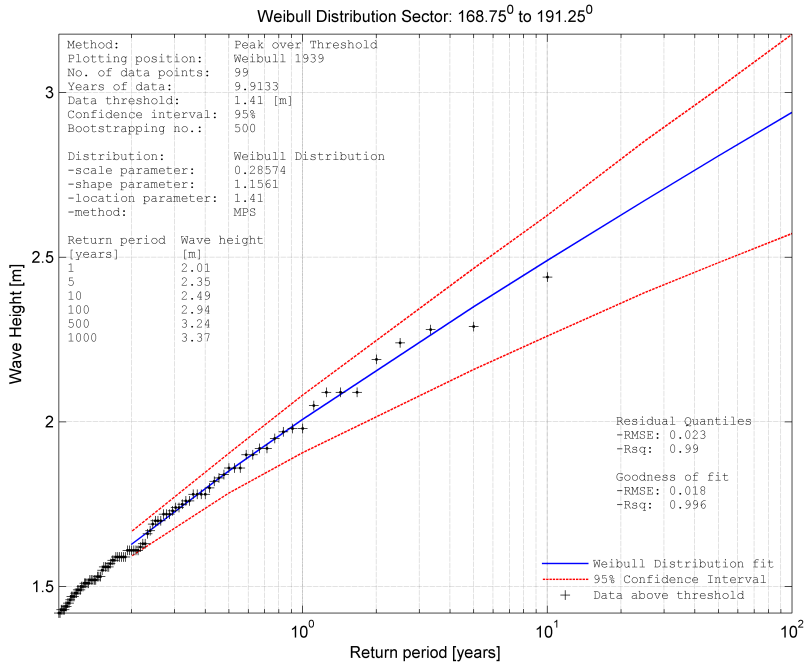

Figure 4.6: Weibull representing the best fit for the extreme significant wave height.

4.2.4. RESULTS

In Table 4.1, the POT results of the extreme values analysis of the wave height are shown. In Figure D.7 and table 4.2, the corresponding wave periods to the extreme wave heights are shown. The table below shows multiple conducted analyses.

Data set H_{m0}	Threshold value	Number of peaks	Distribution	Parameter estimates
Dir.1 [168.8 - 191.3]	1.41	99	Weibull	scale = 0.28574 shape = 1.1561 loc = 1.41
Dir.1 [191.3 - 213.8]	1.793 (m)	89	Weibull	scale = 0.26074 shape = 1.2053 loc = 1.41
Dir.1 213.8 - 236.3]	1.692 (m)	71	Weibull	scale = 0.2138 shape = 1.0905 loc = 1.692
Dir.1 [236.3 - 258.8]	1.645 (m)	70	Weibull	scale = 0.2414 shape = 1.2336 loc = 1.645
Dir.1 [258.8 - 281.3]	1.517 (m)	92	Weibull	scale = 0.33739 shape = 1.3401 loc = 1.517
Dir.1 [281.3 - 303.8]	1.699	106	GPD	scale = 0.18745 shape = 0.31316 loc = 1.699

Table 4.1: Results POT analysis

Directional data set	Combination 1		Combination 2		Combination 3	
	$H_{m0}[m]$	$T_p[s]$	$H_{m0}[m]$	$T_p[s]$	$H_{m0}[m]$	$T_p[s]$
Dir.1 [168.8 - 191.3]	1.77	21.43	2.78	20.59	2.94	14.39
Dir.1 [191.3 - 213.8]	0.96	24.13	2.79	21.34	3.08	7.95
Dir.1 [213.8 - 236.3]	1.94	17.90	2.49	17.36	2.90	7.93
Dir.1 [236.3 - 258.8]	2.40	17.45	2.58	16.22	2.76	8.97
Dir.1 [258.8 - 281.3]	2.00	18.31	2.76	17.10	2.95	9.43
Dir.1 [281.3 - 303.8]	1.91	16.71	2.31	14.47	2.86	8.48

Table 4.2: Offshore 1/100 yr wave conditions

4.3. VALIDATION

4.3.1. FAILURE MECHANISM CALCULATION VALIDATION

The failure mechanism or limit state calculations are validated with Mathcad sheets. Mathcad is software developed to aid in mathematical calculations. It is comparable with Maple. These sheets are constructed and checked by senior engineers from Royal HaskoningDHV. The sources of the equations and calculations differ per failure mechanism but mainly originate from the Rock manual and recent studies.

Three different failure mechanisms are tested on three different Mathcad sheets. In order to test the error and the range of acceptance a test script is written in Python. The script imports the failure mechanism function written in Python and opens the Mathcad sheet. The Mathcad sheet and the corresponding failure mechanism function ought to have the same input parameters. The test file then generates a thousand random values between a given upper and lower bound, per input parameter. It then calculates the outcomes of the Mathcad sheet and failure mechanisms function for all thousand options.

$$error = max\left(\frac{Output_{Python}}{Output_{Mathcad}} - 1.0 \cdot 100\%\right) \tag{4.1}$$

The error is defined by division of the Python answers by the Mathcad answers, as shown in eq. (4.1). The output is the maximum error percentage of all options. In table 4.3, an overview is given with the error percentages for each failure mechanism or calculation script.

Failure mechanism / Equation	Error estimator per 1000 samples [%]
Overtopping	5.12e-13
Armour layer stability (shallow water)	0.0
Armour layer stability (deep water)	0.0
Toe armour stability	2.22e-14
Composite Weibull	7.78e-4

Table 4.3: Failure mechanism, error estimates in comparison to the Royal HaskoningDHV Mathcad sheets

The test files are written to detect writing errors in the self-made Python functions. Furthermore, they serve to maintain the accuracy of the calculations. For instance, a built-in estimator or optimisation tool, can give different results than the Mathcad sheet. This can also be seen in the results in table 4.3. The error in the composite Weibull distribution function is much larger than in the other functions. This is due to the SciPy optimisation code, which follows a different way of optimising than the built-in function of Mathcad.

Moreover, the difference in error magnitude between the failure mechanisms, originates in the estimation of the exponential function. NumPy calculates the exponent in an equation differently than the Mathcad sheets. However, this difference in negligibly small. Ultimately, it can be concluded that compared to the Mathcad sheets, the error in the Python outputs is negligibly small. This concludes that the equations in Python have been successfully written and defined.

4.3.2. PROBABILISTIC CALCULATION VALIDATION

The next step in validating the model is validating the built-in probabilistic calculation functions. TNO has developed a probabilistic calculation toolbox called Prob2b. This software has been validated. Therefore, the implemented code can be tested on the outcome of the Prob2B toolbox, given the same input.

The code which is used to calculate the probabilities of failure in the model, is extracted from Github and is open source. This model is recommended by Deltares Open earth. It is called PyRe (Python Reliability). It is a Python model for structural reliability analysis.

To minimise the risk of writing errors in both Prob2B and the model, another Python library is used as a second check. This is also open source code attainable on Github. The library is called FORM and it only calculates FORM calculations, not Monte Carlo calculations.

The FORM implementation and CMC implementation are validated separately using different approaches and comparisons. To validate the FORM model, a comparison in the output values is made between the three test elements. This is conducted for all failure mechanisms. An error estimate indicates the level of correspondence of the model to other outputs. Since the third test element is only applicable to FORM, another approach is adopted for the CMC evaluation. Moreover, Prob2B supports Monte Carlo calculations, providing a suitable comparison to the model outputs. The coefficient of variation is taken as a validation range.

FORM

Firstly, the outputs of the three comparative systems are compared. The comparison is done by calculating the percent error, shown in eq. (4.2). The inputs differ from each failure mechanism to another and are strictly fictional. This procedure is repeated for every failure mechanism.

$$\delta = 100\% \cdot \eta = 100\% \cdot \frac{\epsilon}{|V_{model}|} = 100\% \cdot \left| 1 - \frac{V_{model}}{V_{module}} \right| \tag{4.2}$$

Where η represents the relative error and ϵ the absolute error. For reasons of conciseness, only the values for the overtopping calculations are shown in Table 4.4. The values for armour and toe stability are shown in Appendix D.

Overtopping	β	Probability of failure	Percentage error
Output Prob2B	0.3766	0.3532	0.0566%
Output Secondary FORM model	0.3782	0.3526	0.2269%
Output Model	0.3761	0.3534	-

Table 4.4: FORM calculation output comparison table - Overtopping

Looking at the probabilities of failure in table 4.4, it can be seen that the FORM calculations for overtopping is accurate to two decimal places for the FORM model and 3 decimal places for Prob2B. In comparison with the form model the error is much larger. The decimal places accuracy is also smaller. This could be the influence different fundamental packages for scientific computing in Python. In particular, the approximation of the exponential functions. This is investigated more thoroughly in chapter 6. The probabilities of failure in table D.5 show that the FORM calculations for this failure mechanism are accurate to 5 decimal places for the FORM model and 3 decimal places for Prob2B. These errors are smaller in comparison with the errors found in the overtopping estimations, especially the FORM approximation model. This could be due to a less complicated limit state equation, as it does not contain any exponential functions. The probabilities of failure in table D.6 show that the FORM calculations for this failure mechanism are for both comparisons accurate to five decimal places. These errors fall in approximately the same range as the errors from the armour layer stability. This could be explained by a comparable level of complexity of the limit state equations.

MONTE CARLO

Monte Carlo calculations use a random sampling approach which gives a different probability of failure each run, depending on the sample size and on the target coefficient of variation (COV). Subsequently, if the probability of failure for the Prob2B output falls within this range, it can be said that the model gives a considerable validated output. The model CMC simulations are conducted by using a sample size of 10000 and a target coefficient of varition (COV) of 0.01. These setting are also used in Prob2B, to account for more accuracy in the comparisons. Again, for conciseness reasons, only the values for the overtopping calculations are shown, in Table 4.5. The values for armour and toe stability are shown in Appendix D.

Overtopping	β	Pf (10000 samples)	Coefficient of variation
Output Prob2B	0.450200	0.32630	-
Output model	0.417654	0.33381	0.01399

Table 4.5: CMC calculation output comparison table - Overtopping

If the coefficient of variation is taken as a range of validity on the probability of failure of the model output, it can be seen that the probability of failure of the Prob2B falls within this range. Thus, with a certain degree of safety it can be said that that the outputs are similar. The outputs of the armour layer stability MC analysis also fall within the range of validity. Like the previous comparisons, this combination of COV and Pf's is similar. However, the target COV is set at 0.01 and the COV's for overtopping, armour stability and toe stability are approx. 0.014, 0.012, 0.048 respectively. For both the overtopping and for the armour stability, the COV's fall within an acceptable range, but the output for the toe is almost 5 times larger. This means that there might be an error in the outputs. This can be investigated by increasing the sample size to generate towards a more accurate COV.

Overall, the outputs generated by the FORM approach contain very small errors « 0.01 %. It can be assumed that the FORM approach functions accordingly and can be safely used. The CMC also behaves accordingly with a minor difference in the COV. For the toe stability this is a little larger. Nevertheless, the probabilities of failure fall within the same range. The only difficulties these minor changes can generate is when the probabilities of failure are extrapolated to a probability of failure over a larger time period. What seem minor changes can become larger differences. This is investigated more thoroughly in chapter 6. Furthermore, the concept of the test scripts can be used for different failure mechanisms and design formulae.

4.3.3. MODEL VALIDATION

In Section 4.1, a case study is introduced. The primary contribution of this case study to this research is the validation procedure. Thus far, the failure mechanism, limit states and probabilistic models have been validated. However, the integration and synergy of the model is not yet been tested and validated.

A means to test the model synergy and the output is to compare its results with an actual preliminary breakwater or revetment design. In this case a breakwater case is used. Naturally, the inputs are equally the same, they are documented in Appendix D.4. In the model, some inputs are set which cannot be altered, such as the damage factors. Its effects on the solution should be analysed in the comparison. An important aspect of this part of the validation is that the model runs deterministically. In the same way the case study is calculated. With the model inputs probabilistic setting are all switched off. In Section 4.1, it is mentioned that the project includes two preliminary designs for two different breakwaters. A breakwater at the southern and northern side, with quarry rock and sand fill Geo-container cores respectively. Therefore, four different comparisons can be made, to get a better understanding of the validity of the model. However, only the southern breakwater validation is handled in this chapter, for reasons of conciseness. The northern breakwater information and validation is given in Appendix D.

The validation is simply a matter of inserting the input values of each breakwater design, document and compare the output with the obtained values from the case study. If they are in accordance the model is validated with only a single case. Preferably, multiple case studies are done; unfortunately only one is available.

After running the model with the same inputs, the outputs are compared. The results of the case study output are found in Appendix D.4. Similarly, the model output is found in Appendix D.4. Conclusively, the model generates the same configurations with the same input, as acquired with the case study. However, the limit state functions show that not all of the outcomes are the same. The output for the toe unit size is slightly larger for the case study than for the model output. This can be explained by the difference in use of empirical formula. The Royal HaskoningDHV case engineers have used the Van Gent and Van der Werf equation with the implementation of the Galland method. The model simply uses the van der Meer equation. Thus, this model might underestimate the toe stability. The overtopping output of the model shows an equal output for the first breakwater option but a different output for the second option. The armour output shows a similar output. It can be concluded that the model is validated for this specific case. However, the use of different inputs and equations cause the scheme to deviate in the exact output.

4.3.4. MODEL BEHAVIOUR OF INTEGRATED COST FUNCTION

The integration of the failure mechanisms and reliability methods is validated. A cost function is also a prominent subject of the model, which requires insight. Since the case study covers a whole breakwater and the model is based on a sole slope structure, the validation procedure is conducted differently. A set of hypotheses is formulated with respect to the influence of different variables on the costs of the rubble mound pro-

tection slope. Only considering the optimisation parameters; the slope angle, the armour layer units, the toe layer units, the crest height and width and the toe height. The hypotheses are stated as follows:

- If a decrease in unit size (i.e. for both toe and armour layer) is inflicted, whilst other parameters remain the same, the costs of the structure decreases.
- If a decrease in crest height is inflicted, whilst other parameters remain the same, the costs of the structure decreases.
- If a decrease in crest width is inflicted, whilst other parameters remain the same, the costs of the structure decreases.
- If a decrease in toe height is inflicted, whilst other parameters remain the same, the costs of the structure decreases.
- If a gentler slope angle is used, whilst other parameters remain the same, the costs of the structure increases.

Subsequently, these hypotheses have been tested on the model in Appendix D.5. In Figure D.11, the influence of each variable is shown as a function of the change in costs. To show the influence per variable, the other variables are kept constant as the variable in question is changed. Table D.19 shows the the upper bounds, lower bounds and step sizes for each variable.

In conclusion, from Appendix D.5 it can be said that there is enough evidence to support the hypotheses. Thus, the model does not show a large deviation in the implied change of the variables on the eventual costs. The difference in influence can be explained by the fact that the variables are all inflicted with the same step size. However, this is a percentile different step size and thus inflicts more change on the outcome than for other variables. For instance, a change of 10 cm in unit size is relatively larger than the same change on a crest width.

5

MODEL APPLICATION

5.1. CASE AND MODEL RESULTS

In this chapter, different methods of the model are compared with each other in terms of differences in output. The following methods are compared:

- Deterministic method without considering uncertainty.
- Deterministic method considering uncertainty.
- Probabilistic method - FORM analysis.
- Probabilistic method - CMC analysis.

These results are also compared to the case study output. Furthermore, the optimisation method output is analysed. The model output of each method is generated with the same input. These inputs can be found in appendix E.0.1.

NOTE: For reasons of conciseness, the discussion and graphical documentation of results for southern breakwater option 2 are disregarded.

5.1.1. CASE OUTPUT

In the previous chapter, chapter 4, the outputs of the case have been introduced. For the following comparison, only the Southern breakwater with quarry run core is used. An illustration of this configuration is shown in Figure 5.1. This configuration is based on the results of RHDHV. As mentioned before, the case study, uses a deterministic approach without considering any uncertainties. The results of the case study output are found in Appendix D.4. Similarly, the input of these results are found in Appendix D.4.
This structure is designed using the conventional deterministic approach. It is design to accept moderate damage to the structure. The actual probability of this event happening, with these dimensions, is not quantified. With the model we can quantify the probability that the structure is going to have moderate damage, henceforth referred to as the probability of failure.

Method	Damage	S_d	N_{od}	Pf_{toe}	Pf_{armour}	$Pf_{overtop}$	$Pf_{toe,TL}$	$Pf_{armour,TL}$	$Pf_{overtop,TL}$	Pf_{tot}
CMC	Moderate	3	1	0.06	0.504	0.076	0.844	1.0	0.907	1.0
FORM	Moderate	3	1	0.0573	0.475	0.0623	0.830	1.0	0.855	1.0

Table 5.1: Probabilities of failure of the case study design per failure mechanism

Table Table 5.1 shows that the total probabilities of failure over the design life of the structure is 1.0, for every case. This means that there is a 100% chance that the structure is going to have moderate damage over 30 years. What the table also shows is that the total probability of failure is determined by the armour layer probability of failure. The overtopping and toe stability have a slightly less chance of failing during the design

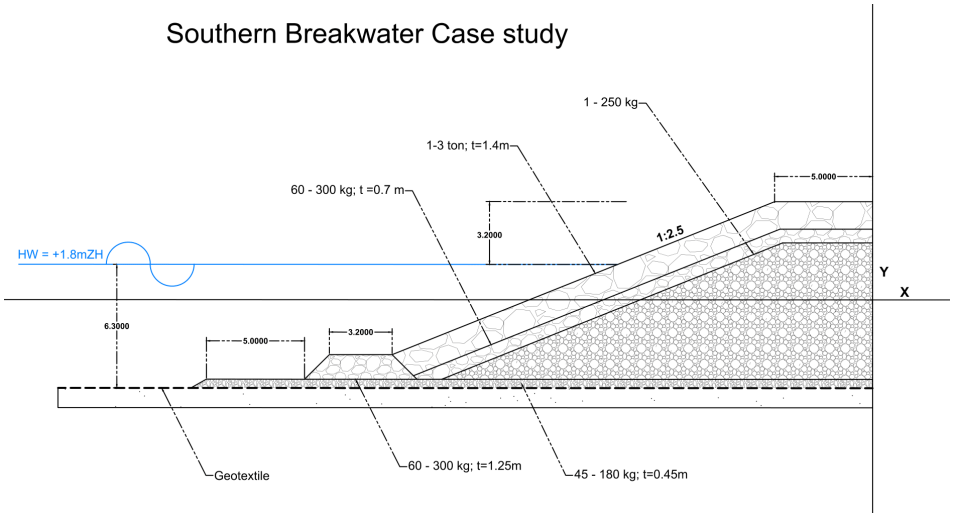

Figure 5.1: Configuration of case study Southern breakwater option 1 (Royal HaskoningDHV, 2018).

life. Nevertheless, all of the design probabilities of failure exceed the target probability of failure. In order to determine which configuration meet the reliability requirements, different configurations are made with the model. Furthermore, the model is compared to the deterministic output as well to see how well it performs in the deterministic design.

5.1.2. MODEL DETERMINISTIC OUTPUT

Firstly, the model output for the deterministic approaches is analysed. An analysis of the whole data set is done. After which the output of the both deterministic analyses are filtered based on the costs. Consequently, two different optimal configurations are obtained, see figs. 5.2 and 5.3. The cost optimal solutions are only analysed for a moderate damage factor. A more thorough comparison between different optimal configuration outputs is discussed in section 5.2.
The table below shows the number of configurations and the computation time of the model. It can be observed that the model generates a large number of configurations in only a small amount of time. If the time and time consumption is compared between the methods. It is concluded that the model generates about 110 options per second. This seems to be a linear relationship, since the ratio holds for all methods.

Method	Damage	Number of configurations	Time consumption
Deterministic	Moderate	43928	06 min 28s
Deterministic w/ uncertainty	Moderate	28968	03 min 17 s

Table 5.2: Model deterministic output Southern Breakwater option 1

Within the data set of the deterministic configurations without considering uncertainty the following is found:

- The first ten options have an overall overlapping slope geometery, appart from the toe dimensions,
- Within the first 100 options the cost difference is only approx. 200 euros.
- Within the first 10 options the cost difference is approx. 50 euros.
- The total cost difference between the cost optimal and worst cost option is 5875,03 euros.
- Within the first 500 options the slope angle remains 1:2.5.
- Within the first 1000 options the the armour stone remains 1000-3000[kg].
- Within the first 10 to 100 or 10 to 1000 options, many different combinations are possible between the toe structure, crest height and width.

Within the data sets of the deterministic configurations with considering uncertainty the following is found:

- The first ten options have an overall overlapping slope geometery, appart from the toe dimensions,
- Within the first 10 options the cost difference is approx. 50 euros.
- Within the first 100 options the cost difference is only approx. 250 euros.
- The total cost difference between the cost optimal and worst cost option is 3950,11 euros.
- Within the first 500 options the slope angle remains 1:1.5, after which different configurations are possible
- For all options the the armour stone remains 3 -6 [ton].
- Within the first 1 to 10, 10 to 100 or 10 to 1000 options, many different combinations are possible between the toe structure, crest height and width.

The configurations in the output of the deterministic analyses are filtered based on the costs. Notably, this is only for moderate damage, since the case study is compared to the optimal costs, and the case study is done for moderate damage. From this two different optimal configurations are obtained, shown in Figures 5.2 and 5.3.

Method	Option	cot_α [-]	$dn50_{armour}$ [m]	Sd [-]	Nod [-]	R_c [m]	w_{crest} [m]	h_{crest} [m]	z_{toe} [m]	$dn50_toe$ [m]	$C_{initial}$ $[euro/m^3/m]$
Deterministic	Moderate	2,5	0,92	3	1	3	3	4,8	-3,25	0,35	4705,75
Detrministic w/ uncertainty	Moderate	1,5	1,22	3	1	4,7	4	6,5	-3,5	0,35	5256,30
Case	Moderate	2,5	0.92	3	0.75	3.2	5	5	-3,25	0.41	5178,76

Table 5.3: Output of cost optimal solutions for the deterministic approaches

Table Table 5.3 shows dimensions and cost of the optimal configurations. For these methods only the construction costs, or the material costs are included. It is seen that the deterministic approach has a few similar dimensions. The deterministic approach with uncertainty is slightly more robust and expensive. Moreover, the case configurations is not observed in this output. This indicates that the considered level of safety, in this case the model strength, disregards the case output. A more thorough comparison between different optimal configuration outputs is discussed in section 5.2.

The cost optimal solution of the deterministic approach without uncertainty is visualised as shown in Figure 5.2.

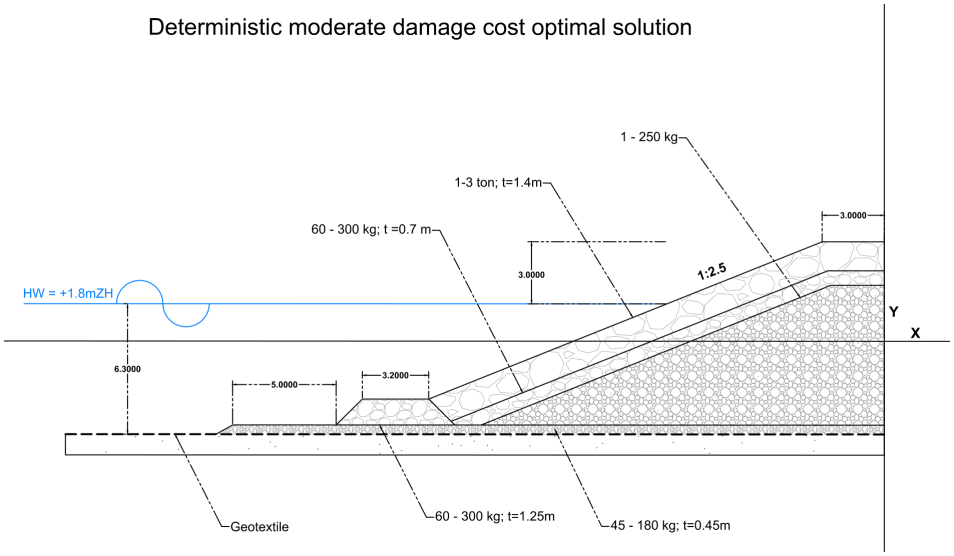

Figure 5.2: Deterministic cost optimal configuration

The cost optimal solution of the deterministic approach with uncertainty is visualised as shown in fig. 5.3.

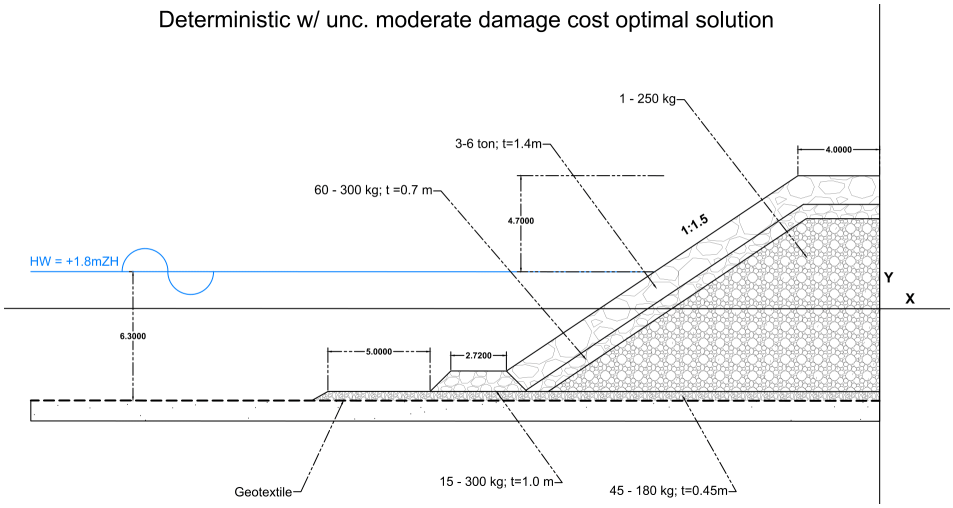

Figure 5.3: Deterministic w/ uncertainty cost optimal configuration

5.1.3. MODEL PROBABILISTIC OUTPUT

Initially the target probability of failure is determined. After which, the results of the output data set are analysed. Finally, the cost optimal solutions are computed.

EFFECT TARGET PROBABILITY OF FAILURE

The target probability of failure is dependent on the target life time and return period of the wave climate. The target life time is not provided by the case study and is assumed to be 30 years. This is shown below:

$$P f_{TL} = 1 - \frac{1}{e^{\frac{T_L}{R_p}}} = 1 - \frac{1}{e^{\frac{30}{100}}} = 0.26 \tag{5.1}$$

Unfortunately, the wave climate exerts a force too large to compare the configurations with such target probabilities of failure, since the probability of failure for the armour layer stability does not reach below 0.89 and the rock grading does not provide larger rocks. Therefore, if possible larger rock sizes, other materials or berm structures should be considered for this specific case study.

The armour layer stability does not allow the configurations to be analysed on the total probability of failure in comparison with the target probability of failure. Alternatively, an analysis is conducted with respect to the probabilities of failure of overtopping and toe stability.

The outputs have been generated with a target life time of 30 years, a return period of 100 years and for moderate damage. Initially, the number of configurations and time consumption is documented, for both the FORM and Crude Monte Carlo analysis, see table 5.4.

Method	Damage	Number of configurations	Time consumption
FORM	Moderate	106	08 min 42 s
CMC	Moderate	304	12 min 31 s

Table 5.4: Model probabilistic output Southern Breakwater 1

The data sets of the FORM analysis and CMC analysis are very similar. Within the data sets with configurations the following is found:

- The first ten options contain different configurations of both toe and crest structure.
- Within the first 10 options the cost difference is only approx. 200 euro.

- Within the all options the difference is approx. 2000 euros..
- The first half of the options the slope angle remains 1:2. After which it becomes 1:2.5
- For all options the armour stone remains 3 - 6 [ton].
- Within the first 1 to 10 or 10 to 100 options, many different combinations are possible between the toe structure, crest height and width.

This output is further visualised in Section 5.2.1.
Subsequently, the output of the probabilistic analyses are filtered based on the costs. Consequently, two different optimal configurations are obtained, shown in Figures 5.4 and 5.5.

Method	Option	cot_α [-]	$dn50_{armour}$ [m]	Sd [-]	Nod [-]	R_c [m]	w_{crest} [m]	h_{crest} [m]	z_{toe} [m]	$dn50_toe$ [m]	$C_{initial}$ $[euro/m^3/m]$	C_{repair} $[euro/m^3/m]$	C_{tot} $[euro/m^3/m]$
FORM	Moderate	2,00	1,22	3,00	1,00	4,50	5,00	6,30	-3,5	0,63	6515,31	697,86	6673,32
CMC	Moderate	2,00	1,22	3,00	1,00	4,30	5,00	6,10	-3,5	0,63	6417,23	686,40	6572,84
Case	Moderate	2,5	0.92	3	0.75	3.2	5	5	-3,25	0.41	5178,76	-	5178,76

Table 5.5: Output of cost optimal solutions if target Pf is not exceeded by overtopping and toe stability

For the configurations above the following probabilities of failure are found:

Method	Damage	Pf_toe	Pf_rock	Pf_overtop	Pf_design_toe	Pf_design_rock	Pf_design_overtop	Pf_tot
FORM	Moderate	0,00	0,12	0,01	0,00	0,98	0,24	0,98
CMC	Moderate	0,00	0,12	0,01	0,00	0,98	0,21	0,98

Table 5.6: Probabilities of failure if target Pf is not exceeded

Tables Tables 5.5 and 5.6 show much differences in dimensions compared to the case study. For instance, steeper slope and larger armour unit sizes. The cost are also higher, but as shown in the probabilities of failure, the probabilistic outputs are more reliable than the case output. A more thorough comparison between different optimal configuration outputs is discussed in section 5.2.

The FORM and CMC cost optimal outputs are shown in the figures below, in Figures 5.4 and 5.5, respectively.

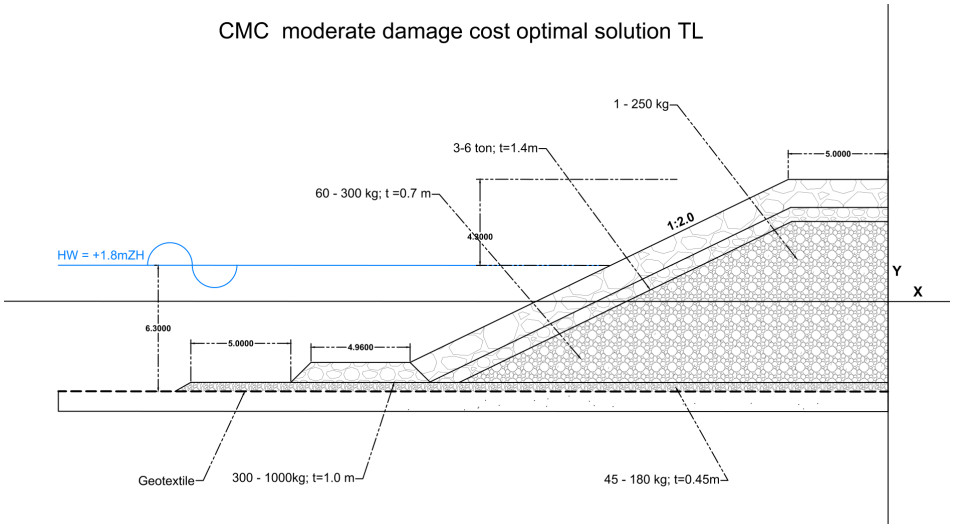

Figure 5.4: Probabilistic cost optimal configuration (CMC)

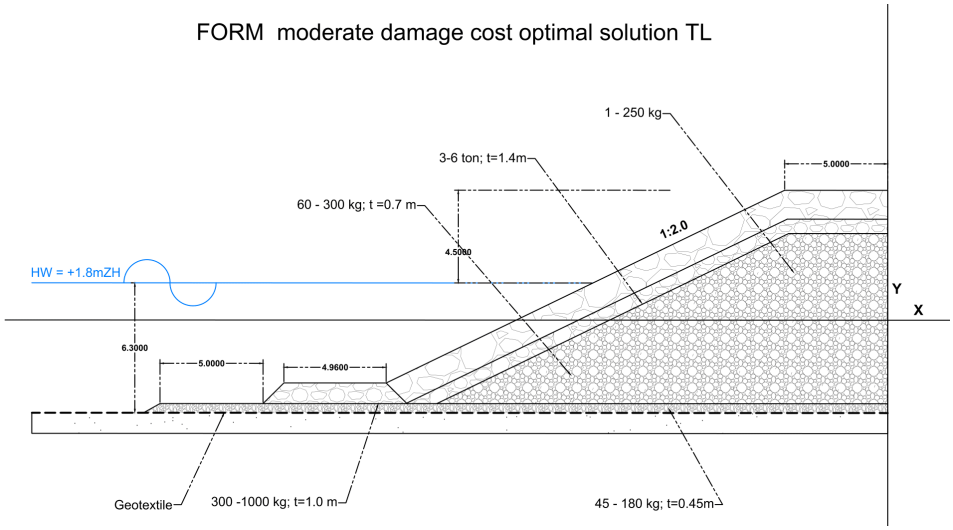

Figure 5.5: Probabilistic cost optimal configuration (FORM)

5.2. CASE AND MODEL COMPARISONS

Firstly, the number of outputs and time consumption are compared. Then a comparison is made between all of the cost optimal configurations of the method outputs.

NUMBER OF CONFIGURATION VS. TIME CONSUMPTION

In the previous sections, the number of outputs and the time consumption is documented. It is clear that the deterministic approaches consume approximately 10 times less computation time than the probabilistic approach. However, if the time consumption and the number of outputs are compared within the probabilistic approach, the time consumption is not linearly dependent on the number of outputs, as both FORM and CMC consume the same amount of time, with a significant difference in number of solutions. In contrast to the probabilistic time consumption and number of outputs, the deterministic methods are more linear. The number of outputs is more in proportion to the time it takes to compute them. This makes the deterministic approach a lot more predictive. Possibly, the difference is that the FORM and CMC analysis both need to converge to a probability of failure. For instance, the FORM analysis makes use of iterations. Thus, for some configurations, more iterations might be needed, which may result in a longer computation time.

Another noticeable difference is the difference between the deterministic approach with and without considering uncertainty, in the amount of solutions. This is due to the deletion of all options with 1 - 3 [t] armour layer units within the uncertainty approach. This results in fewer options. Similarly, the CMC analysis contains three times more configurations than the FORM analysis. This is possibly due to the lack of accuracy of the FORM analysis. Namely, the probabilities of failure are close to the target probability of failure. Once this is exceeded, the solution can be disregarded.

COST OPTIMAL COMPARISONS

It is observed that there is quite some overlap between the different cost optimal configurations. A visual analysis is given of a comparison between all the cost optimal configurations, the configurations considering uncertainty, the deterministic method and case study.

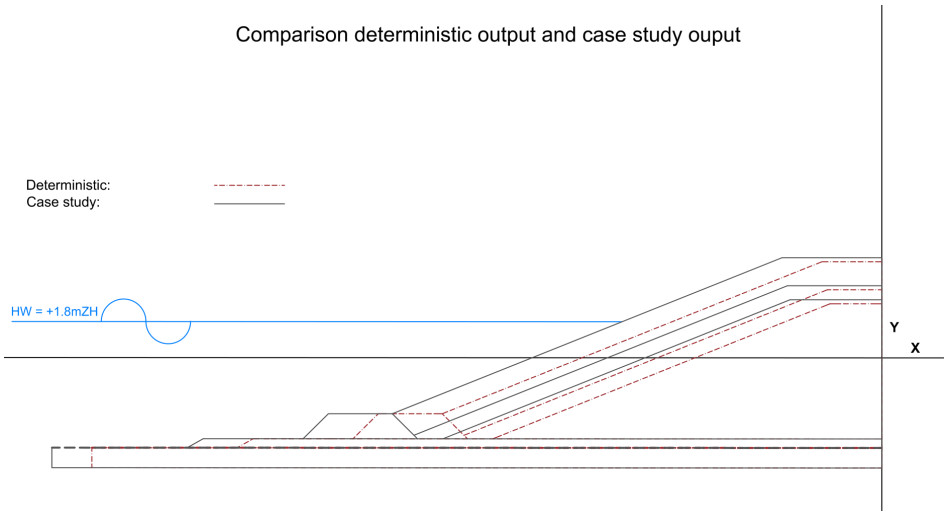

Figure 5.6: Deterministic comparison of cost optimal configurations

Both the case study output and the deterministic output do not consider any form of uncertainty. If the visualisation and the table above are analysed, the difference in geometries is easily noticeable. The case study realises a much broader crest and a slightly broader toe, as an effect of the toe unit size grading. Furthermore, the crest height is slightly higher. This evidently results in a higher construction cost for the case configuration. Moreover, these methods are alike. Thus, the configuration of the case study is searched in the output of the deterministic configuration data set. It is found that the case configuration is ranked place 445 of the 12887 possible configurations. This is relatively a good approximation of the optimal cost optimal configuration.

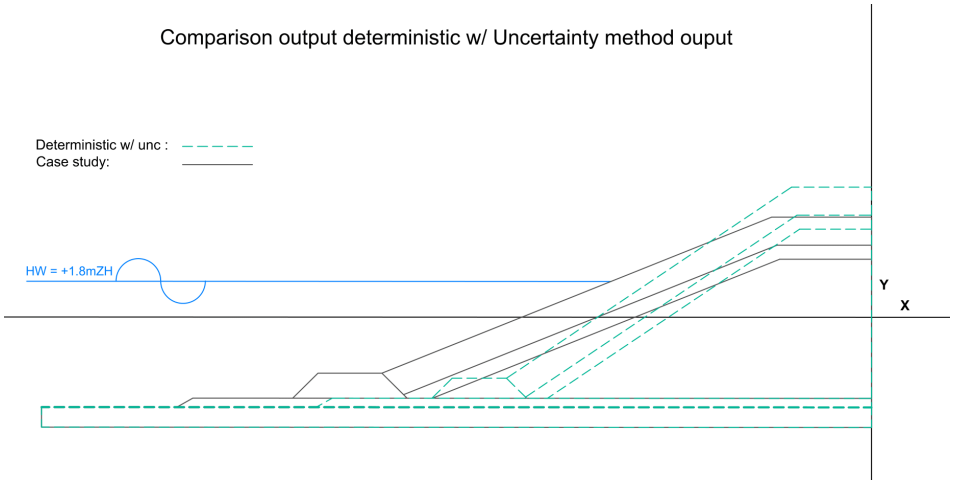

Figure 5.7: Deterministic w/ uncertainty cost optimal configurations comparison

From Figure 5.7 and in Figure 5.3, it is observed that the deterministic approach that considers uncertainty shows very different dimensions and cost than the case study. It has a much steeper slope, larger rock size and a higher crest. The crest width is more narrow. The toe is a little smaller than the case study. The cost of both configurations fall into the same range. The difference can be explained by the model uncertainty which is incorporated in this method and not in the case study. The deterministic approach with uncertainty shows that steeper configurations are more economic. Furthermore, the case configuration is not found in the output of the this method. It is therefore presumed that the uncertainty which is incorporated, disregards the case study option.

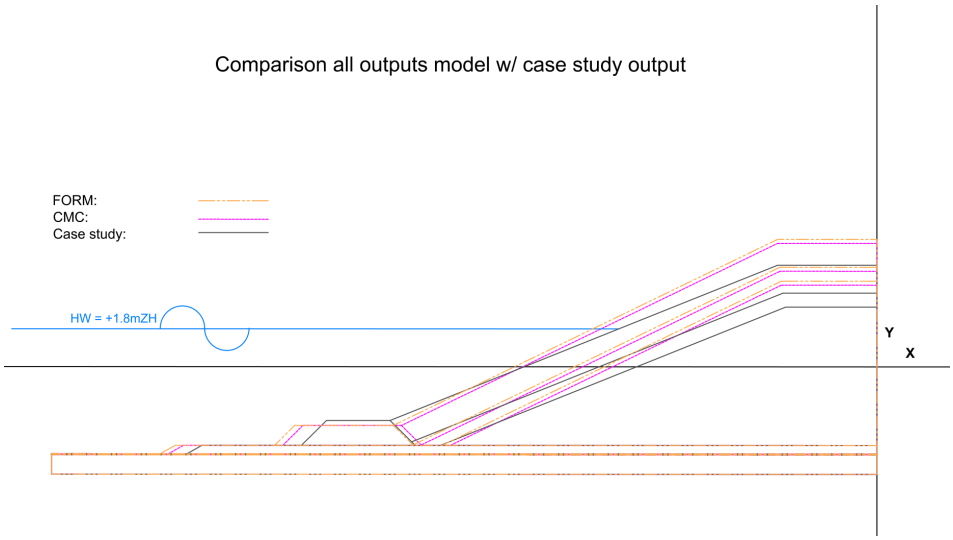

Figure 5.8: Comparison probabilistic cost optimal configurations with case study

In Figure 5.8 the probabilistic outputs are compared with each other and the case study output. From the figure it is seen that the slopes of the probabilistic outputs are a little steeper than the case study. In the tables above it is found that the armour unit sizes are a rock grading higher. However, the structures still have a 100% chance of moderate damage, due to the armour layer stability. The overtopping is accounted for by a larger crest height, but the crest widths are similar. The toe is slightly lower but contains a larger unit size.

DISCUSSION MODEL OUTPUT ON COST OPTIMAL SOLUTIONS

From the outputs discussed in the preceding sections we conclude the following:

- The case study output does not consider any form of uncertainty. From the probabilistic calculations it is concluded that the structure is going to have moderate damage over the life time of the structure.
- The deterministic output, which also does not consider uncertainty, shows that a less robust configuration is possible. This can be considered if the direct incentive is to disregard any reliability regarding moderate damage. This will result in much less costs.
- The deterministic output which considers uncertainty, shows similar costs as the case output, but very different dimensions, much steeper slopes and higher crest. This is due to the damage factor which is considered. For milder slopes and lower crests, the damage factor for moderate damage is higher. This is disregarded in this comparison. This option is however very insightful, if one does not want to conduct a full probabilistic approach.
- The probabilistic approaches show that the structure of the case study is under-dimensioned with respect to the probability of moderate damage. For a more safe structure, the dimensions are different. This results mainly in a slightly higher crest height and larger stone sizes for the toe dimensions.
- The fact that the costs are higher for the probabilistic approaches, is something that the engineer must decide whether to accept or not. However, the model does show that the uncertainties can be quantified more and that this follows through in the costs.

5.2.1. MULTIPLE COST OPTIMAL SOLUTIONS

In the previous section the cost optimal solutions were compared. However, a whole output of configurations is generated. It is therefore analysed if the cost optimal is by far the optimal solution or whether other optimal solutions also fall in the same cost range. This is only done for the Crude Monte Carlo output and the deterministic output. In Figures 5.9 and 5.10, all of the possible configurations of the output acquire in the preceding section are visualised in a 3D plot.

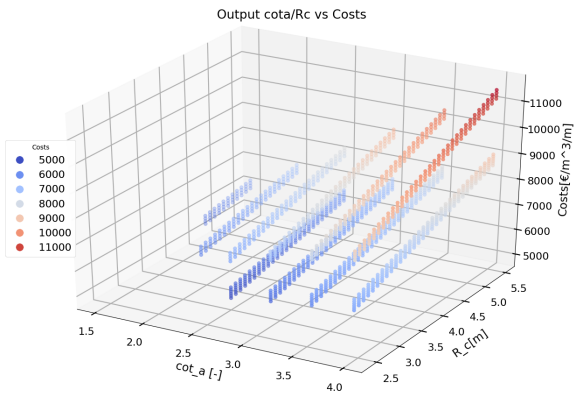

Figure 5.9: Deterministic output

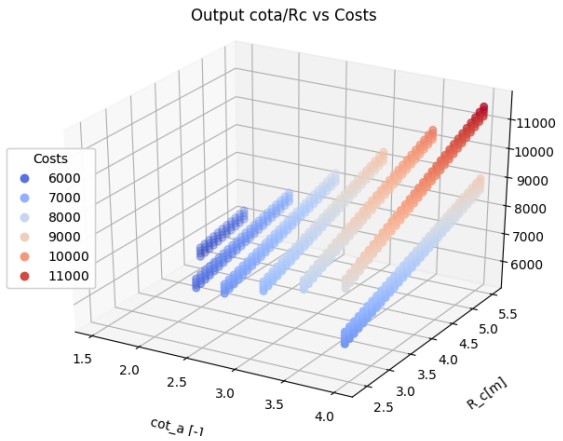

Figure 5.10: Output of the Crude Monte Carlo analysis

The figures above show that the lowest cost range contains many different configurations, with different slope angles and different crest heights. This is observed for both the probabilistic method as the deterministic method. From these figures it can be concluded that converging to a single cost optimal solution, disregards many other possible design with similar costs and different dimensions. It is therefore important that engineers always observe and analyse their output, before concluding and claiming that a certain configuration is the optimal configuration.

5.3. OPTIMISATION SCHEME RESULTS

The theory behind the optimisation method is discussed in section 3.2. Subsequently, this is implemented in the model. The results of which are discussed in this section. The toe structure is fixed, since the dimensions are independent of the other optimisation parameters; and for simplicity reasons.

5.3.1. INITIAL RESULTS OF OPTIMISATION: DETERMINISTIC APPROACH

Firstly, the initial results need to be analysed before conducting an optimisation. The initial results are the deterministic outputs generated with the same inputs as Table E.1b, for the Southern breakwater option 1. These results are also shown and analysed in Section 5.2. For now, however, the computation time and costs per option are interesting. The computation time and amount of options are shown in Tables 5.2 and 5.4 for the deterministic and probabilistic approach respectively. This approach is used as a base input for the optimisation scheme.

In Table 5.7, the number of solutions and computation time is documented for the deterministic approach for both the initial set of configurations and the local minima set.

Method	Computation time	Initial number of config.	Number of local opt. config.
Deterministic	21.8s sec	1292	264

Table 5.7: Deterministic method output of the number of optimal configurations and computation time

The amount of minimum values obtained from the algorithm are 148 for the deterministic approach. This is a drastic decrease in amount of solutions. This decrease in options will eventually result in a lower computation time when applied to the optimisation technique.

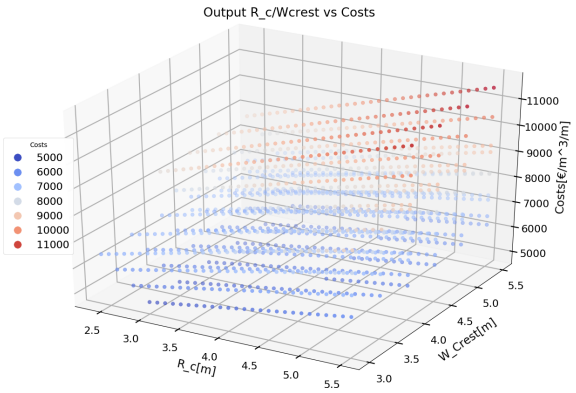

Figure 5.11: Deterministic output Rc / B / Costs

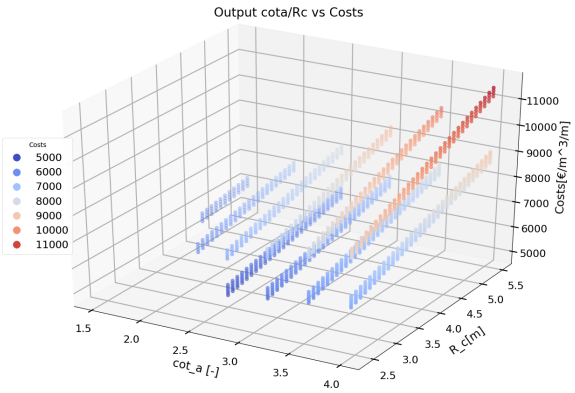

Figure 5.12: Deterministic output cota / Rc / Costs

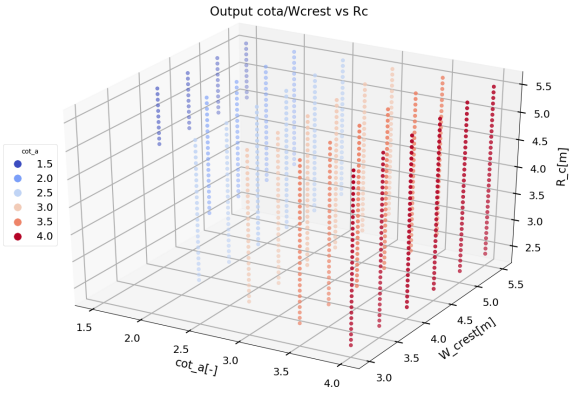

Figure 5.13: Deterministic output cota / B / Rc

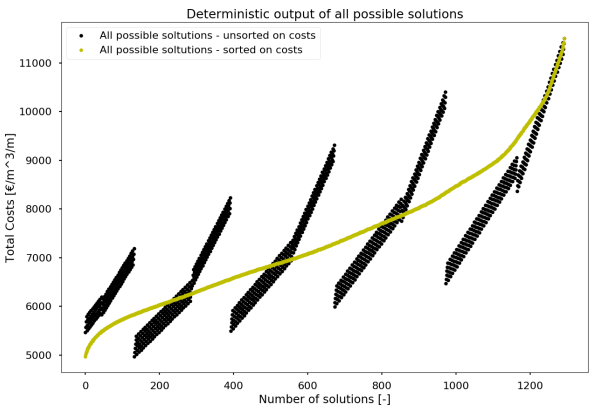

Figure 5.14: Deterministic output of all solutions

In the above figures all of the options are depicted in a 3D plot with different combinations. From these results, it can be seen that both configurations with 1-3 tons and 3-6 tons are considered. Furthermore, very few options have a slope angle of 1:1.5. This means that the limit state of these configurations with a crest height smaller than 4.5 m do not satisfy and will likely fail, given the maximum amount of unit sizes. Figure 5.14 shows all the costs per configuration. The black dots show the configurations and their respective cost. The yellow line is obtained when all of these configurations are sorted from low costs to high. This shows a rapid increase in costs in the low cost segment, a minor stagnation in the mid section and a rapid increase in the high cost segment.

INITIAL RESULTS OF OPTIMISATION: LOCAL MINIMA SELECTION

In Figures 5.15 to 5.18, E.3 and E.4, the results of the local minima selection are visualised. After which, these graphs can be compared to the previous solutions and then with the optimisation output.

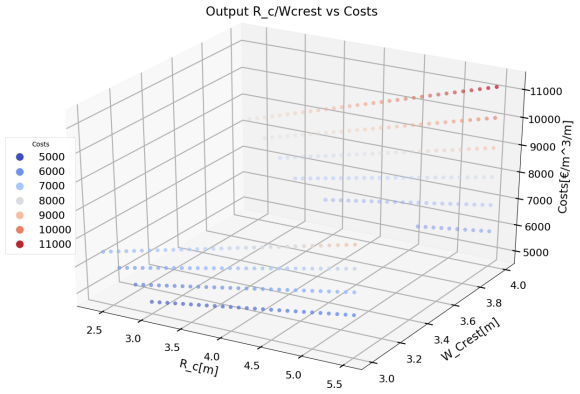

Figure 5.15: Local optimisation output Rc / B / Costs

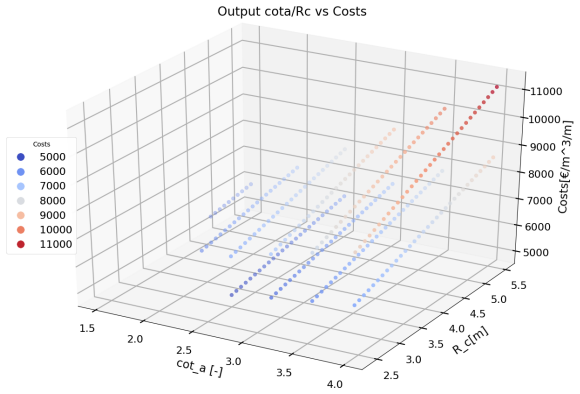

Figure 5.16: Local optimisation output cota / Rc / Costs

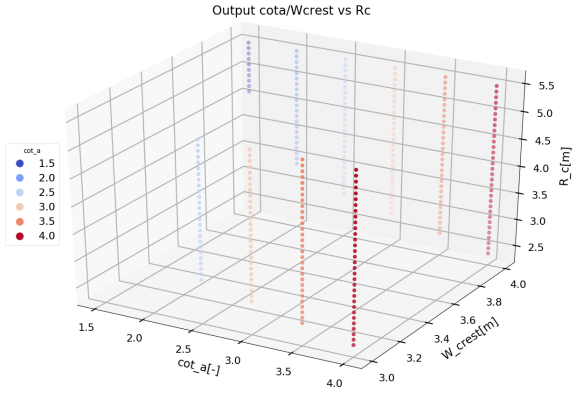

Figure 5.17: Local optimisation output cota / B / Rc

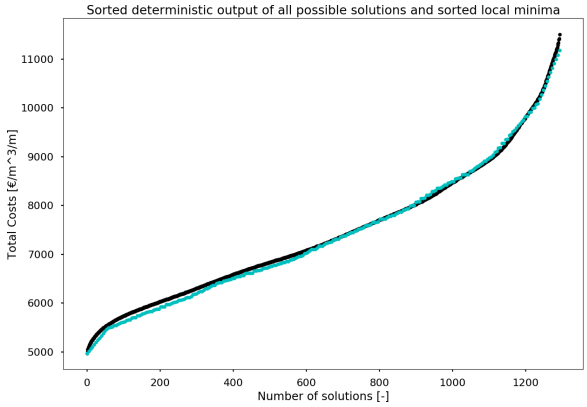

Figure 5.18: Output of locally optimised solutions

From the results it seems that the local minima all favor crest width of 3 or 4 meters, given a toe size as specified. The slope angle and the crest height both generate different configurations. Furthermore, configurations with a slope angle smaller than 1:3 only consider crest widths of minimal 4 meters. Another notable effect is the disregarding of all crest widths larger than 4 meters.
Figure 5.18 shows all the costs per configuration. The black line shows the configurations of the deterministic output and the blue line shows the output of the local minimisation. With less options, the blue line shows an overall decrease in costs, meaning that the most cost optimal configurations from the black line were selected.

5.3.2. RESULTS AFTER OPTIMISATION SCHEME IMPLEMENTATION AND COMPARISON

As a result, only the minimum cost solutions for similar solutions remain. Thus, the amount of options is diminished and selected based on minimum costs. Even though the local optima are determined on minimum costs, this approach mainly benefits the minimisation in computation time. After the implementation

of the optimisation technique, a total of 82 configurations were selected from an initial 1312 deterministic configurations, after which selecting the local optima were 148 solutions.

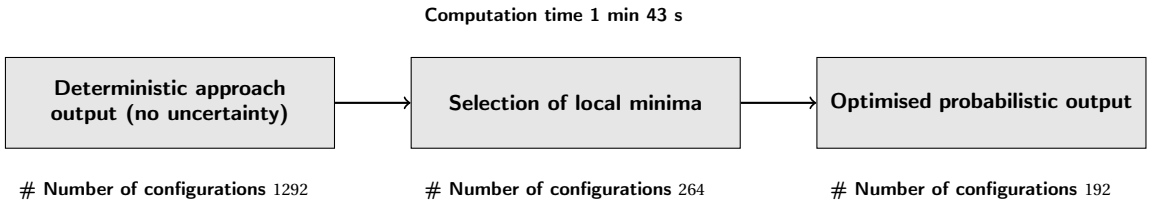

Figure 5.19: Optimisation scheme and process of model output

The observations of the 82 configurations are shown below. In the Figures 5.20 to 5.22, E.5 and E.6, the dimensions of the configurations are plotted against the cost output. If these graphs and all configurations are plotted in a 2D graph on the same axis against the costs, the graph in fig. 5.23 is obtained.

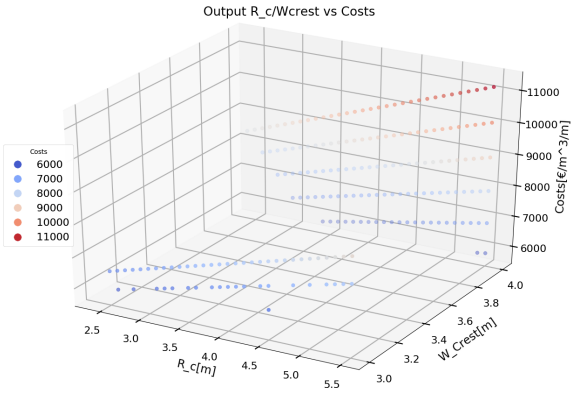

Figure 5.20: Optimisation scheme output Rc / B / Costs

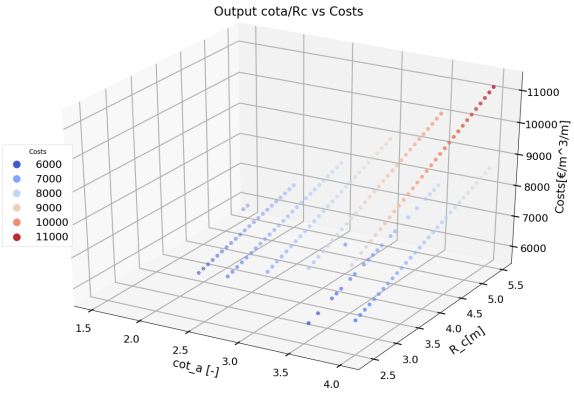

Figure 5.21: Optimisation scheme output cota / Rc / C

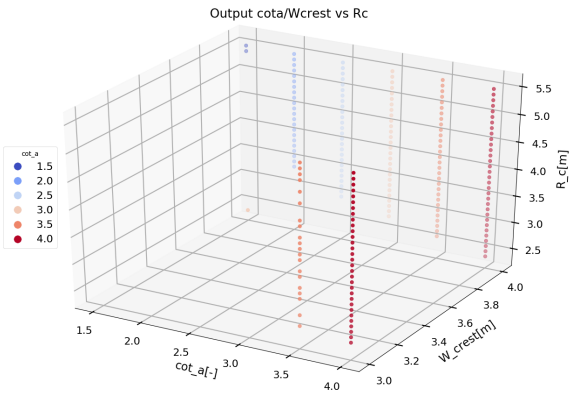

Figure 5.22: Optimisation scheme output cota / B / Rc

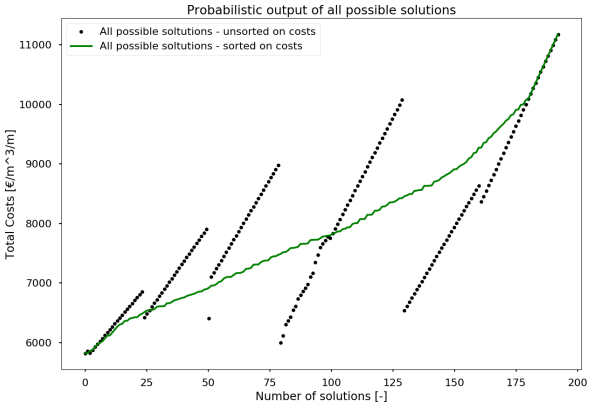

Figure 5.23: Optimisation scheme output of all solutions

These calculations were performed using the CMC analysis, with least accurate setting for reasons of computation time. From these figures above it can be seen that the total number of solutions has drastically been diminished. From Figures 5.22 and E.5, it can be seen that only the slope angle and the crest height are responsible for the change in configuration size. It seems that the armour unit size remains 3 - 6 tons and the crest width stays at a minimum of 4 meters.

5.3.3. RESULTS PROBABILISTIC APPROACH

In order to justify and analyse the output of the optimisation scheme, the outputs of the other methods need to be documented. These are the results of the CMC analysis and the deterministic approac which considers uncertainty. This way the profit in time consumption and optimal configurations can be compared to other methods. The results of the CMC analysis is documented in Appendix E.1 and the resuts of the deterministic approach with uncertainty can be found in Appendix E.1.

Note: The FORM analysis is not part of this analysis, as it disregards many options due to its limited accuracy. However, the results of this analysis with regard to the local optima and the total output are documented in Appendix E.

Method	Computation time	Initial number of config.	Number of local opt. config.
Deterministic w/uncertainty	32 sec	376	46
CMC	2 min 8 sec	192	47
FORM	1 min 54 sec	65	17

Table 5.8: Comparison methods output of the number of optimal configurations and computation time

From the outputs of the probabilistic approaches the following is found:

- FORM disregards many options. This means that the approximation of the probability of failure is much less accurate than the Crude Monte Carlo analysis (which regards more options).
- The analysis considers more options in lower cost segment than the other methods.
- The deterministic approach with uncertainty shows similar outputs as the crude. Monte Carlo analysis.
- The Crude Monte Carlo analysis shows similar outputs as the other methods.
- It also shows crest widths larger than 4 meters.
- It disregards all slope angles smaller than 3.

5.3.4. DISCUSSION OPTIMISATION APPROACH

Ultimately, the optimisation scheme is discussed. The criteria of this scheme are the reduction in computation time and increase in insight into the optimal configurations, by reducing the amount of initially generated configurations. As a result the following is found:

- The optimisation approach does indeed require less computation time than the probabilistic approaches. Evidently, the deterministic approaches still require less computation time.
- The optimisation methods proves to generate a smaller output load; giving more insight in the different dimensions and costs of the possible configurations, for the same input.
- Apparently, the scheme filters the local minima on the crest width, giving room for different configurations to the crest height and slope angle.
- By optimising on the crest width, the scheme disregards many options which fall in the same cost category with different crest dimensions.
- It becomes difficult to see whether other options, such as crest width configurations have the same costs and should therefore also be considered in the design process.
- The scheme is still a "brute forced" approach. It does not learn from its output and does not consider alternatives which have already been disregarded. This means that a large surrender lies in the insight of the configurations and does not confirm the best options with full certainty.

5.3.5. RESULT KEYPOINTS

METHOD COMPARISONS

- The model generates a large number of possible configurations, for all methods.
- The deterministic approaches require approximately 10 x less computation time than the probabilistic approaches. However, unlike the deterministic approaches, the probabilistic approaches are not linearly in correspondence with the amount of output configurations.
- The deterministic approach with and without considering uncertainty, deviates largely in the amount of output solutions.
- The CMC analysis contains three times more configurations than the FORM analysis. Possibly due to the lack of accuracy, many options are disregarded based on exceeding a certain probability of failure.
- The probabilistic approaches show that the structure of the case study is under-dimensioned with respect to the probability of moderate damage. For a more safe structure, the dimensions are different. This results mainly in a slightly higher crest height and larger stone sizes for the toe dimensions.
- Converging to a single cost optimal solution, disregards many other possible designs with similar costs and different dimensions.

OPTIMISATION SCHEME

- The local optimisation scheme indeed selects the most cost optimal configurations from the initial configuration data set.
- It seems that the scheme filters the local minima on the crest width.
- The optimisation approach indeed requires less time than the probabilistic approaches and also generates a smaller configuration date set.
- The scheme is still a "brute forced" approach. It does not learn from its output and does not consider alternatives which have already been disregarded, meaning that a large surrender lies in the insight of the configurations and does not confirm the best options with full certainty.

6

SENSITIVITY ANALYSIS

6.1. INTRODUCTION

As mentioned before, the model should only be used and reviewed by experts and competent engineers to avoid unrealistic outcomes. The model follows an integrated design of multiple failure mechanisms and equations. Therefore, it can be valuable to know the effect of different inputs on the costs of the design and probability of failure. Consequently, a study is done to asses the impact of different input variables, such as the geometric variables and standard deviations, on the probability of failure.

The model is applied to the preliminary and final design phase. Conventionally a design process tests an amount of configurations, determined in the preliminary design phase, in the lab with model tests. With these tests uncertainty in the empirical approach can filtered. However, if these uncertainties are already diminished and quantified beforehand, the model test configurations can be optimised more thoroughly, avoiding unnecessary extensive and repetitive tests and costs. Consequently, a sensitivity analysis of the uncertainty parameters is done.

Furthermore, in the preliminary design phase, realising many configurations will cost a lot of time. Therefore, the model should not exceed the current time consumption. The probabilistic method in the model can make use of multiple sets of accuracy and time parameters. This chapter also describes the effect of different parameters on the computation time and accuracy.

6.2. PROBABILITY OF FAILURE DISTRIBUTION OVER DIFFERENT FAILURE MECHANISMS

An initial hypothesis suggests that a slope protection with a smaller footprint is a more economical option than a slope protection with a larger footprint. This means that a slope with a more gentle structure is more costly than a slope protection with a steeper slope. However, a more steeper slope requires a larger armour unit size to maintain an acceptable probability of failure. Furthermore, a wider crest means a larger structure. If the crest width would be diminished, the crest height should be increased, again to maintain an acceptable overtopping rate and a compliant probability of failure. For the toe dimensions, a smaller toe volume means a toe level as low as possible, for both a smaller volume and smaller armour unit size due to smaller wave induced forces. This hypothesis is tested by a comparison of two combinations. An initial combination of input variables suggests a slope protection with a more gentle slope and a relatively higher toe height. After which the variables are altered in correspondence with the idea that a smaller slope protection footprint, would be a more economical option. Furthermore, if these changes in geometry are made, the distribution of dominant failure mechanisms are likely to change. Thus, for a fair comparison, the total probability of failure should be kept constant. In Table 6.1 the values for the input variables are given, and in Figures 6.1 and 6.2 the distributions of failure mechanisms are shown.

Variable	Combinatin 1	Combination 2
cot_{α}	3.5 [-]	1.5
$dn50_{armour}$	1.3[m]	1.55 [m]
R_c	2.0 [m]	4.8 [m]
w_{crest}	10.0 [m]	3.3 [m]
z_{toe}	-2.0 [m]	-3.5 [m]
$dn50_{toe}$	0.625[m]	0.458 [m]

Table 6.1: Input values comparison of combinations of different footprint sizes.

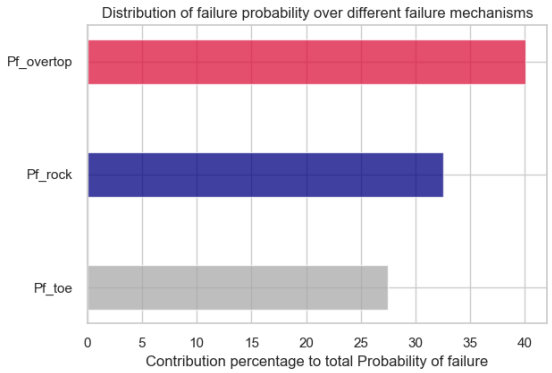

Figure 6.1: Distribution of the probability of failure over different failure mechanisms, initial combination

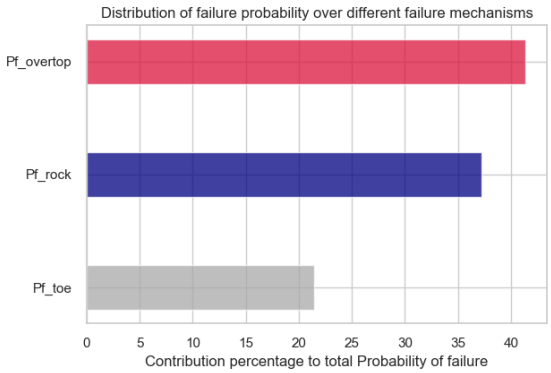

Figure 6.2: Distribution of the probability of failure over different failure mechanisms, comparative combination

In Table 6.2, an overview is given of the results for combinations 1 and 2, expressed on the probabilities of failure per failure mechanisms and the costs in initial, repair and total. This comparison is done for the serviceability limit state. Moreover, the effect that a larger rock size is more costly than a smaller rock size is not considered. Looking at the results, it seems that even though a smaller footprint is realised, the costs have not been minimised that much for an almost equal probability of failure. This can be explained by the increase in costs for armour layer units as the area increases due to a larger stone size. Moreover, the crest height increases proportionally to the decrease in width as the probability of failure stays almost the same.

Variable	Combinatin 1	Combination 2
$P_{f,overtop}[-]$	0.122494	0.137
$P_{f,toe}[-]$	0.144795	0.155
$P_{f,armour}[-]$	0.178263	0.165
$C_{initial}[euro/m^3/m]$	9201.81	9121.86
$C_{repair}[euro/m^3/m]$	1061.02	1172.24
$C_{total}[euro/m^3/m]$	9245.57	9166.66

Table 6.2: Ouput distribution of comparative combination when footprint is smaller

Some variables only undergo a small change, such as the armour unit size, and others require much more change, such as the crest width. The only parameter which has an influence on multiple systems is the slope angle. Figure 6.3 shows the distribution of failure, when the slope angle is changed. It can be seen that initially, the probability of failure for both armour layer stability and overtopping is contributing in almost the same amount, where the toe probability of failure is dominant. As the slope angle is decreased, the overtopping probability of failure contribution increases quite rapidly, whereas the armour stability increases more calmly with a sudden jump at slope angle of 3.0. Finally, at a slope angle of 2.5, the overtopping probability of failure is dominant, while it initially had the lowest contribution. Thus, it seems that changing the slope angle has more influence on the increase or decrease in the overtopping failure mechanism and less on the armour stability mechanism.

In Figure 6.4, only the armour size of the armour layer is changed, while the other parameters are kept constant. The first part from sizes 1.9 to 1.7 confirms that this parameter only influences the armour layer stability probability of failure. As it decreases further, it seems that from a size of 1.5 m the probability of failure for armour increases quite rapidly. This indicates a high influence on the probability of failure for armour layer stability. The quantification of the influence of these parameters is discussed in the next section.

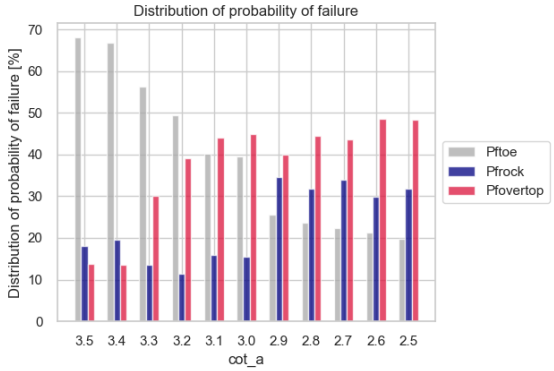

Figure 6.3: Probability of failure distribution of cota over failure mechanisms using CMC

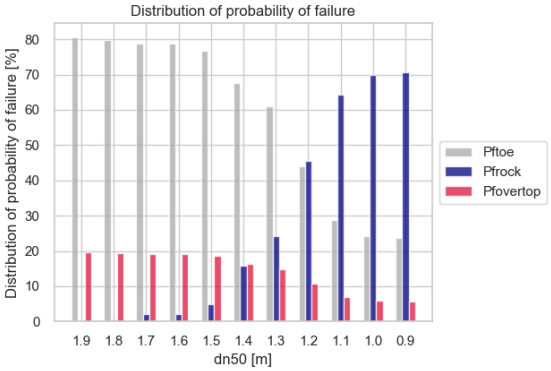

Figure 6.4: Probability of failure distribution of dn50 over failure mechanisms using CMC

6.3. INFLUENCE ON THE PROBABILITY OF FAILURE BY EACH VARIABLE

Solutions which do not meet the predetermined requirements or threshold for the probability of failure are considered negligible. Thus, in order to know how the parameters correspond to the probability of failure, their influences are investigated. In Figure 6.5, the influence of each variable is shown as a function of the change in probability of failure. The same approach is used for Figure D.11. Moreover, different combinations are used, as shown in Table 6.3. However, the rate of change in variables is kept the same.

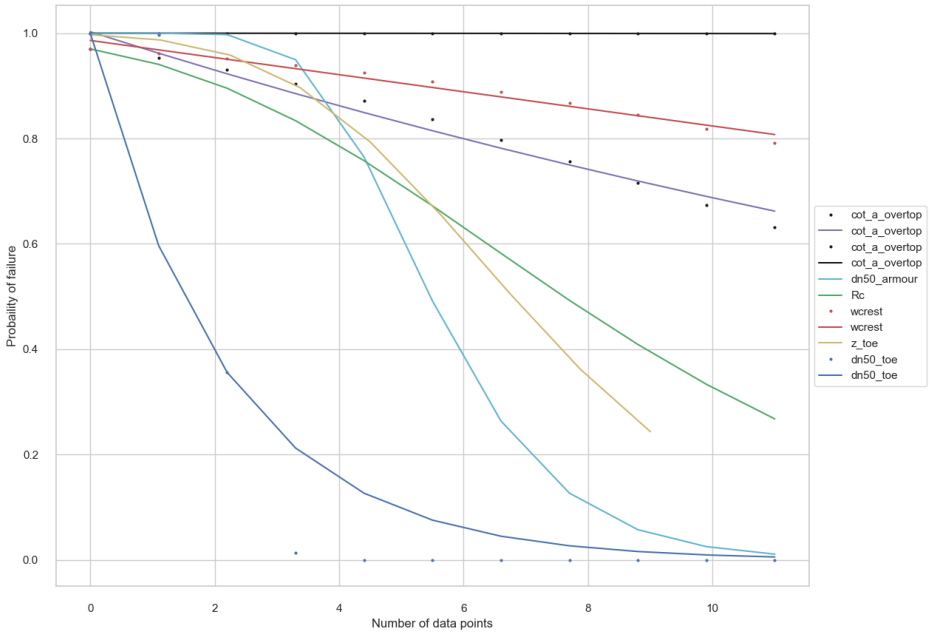

Figure 6.5: This figure represents the change in probability of failure per variable, when all other variables are kept constant, each x-axis of the curve is given in table 6.3

Variable	0	1	2	3	4	5	6	7	8	9	10
$Slopeangle$	2.5	2.6	2.7	2.8	2.9	3.0	3.1	3.2	3.3	3.4	3.5
$dn50_{armour}$	0.9	1.0	1.1	1.2	1.3	1.4	1.5	1.6	1.7	1.8	1.9
R_c	3.0	3.1	3.2	3.3	3.4	3.5	3.6	3.7	3.8	3.9	4.0
w_{crest}	5.0	5.1	5.2	5.3	5.4	5.5	5.6	5.7	5.8	5.9	6.0
z_{toe}	-3.0	-3.1	-3.2	-3.3	-3.4	-3.5	-3.6	-3.7	-3.8	-3.9	-4.0
$dn50_{toe}$	0.3	0.4	0.5	0.6	0.7	0.8	0.9	1.0	1.1	1.2	1.3

Table 6.3: Combination table for probability of failure sensitivity analysis

In the figure above, it is immediately visible that the probability of failure is most strongly influenced by the armour size of the toe layer units. Followed by the armour size units of the armour layer. However, these sizes have been predetermined, following the standard rock gradings. Even though they are predetermined, it is noticeable that within the given bounds with a 10 cm step size, this is a very sensitive parameter and strongly influences the probability of failure. Moreover, the toe height is bounded by ht/h, so the sensitivity of 10 cm change in height is an accurate step size. The crest height also strongly influences the probability of failure. The gradient is slightly less steep than the aforementioned parameters. Thus, its effect is probably still recognisable if the upper bound was set higher and the step size set larger. Its sensitivity would probably be more influential and feasible for 20 cm. This is even more noticeable for the crest width. Thus a crest width sensitivity is more likely to be accurate for steps of 0.5 m. The slope angle is not of great influence for the probability of failure for the overtopping as well as for the probability of failure for armour stability. Especially for the armour failure it is almost negligible. For the overtopping probability of failure it is more influential. However, since its bounded and the influence is fairly low, the sensitivity is quite small. Thus, a large step size is recommended.

These observations are more of a qualitative nature, since the rate of change is self-inflicted and not in ratio with other parameters. To gain more insight in the latter, the rate of change and its effects need to be quantified in order to implement in further research. With a FORM II analysis, it is possible to determine to some extend the gravity of the influence of the parameters. This can be done through the use of alpha values, the omission factor and the reliability elasticity coefficient.

6.3.1. SENSITIVITY OF VARIABLES TO THE PROBABILITY OF FAILURE

The alpha value, $\alpha_i (i = 1, ..., n)$, represents the direction cosines at the design point (Naess and Moan, 2005). Alternatively, these are sensitivity parameters. They give an indication of the relative influence of a random variable to the overall reliability of the limit state function. The larger the value, the greater the influence of the variable on the reliability. A negative sign signifies that the respective variable is considered a resistance variable and a positive sensitivity factor is considered a load variable (Naess and Moan, 2005). Surely, this is dependent on the how the limit state function is defined, but generally this is the annotation.

SENSITIVITY FACTORS, α_i

These sensitivity parameters are strongly dependent on the values for the standard deviations which have been chosen. The alpha values are determined for the different failure mechanisms and the probability of failure for each respective failure mechanism.

Variable v_i	$\frac{d}{dH_s}$	$\frac{d}{dH_2}$	$\frac{d}{dTm10}$	$\frac{d}{dTm}$	$\frac{d}{drhos}$	$\frac{d}{dSd}$	$\frac{d}{dP}$	$\frac{d}{dcot_a}$	$\frac{d}{ddn50_{armour}}$	$\frac{d}{dcsw}$	$\frac{d}{dXhs}$
Sensitivity factor α_{nu_i}	-0.182	0.578	0.219	-0.046	-0.142	0.056	-0.106	-0.116	-0.106	-0.412	0.420

Table 6.4: Sensitivities of each variable to the total probability of failure for Armour layer stability failure mechanism for the serviceability limit state

Variable v_i	$\frac{d}{dH_{m0}}$	$\frac{d}{dcot_a}$	$\frac{d}{dTm10}$	$\frac{d}{\beta}$	$\frac{d}{R_c}$	$\frac{d}{dgamma_f}$	$\frac{d}{dw_{crest}}$	$\frac{d}{dA}$	$\frac{d}{dB}$	$\frac{d}{dC}$	$\frac{d}{dD}$	$\frac{d}{dE}$	$\frac{d}{dXhs}$
Sensitivity factor α_{nu_i}	0.742	-0.096	0.189	-0.0	-0.040	0.065	-0.040	-0.0	-0.0	0.107	-0.40	-0.0	0.477

Table 6.5: Sensitivities of each variable to the total probability of failure for Overtopping failure mechanism for the serviceability limit state

Variable v_i	$\frac{d}{dH_s}$	$\frac{d}{drho_s}$	$\frac{d}{dSWL}$	$\frac{d}{dz_{bed}}$	$\frac{d}{dz_{toe}}$	$\frac{d}{ddn50_{toe}}$	$\frac{d}{dgamma_{toe}}$	$\frac{d}{dXhs}$
Sensitivity factor α_{nu_i}	0.680	-0.155	-0.003	-0.014	0.0844	-0.452	-0.271	0.478

Table 6.6: Sensitivities of each variable to the total probability of failure for Toe stability failure mechanism for the serviceability limit state

Evidently, the environmental conditions have a large impact on the reliability of the limit state function. The effect of the uncertainty factors, e.g. c_{sw}, X_{H_s}, etc., are further investigated in Section 6.3.3. The slope angle as previously predicted, has a small impact on the reliability for both the overtopping failure mechanism as well as the armour layer stability. Even though the crest height is previously predicted to have a slightly larger impact than the crest width, it seems that the impact of the sensitivity factors is almost the same. Conform with the previously determined impacts of the armour sizes for both the armour layer as the toe, the impact quite large, with a larger influence of the unit size of the toe elements than that of the armour layer elements. Notably, the toe height has a larger influence than the crest width, height and the slope angle, as shown in Figure 6.5. This variable is also considered a load factor, as an increase in toe height also increases the probability of failure of the system.

In conclusion, these sensitivities in the reliability of the system can be of further use in an optimisation scheme. Furthermore, the knowledge of the influence of these variables can be used to alter inputs and for users to determine their inputs for other projects.

THE OMISSION SENSITIVITY FACTOR, ς_i

Another sensitivity measure related to α_i is the omission sensitivity factor ς_i suggested by Madsen (Madsen, 1988). This factor gives the relative importance of a variable on the reliability index by assuming that stochastic variable i, i.e. it is considered a deterministic quantity (Sørensen, 2004). The omission factor is calculated as follows:

$$\varsigma_i = \frac{1}{\sqrt{1-\alpha_i^2}} \tag{6.1}$$

This parameter is specifically valuable to reduce the number of random variables. Especially if one deals with a large number of input variables. In Tables 6.7 to 6.9, the omission sensitiviy factors are considered for armour layer stability, overtopping and toe stability respectively.

Variable ς_i	H_s	H_2	$Tm10$	Tm	$rhos$	Sd	P	cot_a	$dn50_{armour}$	csw	Xhs
Sensitivity factor ς_{η_i}	1.0067	1.1829	1.0140	1.00089	1.0085	1.0013	1.0142	1.0003	1.0047	1.2094	1.0840

Table 6.7: Omission sensitivity factor for Armour layer stability failure mechanism for the serviceability limit state

Variable ς_i	H_{m0}	cot_a	$Tm10$	β	R_c	$gamma_f$	w_{crest}	A_{ov}	B_{ov}	C_{ov}	D_{ov}	E_{ov}	Xhs
Sensitivity factor ς_{η_i}	1.45166	1.00485	1.01816	1.0	1.00059	1.00239	1.0007	1.0	1.0	1.00607	1.11006	1.0	1.13355

Table 6.8: Omission sensitivity factor for Overtopping failure mechanism for the serviceability limit state

Variable ς_i	H_s	rho_s	SWL	z_{bed}	z_{toe}	$dn50_{toe}$	$gamma_{toe}$	Xhs
Sensitivity factor ς_{η_i}	1.32594	1.02127	1.000006	1.00016	1.00587	1.05854	1.07969	1.16713

Table 6.9: Omission sensitivity factor for Toe stability failure mechanism for the serviceability limit state

(Madsen, 1988), states that if the α_i factor < than ±0.14, than the omission factor ς_i would be < 1.01, i.e. the error in the reliability index is less than 1% if the respective value would be deterministic. For the armour stability this holds for several factors, but especially the optimisation parameters, i.e. the slope angle and rock size. Again for overtopping optimisation parameters, slope angle, freeboard and crest width have a very low

influence. For the toe stability, this only holds for the toe height.

To conclude, this information can be useful for further optimisation techniques and engineers willing to continue with probabilistic design on structures. However, the reason for the small errors regarding the optimisation parameters may be due to the larger impact of the environmental parameters and uncertainty parameters. Thus, a relative contribution to the reliability amongst these parameters is relevant to know. This is discussed in the next section.

THE RELIABILITY ELASTICITY COEFFICIENT, e_p

Another very important sensitivity measure is the reliability elasticity coefficient.

$$e_p = \frac{d\beta}{dp}\frac{p}{\beta} \tag{6.2}$$

Where p is a parameter in a distribution function (e.g. the expected value or the standard deviation) or p is a constant K in the failure function. From Figure 6.6, it is seen that if the parameter p is changed by 1%, then the reliability index is changed by e_p%. The change in reliability for a change in 1% in armour rock size is shown in Figure 6.6.

Figure 6.6: Sensitivity of $dn50_{armour}$ change by 1% to the reliability index β

The factor $\frac{d\beta}{dp}$ is determined by estimating the slope shown in Figure 6.6. An increase in the reliability index means a decrease in the probability of failure, also visualized in Figure 6.7. From Table 6.10a, it is seen that if the armour rock size is increased by 1%, the reliability index increases approximately by 2%. Primarily the changes in the mean value of the optimisation factors are investigated by $e_{\mu,i}$. The results are shown in Tables 6.10a, 6.10b and 6.11, for the armour stability, overtopping and toe stability failure mechanism respectively.

Variable, η_i	$cota_\alpha$	$dn50_{armour}$
e_μ	1.020	2.0318

(a) Elasticity coefficient e_μ for Armour layer stability

Variable, η_i	z_{toe}	$dn50_{toe}$
e_μ	2.3904	1.60392

(b) Elasticity coefficient e_μ for Toe stability

Variable, η_i	$cota_\alpha$	R_c	w_crest
e_μ	0.93377	1.9722	0.7834

Table 6.11: Elasticity coefficient e_μ for Overtopping

Evidently, the influence of the armour size difference has twice the impact than that of the slope angle. With regard to overtopping, the same holds for the crest height. The toe height is more influential than the armour rock size. However, the influences of both the toe parameters have significantly more influence on the reliability than the parameters of the armour layer and the overtopping failure mechanisms. In Figure 6.7 the increase in the rate of change is visualised for the change in armour rock size. A 1% difference in this parameter means a decrease in probability of failure of approximately 0.003. This seems quite low. However, when taken over a lifetime of 25 to a hundred years this becomes 10 times as much and is more in the order of 0.03 which is a more considerable change.

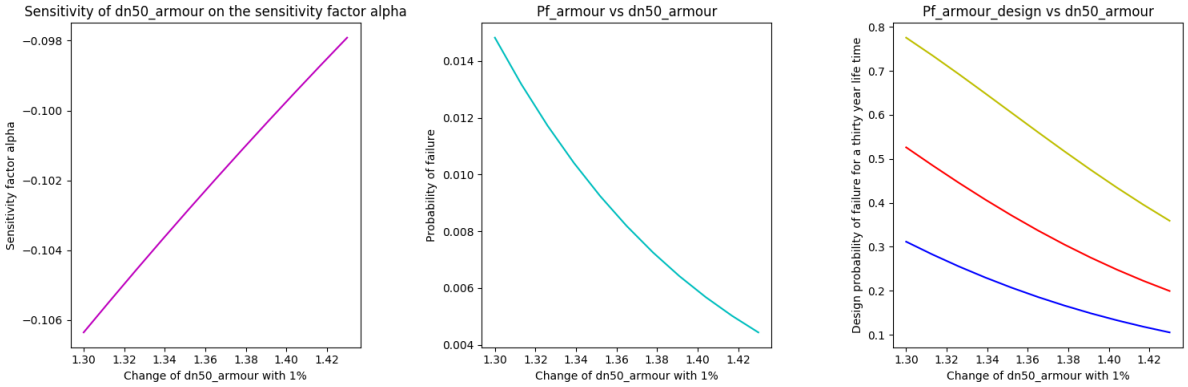

Figure 6.7: Sensitivity of $dn50_{armour}$ change by 1% to the sensitivity factor α and probability of failure

6.3.2. STANDARD DEVIATION SENSITIVITIES

Previously, the reliability elasticity coefficients of the mean values of the optimisation factors were investigated. However, a large uncertainty lies in the determination of the standard deviation of parameters. To see the influence that these parameters have on the reliability of the model, the same analysis is made except for the p is σ_i. The results are shown in tables 6.12 to 6.14, for the armour stability, overtopping and toe stability failure mechanism respectively.

Variable, η_i	cot_α	$dn50_{armour}$
e_σ	-0.000622	-0.01126

Table 6.12: Elasticity coefficient e_σ for Armour layer stability

Variable, η_i	cot_α	R_c	w_{crest}
e_σ	-0.01023	-0.0012378	-0.0014728

Table 6.13: Elasticity coefficient e_σ for Overtopping

Variable, η_i	z_{toe}	$dn50_{toe}$
e_σ	-0.04673	-0.107965

Table 6.14: Elasticity coefficient e_σ for Toe stability

Regarding the rock armour stability parameters, slope angle and the armour size, the standard deviation of the armour size is significantly more influential than the standard deviation of the slope angle, even though the standard deviation of the slope angle is much larger than that of the armour size. Meanwhile, for the overtopping failure mechanism, the standard deviation of the slope angle is most influential, while they all fall in the same range. Regarding the toe stability, a similar observation is drawn as the one for the armour size. Moreover, the effect of the toe armour size standard deviation is significantly larger than the standard

deviation of the other parameters. This is possibly due to the closeness of the order of magnitude of the mean value and the standard deviation of the toe armour size.

6.3.3. EFFECT OF THE MODEL UNCERTAINTIES ON THE PROBABILITY OF FAILURE

Previously, the influence and the sensitivity of the resistance parameters on the probability of failure was investigated. This showed the effect of the mean values and their default standard deviations on the cost optimal solution. However, a greater uncertainty lies in the inputs of the mean values and the standard deviations of the model uncertainty parameters. Subsequently, the effect thereof is investigated in the section. Some of the uncertainty parameters have already been determined and investigated. These are mainly the uncertainty parameters which give an indication of the level of uncertainty that is inherent to the formulas which have been empirically derived. Even though the values for the means and standard deviations of these parameters are fixed, they are quantified with respect to this model. These uncertainty parameters are the following:

- $c_{s,s}, c_{s,pl}, c_{d,s}, c_{d,pl}$, (Armour layer stability)
- γ_{toe}, (Toe stability)
- A, B, C, D, E, (Overtopping)

The uncertainty parameters which are less clearly determined, with more room for interpretation, are more interesting to investigate further. These are the following parameters:

- Wave height uncertainty: X_{H_s}
- Model correspondence uncertainty parameters: $\gamma_{armourstab}, \gamma_{toestab}, \gamma_{overtop}$

MODEL UNCERTAINTIES

The values of the sensitivity factors α_i for the model uncertainty parameters are shown in Tables 6.4 to 6.6. Within the specified empirical function for armour layer stability, the c_{sw} has a significant share in the reliability of the model. It has a negative value, meaning a large share in the resistance of the model. The value γ_{toe} is relatively twice or three times smaller than the effect of the environmental conditions and the statistical uncertainty, and also contributing to the resistance. The value for C is contributing to the load in the model and is relatively smaller than the effect of the statistical uncertainty and the environmental variable effects. D is more significant and contributing to the resistance. These values represent the uncertainty in the empirical formulas. Especially, in armour layer stability and overtopping they contribute largely to the overall reliability of the model. The indication of a large contribution to the reliability and uncertainty of the empirical model, means that the fit contains a very large uncertainty and spread. Notably, the uncertainty follows through in the possibility of different outcomes. This can be considered when performing model tests.

The values of the omission factors η_i for the model uncertainty parameters are shown in Tables 6.7 to 6.9. It can be concluded that none of these parameters can be considered deterministic. This would also not make any sense since these parameters account for inherent uncertainties and fit the empirical formula on deviating outcomes.

STATISTICAL UNCERTAINTY

An initial indication of the sensitivity of the wave uncertainty parameter

Failure mechanism statistical uncertainty factor	Sensitivity factor for uncertaintyα_i, $\frac{d}{dXhs}$
Toe stability	0.478
Armour layer stability	0.432
Overtopping	0.477

Table 6.15: Sensitivities of the statistical uncertainty to the total probability of failure for the serviceability limit state

The statistical uncertainty is investigated by quantifying the increase in the sensitivity of the uncertainty parameter X_{H_s}. This increase in sensitivity is basically an increase in contribution to the total reliability. In Section 6.3.1, an error of 8 to 16% is found on the reliability of the model, if considered deterministic.

However, the standard deviation of the uncertainty factor X_{Hs} ranges from 0.05 to 0.15, which indicates a large range of uncertainty. To quantify its effect, the standard deviation is changed by 1%, determining the reliability elasticity coefficient. The increase in probability of failure is also expected since an increase in standard deviation is equally in line with an increase in uncertainty of the random variable.

Variable, ς_i	Armour layer stability	Overtopping	Toe stability
e_σ	-0.0678	-0.0956	-0.1102

Table 6.16: Elasticity coefficient e_σ for X_Hs

Table 6.16 shows the values for the reliability elasticity coefficients. The change in standard deviation by 1% has the most impact on the reliability of the toe stability. In Figure 6.8 the effect of a 1% change in the standard deviation of the given parameter on the probability of failure of rock armour is shown. If a life time of 25 to 100 years is considered a 1% change indicates a ±0.01 change in probability of failure, which is a considerable change, given for instance a target probability of failure of 0.2.

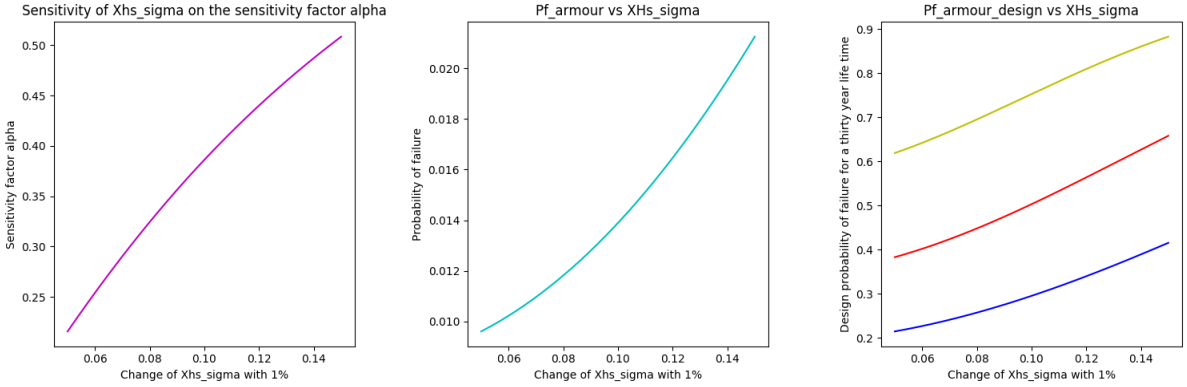

Figure 6.8: Sensitivity reliability index β when changes in standard deviation are made

MODEL CORRESPONDENCE UNCERTAINTY

The same approach which is followed in Section 6.3.3 is handled for the sensitivity analysis of the standard deviation of the model uncertainty correspondence factor. The results of the reliability elasticity coefficients are shown in Table 6.17.

Variable, ς_i	$\gamma_{armourstab}$	$\gamma_{overtop}$	$\gamma_{toestab}$
e_σ	-0.0668	-0.0027	-0.0815

Table 6.17: Elasticity coefficient e_σ for MCU values

Compared to the wave uncertainty parameter, the overtopping model correspondence uncertainty parameter is much less influential. The influence of the toe stability factor and armour stability are in the same range.

6.4. PROBABILISTIC METHOD SENSITIVITIES

6.4.1. MONTE CARLO COMPUTATION TIME SENSITIVITY ANALYSIS

Monte Carlo calculations use random sampling approach, by performing N simulations, which gives a different probability of failure each run, depending on the sampling size (N) and on the target coefficient of variation (COV). The number of simulations N is determined in function of the number of significant digits with which one wants to calculate Pf or based on the relative accuracy (Jonkman et al., 2015).

Thus a larger number of simulations and a more defined target coefficient of variation leads to a more accurate result of the prediction of the probability of failure. However, a larger sampling size also leads to a larger

computation time. Especially in cases where a large number of options need to be calculated, this can be a very time consuming operation. A sensitivity study is done in order to know the computation time of a larger sample size and a smaller coefficient of variation. This is done by performing one calculation of only a single slope structure with the CMC analysis for different settings. A sample size range is given as follows: 1000, 10000 and 100000. The coefficient of variation is varies by: 0.1, 0.05 and 0.01. The effect of different target coefficient of variations and sample sizes in contrast to the accuracy of the results and the computation time, is shown in table 6.18.

COV / Sample size	1000	10000	100000
0.1	Accuracy: 3 dec Time: 0.840 s	Accuracy: 3 dec Time: 1.852 s	Accuracy: 3 dec Time: 1.956 s
0.05	Accuracy: 3 dec Time: 0.813 s	Accuracy: 3 dec Time: 4.237 s	Accuracy: 4 dec Time: 6.411 s
0.01	Accuracy: 3 dec Time: 0.807 s	Accuracy: 4 dec Time: 4.982 s	Accuracy: 4 dec Time: 48.58 s

Table 6.18: Time and accuracy sensitivity of Crude Monte Carlo analysis of only structure option

From Table 6.18, it can be concluded that a sample size of 100000 with a COV of 0.01, takes the largest amount of computation time, but it is also most accurate. This can be a desirable setting for a very small amount of calculations, where a more thorough view is needed on the probability of failure. The calculations with a COV of 0.1 only have an accuracy of 3 decimals, and it does not become more accurate by increasing the sample size. A, more accurate result with a considerable acceptable amount of computation time would be either a calculation with a sample size of 10000 and a COV of 0.01 or a sample size of 100000 and a COV of 0.05. The first option is more beneficial in terms of time and variation. Calculations with 1000 samples can be done for large amounts of calculations and a first glance.

6.4.2. FORM CONVERGENCE

In the FORM outputs, if a probabilistic analysis is performed, possibly a NaN (Not a Number) value can be produced. This is an indication that the FORM analysis could not produce a probability of failure. This issue is largely due to the problem of non-covergence. Generally, a function which is linear or weakly non-linear, would reach convergence after a couple of iterations. However, when this non-linearity increases, the sequential points during iteration may not reach convergence (Yang et al., 2006). The FORM convergence for each iteration is defined by a convergence tolerance. If this is not met, the simulation stops. In order for highly non linear limit state functions to reach the convergence criterion, a smaller step size needs to be chosen (Mínguez et al., 2006). However, the script follows the Armijo rule for determining the step size and can therefore not be altered. Hence, if a highly non-linear limit state function is entered, such as the overtopping limit state function, it is recommended to use the CMC analysis.

6.5. RESULT KEYPOINTS

PROBABILITY OF FAILURE DISTRIBUTION OVER DIFFERENT FAILURE MECHANISMS

- Even though a smaller footprint is realised, the costs do not differ that much for an almost equal probability of failure.
- It seems that by increasing or decreasing the slope angle,the influence in the rate of change on the overtopping failure mechanism is more significant than the rate of change in the probability of failure of the armour stability mechanism.

PROBABILITY OF FAILURE SENSITIVITY ANALYSIS

- The armour unit sizes are the most influential parameter with regard to the probability of failure. Even though in this research a standard grading is followed, for other rubble mound elements this can be significant.
- Toe height is bounded by the ht/h parameter. It is concluded that a step size of 10 cm is within a good range.
- With regard to the settings and failure mechanisms used in this research, the crest height step size is best set at 20 cm and the crest width at 50 cm.
- From the alpha values it can be confirmed that the environmental variables and the uncertainty factors have the most influence on the reliability of the limit state function.
- The model uncertainties indicate a large contribution to the uncertainty of the empirical model, which means that the fit contains a very large spread. This uncertainty or output spread within certain bounds can be considered when performing model tests.
- From the omission factors it seems that the optimisation parameters do not necessarily have to be randomly distributed and can also be considered deterministic.
- From the elasticity coefficient it is observed that once again the armour unit sizes have the largest impacts. The toe parameters and toe failure mechanism as a whole as well. Within the overtopping FM the crest height has the largest influence.
- Compared to the wave uncertainty parameter, the overtopping model correspondence uncertainty parameter is much less influential. The influence of the toe stability factor and armour stability are in the same range.
- From both the statistical uncertainty and the model correspondence uncertainty. The change in 1% of the standard deviations can inflict large change in probability of failure over a long structure life time.

SENSITIVITY OF PROBABILISTIC APPROACHES

- The FORM analysis does not perform consistently for non-linear functions. Therefore, if such a function is considered, CMC is recommended.
- FORM is faster than the CMC analysis.
- It is found that the best settings for the CMC analysis are either 10000 samples and a COV of 0.01 or 100000 samples and a COV of 0.05.

7

Discussion, Conclusions & Recommendations

7.1. Discussion

The model is validated and applied to a case study. With a sensitivity analysis the effects of the several parameters on the probability of failure are quantified. These analyses are all bounded by an initial set of design boundaries, which are discussed in Chapters 1 and 3. In the introduction and background information, a few studies have been mentioned regarding parametric engineering, optimisation techniques and sensitivity analyses. In this discussion, this research is compared to those studies, and it is discussed how this fits into the current scientific knowledge. Furthermore, this discussion reflects on the limiting effects which several of the inflicted design boundaries have on the results.

7.1.1. Scientific reflection

Primarily, the optimisation techniques, which have already been implemented by for instance (Castillo et al., 2006; Mínguez et al., 2006), consider an optimisation technique towards a global optimal cost design. In these researches, it is assumed that a single solution is an optimal solution. This research shows that the optimal solution can differ with a slight difference from the second optimal solution. By converging towards only a single solution, many other options are neglected, thereby losing insight and transparency in the design process and other alternatives. Furthermore, the comparisons and the insight into the ratio between different failure mechanisms are lost within these optimisation techniques. These optimisation techniques also do not consider the sensitivity of certain parameters in advance, only afterwards. With this model, these considerations can be considered in advance.

Parametric design applied to breakwaters and revetments is still developing. This model generates multiple solutions and integrates a probabilistic design method, which is currently still lacking in scientific knowledge. Only the work of (A. Vittal Hegde and Bhat, 1998), proposes a parametric algorithm. Their approach is the first proposal towards a parametric model for the design of rubble mound breakwaters. They state that predecessors did not take into account all of the parameters. Although they aimed to do so, they did not take into account multiple failure mechanisms and only considered Hudson and Van der Meer formulas. This research contributes well to their initiative.

Regarding the sensitivity analyses conducted in the same studies, a correspondence is found between the overtopping sensitivity studies of (Mínguez et al., 2006) and the sensitivity studies in this research. They both state that the crest height or freeboard is the most influential parameter in the reliability of the overtopping failure mechanism. The reliability elasticity coefficient has not been widely used, only in (Sørensen, 2004; Poulsen et al., 2012). It does, however, prove to be a good indicative and should be implemented in further studies regarding the combination of a FORM and sensitivity analysis.

7.1.2. RESULT ANALYSIS AND LIMITATIONS

FAILURE MECHANISMS

Three failure mechanisms are considered: overtopping, armour layer stability and toe stability. In order to represent these failure mechanisms only three design formulae are chosen, namely one formula per mechanism. These formulas only represent a small part of a real revetment or breakwater. Furthermore, only rock armour is considered. But many other rubble mound elements exist and are used such as accropodes and concrete blocks. As a result, the model contains the following limitations:

- Only a small number of elements are included which compromises the applicability range of the model. Similarly, the input flexibility for the engineer is limited.
- The total probability of failure is does not necessarily include the governing failure mechanism within a system, since the latter is a simplification.

LIMIT STATE EQUATIONS

In the model, the limit state equations are constructed in a particular way. The admissible overtopping is compared to the calculated overtopping. In this limit state equation, the overtopping is a quantification of damage. The exceedance of this limit state equations shows to what extend the failure mechanism is subject to damage. The toe stability and armour layer stability limit state equations are constructed differently. They compare the required armour unit sizes to the chosen armour unit size. Alternatively, this can be restructured to the damage number. This represents a more correct limit state equation. Consequently, damage distributions can be extracted, from which an engineer can derive more meaningful conclusions.

MODEL SIMPLIFICATIONS

In this research, assumptions and simplifications are made, because of time and workload restrictions. The main simplifications are described below:

- The geometries functions are simplified versions of actual dimensions and sizes of certain structural elements.
- The cost function is a function of the geometry functions and therefore contain an inherent simplification.
- Armour unit costs, or cost per rock grading, increases as the rock grading sizes increase. This effect is not considered. Each rock grading is equally priced.
- Filter layer rules are not included. A simplified rule is applied. This means that the rock gradings of the under layer and the core are a simplified function of the armour layer rock grading.
- The probabilities of failure are considered fully dependent. Actual representation of the correlation between different failure mechanisms is not represented.

The costs and volumes are thus a mere simplification of a real configuration. Consequently, the sketches which are generated by the model are representations of a revetment which would not be fit for construction.

VALIDATION

The extent of the integrated design process has been validated through a single case study only. Even though the case study has confirmed the integrated design process of the model by comparison of the output, it remains only a single comparison. Thus, for more reliable conclusions, multiple case studies with different environmental conditions should be tested. Furthermore, from Chapter 5, it is found that not all input is known or poorly documented; this makes the model less profitable in the preliminary design phase as it increases the level of uncertainty in the input. This is especially present in the input for the probabilistic analysis, i.e. unknown distributions and standard deviations.

MODEL APPLICATION

From the model application multiple limitations are derived as a result of a single case with predetermined design decisions. The main limitations and assumptions are described below:

- In this case the probability of failure indicates the probability that the structure is subjected to moderate damage. Alternatively, a case is preferred to test the model application to total failure.
- The application comparisons show that the armour layer stability is definitely going to fail on moderate damage as larger rock size are not included in the design. Conclusions regarding the complete reliability of the structure is therefore not possible. A case with milder environmental conditions should therefore be applied.
- The optimal design configurations are only optimal within the materialisation of the design. An engineer also needs to other design requirements, such as the constructability of the design which can lead to alternative solutions.
- A target lifetime of 30 years is chosen. This is an assumption by the author, because actual information on this matter was not available. Alternative design lifetimes result in different allowable probabilities of failure, i.e. different optimal solutions.

OPTIMISATION

The output of the model remains a product of the input of the engineer and should therefore always be revised. Moreover, the solution set still contains a very large amount of possible designs. This is one of the downsides as well as one of the assets for a parametric engineer. While many different solutions are generated, one could not analyse them all. Therefore, the optimisation technique proposes a promising start towards narrowing down such large data sets. However, it still very brute-forced and a crude technique. It consumes more time as new data sets are made. This should be approached with a smarter and softer solution. It does, however, use the deterministic and probabilistic approach together as some sort of importance sampling technique, by first determining the deterministic optima and then probabilistic calculations and selection.

SENSITIVITY ANALYSIS

The outputs of the sensitivity analysis are determined by order of magnitude of the inputs between the mean and standard deviation of the variables. Since this is only done for a single solution, it is not safe to say that these sensitivities are such completely reliable values. Additionally, when other failure mechanisms or design formulae are implemented, the approach in this research could be used to study the mutual relationships and proportions. However, the outputs of the sensitivity analysis are now only done for the serviceability limit state; this is simply limited research and should be investigated for other limit state functions as well.

7.2. CONCLUSIONS

The main objective of this research is described as follows:

> "Develop a model which parametrically determines multiple configurations of a rubble mound slope protection also integrating a probabilistic design method to account for multiple different uncertainties."

From this objective, three research questions are established:

1. Is it feasible to create a parametric design-tool, which simultaneously incorporates a probabilistic approach, for the preliminary design of a rubble mound slope protection?
2. What are the advantages of the integration of the probabilistic analysis in the proposed model as opposed to the current design process?
3. What is the practical added value of the model in the design process?

Based on these questions, the conclusions of the main findings in this research are explained.

IS IT FEASIBLE TO CREATE A PARAMETRIC DESIGN-TOOL, WHICH SIMULTANEOUSLY INCORPORATES A PROBABILISTIC APPROACH, FOR THE PRELIMINARY DESIGN OF A RUBBLE MOUND SLOPE PROTECTION?

The model shows promising results, and it can be concluded that a parametric design-tool is feasible. The integration of different failure mechanisms and simultaneously calculating their limit state functions with a single input is completed for the armour layer stability, overtopping and toe stability. This model shows that full integration is a very complex structure and design method, due to many interdependencies and implications, but it can be achieved in time. Moreover, the question is twofold, concerning the integration of the probabilistic approach, it can also be safely concluded that this has been successfully implemented in the model as well. The model integrated both FORM and a Monte Carlo method. Furthermore, also a conventional method, which incorporates uncertainty, is implemented. Below a few key findings regarding the feasibility of the model are explained:

Feasibility of parametric design-tool and model integration:

- The model has been validated on many different elements, which provides a basis for further validation.
- The model successfully incorporates three different failure mechanisms and provides a basis for further implementation of different empirical formulae and other failure mechanisms.
- Two different probabilistic tools are fully integrated into the model. However, the accuracy setting still needs to be manually altered in the code.
- In Chapter 5, the model is successfully applied to a case study design comparison, even though not all failure mechanisms are considered. This shows it is feasible to apply this model to the preliminary design phase.

WHAT ARE THE ADVANTAGES OF THE INTEGRATION OF THE PROBABILISTIC ANALYSIS IN THE PROPOSED MODEL TO THE CURRENT DESIGN PROCESS?

One of the main problems within the preliminary design phase is the lack of insight in the uncertainties of the preliminary configurations. It is found that by integrating two probabilistic design methods, within an integrated system, it is possible to incorporate different uncertainties, e.g. statistical and model uncertainties flexibly. The main advantage is that an engineer acquires more insight into the reliability of a proposed configuration and also the number of extra costs that come with a more reliable structure. Furthermore, the implementation of both FORM and CMC provide an easy and accessible basis for sensitivity analysis, by, for instance, using the alpha values from the FORM output. Below some key findings are outlined:

Model application:

- The implementation of a probabilistic analysis in this design phase gives more insight into the uncertainty of different configurations. This is observed in the model application where probabilistic approaches show that the structure of the case study is under-dimensioned with respect to the probability of moderate damage. For a more safe structure, the dimensions are different. This results mainly in a slightly higher crest height and larger stone sizes for the toe dimensions.
- Conventionally, from the extrapolated wave height, only a mean value or a slightly higher value is chosen to account for some degree of uncertainty. With a probabilistic analysis the whole distribution can be included which increases the reliability of the configuration.
- The uncertainties in costs can be quantified, and for instance, the probability of failure can be used in the calculation of the maintenance costs.
- From the case study, it is seen that configurations which are composed using the conventional approach can be either under dimensioned or even over-dimensioned. The probabilistic analysis shows if this is the case, and if so, how much extra costs would be required to attain a more reliable structure.

Sensitivity analysis:

- With an incorporated probabilistic analysis, the rate of change which different parameters inflict on the reliability of the model and configurations can be quantified.
- In this research, it is found, from the omission factors that the optimisation parameters do not necessarily need to be randomly distributed. Consequently, this diminished the computation load.
- From the reliability, elasticity factors it is found that the crest width and unit size inflict the largest rate of change in the overall reliability. Furthermore, the probability of the toe stability has the most significant influence.

WHAT IS THE PRACTICAL ADDED VALUE OF THE MODEL IN THE DESIGN PROCESS?

This question is focused on the problem that the current design process is time-consuming and engineers are only able to design a limited amount of configurations. From this research, it can be concluded that the model has proven to tackle these problems successfully. The time consumption of this analysis shows that it can generate many configurations in a short amount of time relative to the time that is currently required, given conventional design tools. This asset is very beneficial for the preliminary design phase, as it provides more insight into different possible configurations for the same input. Additionally, an optimisation scheme promises to give more insight in the output of the model and also a decrease in computation time.

Model application:

- In the case study and from Chapter 5, it can be concluded that the model can generate thousands of different configurations within a few minutes.
- The model gives an insight into the cost-optimal solutions. Converging to a single cost optimal solution, disregards many other possible designs with similar costs and different dimensions.
- This model makes it possible for an engineer to quickly and widely diverge at the start of the design phase and quickly converge to a more optimised design — this way the full spectrum of all possible configurations can be considered. This saves a lot of man-hours, effort and precious time. Moreover, more time can be spent to determine the cost-optimal and most reliable structure rather than relying entirely on expert judgement and the workload of generating just a couple of configurations.

Optimisation:

- The optimisation scheme shows a decrease in computation time and the selection of cost-optimal solutions.
- By decreasing the size of the output, a more precise overview of the output is acquired. On the other hand a decrease in insight is the coupled effect as it does not show the disregarded options, which might very well be applicable too.
- It provides a basis for further research and should not yet be implemented, because a precise understanding of the trade-off between overview and insight is still lacking.

7.3. RECOMMENDATIONS

Within this thesis, three main components are recommended for further research: model enhancements, i.e. expansion and improvement, more elaborate sensitivity analysis and different possibilities regarding optimisation approaches.

7.3.1. MODEL ENHANCEMENT

The improvement of the model is subdivided into three subtopics, the model framework & application, setup and validation.

MODEL FRAMEWORK AND APPLICATION

- The model is a simplified representation of all of the processes and options included in the design of breakwaters and revetments. It only considers three failure mechanisms and only a single empirical formula per failure mechanism. For the model to become more integrated and complete, multiple failure mechanisms should be included, such as scour, settlement and sliding. Furthermore, engineers use different empirical formulae per failure mechanism; therefore, many different formulae should be incorporated.
- The whole geometry is a simplification of either a revetment design or a breakwater design. These structures also include berms, buried toes, rear slopes and different rubble mound materials, such as concrete blocks or accropodes. By considering more geometry options, the model can also be used in the feasibility design phase.
- Apart from the neglected geometries, the considered geometry calculation and configuration should also be further optimised. Such as the toe structure, which does not consider an under layer. Furthermore, the armour layer filter rules are very simplified. In the end, an enhanced specification of the volumes also results in a better representation of the costs.
- The costs function only includes construction costs and maintenance costs. However, in cases of breakwaters or populated hinterlands, downtime costs and potential costs of life should be included as well.

MODEL SETUP

- The adaptability and accessibility should be improved. For instance, the code should be written in classes rather than functions. This enables the user to alter the distributions, offset of probabilistic specifications, such as step size and it makes the PyRe library more accessible.
- The GUI is now made in Microsoft Excel. This is an error sensitive interface and relatively heavy to load each run. To make the input more transparent and professional, a GUI made with Django or another web-framework of choice is recommended.

VALIDATION

- The model is validated on only a single case study. For the sake of reliability of the model, multiple case studies should be done, with different environmental conditions.
- As discussed, environmental parameters such as the wave height and period are correlated. An uncertainty lies in the assumption of them being uncorrelated. Therefore, for a more optimal results the correlation of different environmental variables should be considered as well, for instance through a copula based approach.

7.3.2. OPTIMISATION

- In the sensitivity analysis the omission factor was determined for different parameters. For some variables an omission factor with a small percentile error was observed. By considering these as variables as deterministic variables, the computational load of the probabilistic analysis diminishes. This information could be applied in an optimisation method. It is recommended that the effect of this is further analysed.
- This optimisation technique is a brute-forced technique and does not use smart solutions. Therefore, different optimisation techniques and algorithms could be used, such as a global optimisation in combination with a small step size difference to generate multiple outcomes. Moreover, genetic algorithms or machine learning can be applied as well.

7.3.3. SENSITIVITY ANALYSIS

- The sensitivity analysis is conducted for the serviceability LS only. Other limit states have a different impact on the outcome of the solutions for both probability of failure as for the cost-optimal solutions, due to a difference in allowable damage. For a more reliable sensitivity analysis, thus influence of different parameters, these limit states should be analysed as well.

- The probabilistic analysis is either done in FORM or with CMC and less accurate setting, i.e. smaller amount of samples and a coarser defined coefficient of variation. The reason for this is a lower computation time. However, with the use of cloud computing or multithread processing, multiple cores can be used, resulting in more computation power. This makes it possible to expand analyses. The influence on the accuracy can be analysed in more detail, possibly the effect of which on the costs and probability of failure.

- The sensitivity analysis only incorporates the effects of the optimisation parameters, i.e. slope angle, crest height, and the uncertainty parameters. However, the effects of the environmental conditions, roughness factor, porosity and rock density are not analysed. Especially the environmental conditions contain a significant uncertainty and have an enormous impact on the solution and they should, therefore, be studied in more depth. Likewise, the roughness factor and the porosity differ for different armour stone sizes.

REFERENCES

A. Vittal Hegde, B. S. and Bhat, T. (1998). An Algorithm for Computer Aided Optimum Design of Rubble Mound Breakwaters. *Journal of Coastal Research*, pages 80–87.

Allsop, N. W. H., Oumeraci, H., De Groot, M. B., Crouch, R. S., and Vrijling, J. K. (1999). MAST III / PROVERBS Probabilistic Design Tools for Vertical Breakwaters VOLUME I. Technical report, Technical University of Braunschweig.

Allsop, W., Bruce, T., Allsop, N. W. H., Franco, L., Bellotti, G., Bruce, T., and Geeraerts, J. (2009). Hazards to people and property from wave overtopping at coastal structures. In *HR Wallingford - Working with Water*, volume 1.

Booshi, S. and Ketabdari, M. J. (2016). Parametric Study on Wave Interaction with a Porous Submerged Rubble Mound Breakwater Using Modified N-S Equations and Cut-Cell Method. *International Journal of Maritime Technology*.

Burchart, H. F. (1995). Rubble Mound Breakwater Failure Modes. Technical report, Aalborg Universitet.

Burchart, H. F. and Hughes, S. (2006). Types and Functions of Coastal Structures. In *Types and Functions of Coastal Structures*, chapter 2. Aalborg University, Aalborg.

Burcharth, H., Falk, ., Sørensen, J., Dalsgaard, ., and Kim, S.-W. (2018). Optimum breakwater safety levels based on life-cycle cost optimization. Technical report, Aalborg Universitet.

Burcharth, H. F. and Hughes, S. (2006). Types and Functions of Coastal Structures. In *Types and Functions of Coastal Structures*, chapter 2. USACE.

Burcharth, H. F. and Liu, Z. (1995). Rubble Mound Breakwater Failure Modes. Technical report, Aalborg Universitet.

Burcharth, H. F. and Sørensen, J. D. (2006). On Optimum Safety Levels of Breakwaters. Technical report, Aalborg Universitet.

Castillo, C., Mínguez, R., Castillo, E., and Losada, M. A. (2006). An optimal engineering design method with failure rate constraints and sensitivity analysis. Application to composite breakwaters. *Coastal Engineering*.

Castillo, E., Conejo, A. J., Mínguez, R., and Castillo, C. (2003a). An alternative approach for addressing the failure probability-safety factor method with sensitivity analysis. *Reliability Engineering and System Safety*.

Castillo, E., Losada, M. A., Mnguez, R., Castillo, C., and Baquerizo, A. (2003b). Optimal Engineering Design Method that Combines Safety Factors and Failure Probabilities: Application to Rubble-Mound Breakwaters. *Journal of Waterway, Port, Coastal, and Ocean Engineering*.

CIRIA/CUR (2007a). Chapter 2 - Planning and designing rock works. In *The Rock Manual*, chapter 2. CIRIA, 2007 edition.

CIRIA/CUR (2007b). Chapter 5 - Physical processes and design tools. In *The Rock Manual - version 2007*. CIRIA/CUR.

CIRIA/CUR (2007c). Chapter 6 - Design of marine structures. In *The Rock Manual - version 2007*. CIRIA, en 13383:5–8. edition.

De Smet, L. (2015). *Rubble-mound and caisson breakwaters Excel-based design tool for the assessment of*. PhD thesis, Delft University of Technology.

Deltares (2018). BREAKWAT.

Everts, P. (2016). *Probabilistic Design of a Rubble Mound Breakwater*. PhD thesis, Delft University of Technology.

Galiatsatou, P., Makris, C., and Prinos, P. (2018). Optimized Reliability Based Upgrading of Rubble Mound Breakwaters in a Changing Climate. *Journal of Marine Science and Engineering*.

Genest, C., Kojadinovic, I., Nešlehová, J., and Yan, J. (2011). A goodness-of-fit test for bivariate extreme-value copulas. *Bernoulli*, 17(1):253–275.

Gerding, E. (1993). Toe structure stability of rubble mound breakwaters. Technical report, TU Delft Hydraulic Engineering Group, Delft.

Haldar, A. and Mahadevan, S. (1995). First-order and second- order reliability methods. In C. Sundararajan, editor, *Probabilistic Structural Mechanics Handbook*, chapter 3. Chapman & Hall.

Holmes, S. (2000). RMS Error.

inFERENCe (2015). Idea of the Week: Maximum Spacing Estimation, Gaussianisation and Autoregressive Processes.

Institution of Civil Engineers (Great Britain) (1988). *Design of breakwaters : proceedings of the conference Breakwaters '88 organized by the Institution of Civil Engineers and held in Eastbourne on 4-6 May 1988*. Telford.

Janardhan, P. (2013). *Parametric Studies On Stability Of Reshaped Berm Breakwater With Concrete Cubes As Armor Unit*. PhD thesis, National Institute of Technology Karnataka, Surthkal, Mangalore.

Jeon, B., Kim, J., Lim, K., Choi, Y., and Moon, M. (2017). Calculation of Detector Positions for a Source Localizing Radiation Portal Monitor System Using a Modified Iterative Genetic Algorithm. *Journal of Radiation Protection and Research*, 42(4):212–221.

Jonkman, S. N., Steenbergen, R. D. J. M., Morales-Nápoles, O., Vrouwenvelder, A. C. W. M., and Vrijling, J. K. (2015). *Probabilistic Design: Risk and Reliability Analysis in Civil Engineering Lecture notes CIE4130*. Delft University of Technology, Delft, 1 edition.

Katz, R. W., Parlange, M. B., and Naveau, P. (2002). Statistics of extremes in hydrology. Technical report, Advances in water resources.

Kumar Singh, R., Kumar Singh, S., and Singh, U. (2016). Maximum product spacings method for the estimation of parameters of generalized inverted exponential distribution under Progressive Type II Censoring. *Journal of Statistics and Management Systems*, 19(2):219–245.

Lopez, R. H. and Beck, A. T. (2012). Reliability-based design optimization strategies based on form: A review.

L.P.L. van der Linden (2018). *CIE4210 - Parametric Engineering Lectore Notes*. Delft University of Technology, Delft, 1.0 edition.

Madsen, H. O. (1988). Omission sensitivity factors. *Structural Safety*, 5(1):35–45.

Manoj, N. R. (2016). *First - order Reliability Method : Concepts and Application*. PhD thesis, Delft University of Technology.

Medina, J. R. (1992). Deterministic computer-aided optimum design of rock rubble-mound breakwater cross-sections, by W. de Haan. *Coastal Engineering*, 15(3-4):279–282.

Mínguez, R., Castillo, E., Castillo, C., and Losada, M. A. (2006). Optimal cost design with sensitivity analysis using decomposition techniques. Application to composite breakwaters. *Structural Safety*.

Muttray, M. (2013). A pragmatic approach to rock toe stability. *Coastal Engineering*, 82:56–63.

Naess, A. and Moan, T. (2005). Probabilistic Design of Offshore Structures. In SUBRATA K. CHAKRABARTI, editor, *Handbook of Offshore Engineering*, chapter 5, pages 197–277. Elsevier Science.

Pezzutto, P. (2013). On Floating Breakwaters Efficiency-a 2DV Parametric Based Analysis. Technical report, Universitá degli Studi di Padova.

Pezzutto, P., Ruol, P., and Martinelli, L. (2012). A Parametric Analysis of Dissipation Capacity for {Π}-type Floating Breakwaters. Technical report, Universitá degli Studi di Padova.

Poulsen, A. S., Randers, M. B., and Sørensen, T. (2012). *Probabilistic Design Of Gravity Based Foundations Master's Thesis*. PhD thesis, Aalborg University.

Prudhomme, C., Kundzewicz, Z. W., and Hanel, M. (2010). Methodologies for the space-time development of large-scale floods at the river-basin, regional and continental scales. Technical report, The WACH project, Wallingford.

Puertos del Estado and Ministerio de Fomento, S. (3002). Procedimiento general y bases de calculo en el proyecto de obras maritimas y portuarias. *ROM 0.0*, pages 1–30.

Royal HaskoningDHV (2018). Royal HaskoningDHV - Company profile.

Schiereck, G. J. and Verhagen, H. (2012). *Introduction to Bed, bank and shore protection*. VSSD, Delft, 2nd editio edition.

Schnabel, M. A. (2012). Learning Parametric Designing. In *Computational Design Methods and Technologies*. The Chinese University of Hongkong.

Schüttrumpf, H., Kortenhaus, A., Fröhle, P., and Peters, K. (2008). ANALYSIS OF UNCERTAINTIES IN COASTAL STRUCTURE DESIGN BY EXPERT JUDGEMENT. Technical Report August, Chinese-German Joint Symposium on Hydraulic and Ocean Engineering, Darmstadt.

Simm, J. (2005). Breakwaters and Closure Dams. *Maritime Engineering*, 157(3):143–143.

Singh, U., Singh, S. K., and Singh, R. K. (2014). A Comparative Study of Traditional Estimation Methods and Maximum Product Spacings Method in Generalized Inverted Exponential Distribution. *Journal of Statistics Applications & Probability*, 3(2):153–169.

Sørensen, J. D. (2004). Structural Reliability. In *Notes in Structural Reliability Theory And Risk Analysis*, chapter 2. Aalborg University, Aalborg.

van der Meer, J., Allsop, N., Bruce, T., De Rouck, J., Kortenhaus, A., Pullen, T., Schüttrumpf, H., Troch, P., and Zanuttigh, B. (2018). EurOtop Manual. Technical report, EurOtop.

van der Meulen, T., Schiereck, G. J., and d'Angremond, K. (1996). Toe stability of rubble mound breakwaters. In *Coastal Engineering*, chapter 153. Delft University of Technology, Faculty of Civil Engineering, Delft.

Verhagen, H., d' Angremond, K., and van Roode, F. (2009). *Breakwaters and closure dams*. VSSD, Delft, 2nd edition.

Verhagen, H. and Van den Bos, J. (2018). Breakwater design: Lecture notes CIE5308.

Wicklin, R. (2017). The method of moments: A smart way to choose initial parameters for MLE.

Yang, D., Li, G., and Cheng, G. (2006). Convergence analysis of first order reliability method using chaos theory. *Computers and Structures*, 84(8-9):563–571.

Zhao, Y.-g. and Ono, T. (1999). A general procedure for First / second-order reliability method (FORM / SORM). *Structural Safety*, 21:8–9.

A

APPENDIX A

A.1. DESIGN PHASING

Design Phase	Explanation
Problem understanding	Functional requirements Performance criteria Constraints: budget, access, materials, environment, maintenance Available materials
Information requirements	Hydraulic conditions (e.g. waves, currents, water levels) Bathymetry and topography Ground conditions Structure layouts and types
Conceptual design	Identify information requirements Review project feasibility Analytical studies and modelling
Preliminary design	Assess alternatives against performance criteria and constraints Cost estimates Compare alternatives (technical, environmental and economic)
Detailed design	Calculate detailed structure dimensions Design transitions, end protection, drainage, services, etc.
Implementation	Construction Monitoring
Operation	Maintenance Decommissioning or removal

Table A.1: Design phases

A.1.1. COMPANY INVOLVEMENT - ROYAL HASKONINGDHV

Currently, Royal HaskoningDHV is planning on investing more in innovation. This includes providing services and automation technologies. This technological innovative mindset is being pursued throughout the whole company, including the coastal protection business and breakwater and revetment design. Momentarily it is being investigated if it is possible to create an automated design tool which would help the design process of breakwaters and revetments. This is an initiative which connects well to this research. This tool generates deterministic designs of breakwater cross-sections.

B

APPENDIX B

B.1. FAILURE MECHANISMS

Hazard type and reason	Mean discharge q (l/s per m)	Max volume V_{max} (l per m)
Rubble mound breakwaters; H_{m0} > 5 m; no damage	1	2,000-3,000
Rubble mound breakwaters; H_{m0} > 5 m; rear side designed for wave overtopping	5-10	10,000-20,000
Grass covered crest and landward slope; maintained and closed grass cover; H_{m0} = 1 – 3 m	5	2,000-3,000
Grass covered crest and landward slope; not maintained grass cover, open spots, moss, bare patches; H_{m0} = 0.5 – 3 m	0.1	500
Grass covered crest and landward slope; H_{m0} < 1 m	5-10	500
Grass covered crest and landward slope; H_{m0} < 0.3 m	No limit	No limit

Figure B.1: Limits for wave overtopping for structural design of breakwaters, seawalls, dikes and dams (van der Meer et al., 2018)

Hazard type and reason	Mean discharge q (l/s per m)	Max volume V_{max} (l per m)
Significant damage or sinking of larger yachts; H_{m0} > 5 m	>10	>5,000 – 30,000
Significant damage or sinking of larger yachts; H_{m0} = 3-5 m	>20	>5,000 – 30,000
Sinking small boats set 5-10 m from wall; H_{m0} = 3-5 m Damage to larger yachts	>5	>3,000-5,000
Safe for larger yachts; H_{m0} > 5 m	<5	<5,000
Safe for smaller boats set 5-10 m from wall; H_{m0} = 3-5 m	<1	<2,000
Building structure elements; H_{m0} = 1-3 m	≤1	<1,000
Damage to equipment set back 5-10m	≤1	<1,000

Figure B.2: General limits for overtopping for property behind the defence (van der Meer et al., 2018)

Hazard type and reason	Mean discharge q (l/s per m)	Max volume V_{max} (l per m)
People at structures with possible violent overtopping, mostly vertical structures	No access for any predicted overtopping	No access for any predicted overtopping
People at seawall / dike crest. Clear view of the sea.		
H_{m0} = 3 m	0.3	600
H_{m0} = 2 m	1	600
H_{m0} = 1 m	10-20	600
H_{m0} < 0.5 m	No limit	No limit
Cars on seawall / dike crest, or railway close behind crest		
H_{m0} = 3 m	<5	2000
H_{m0} = 2 m	10-20	2000
H_{m0} = 1 m	<75	2000
Highways and roads, fast traffic	Close before debris in spray becomes dangerous	Close before debris in spray becomes dangerous

Figure B.3: Limits for overtopping for people and vehicles (van der Meer et al., 2018)

Instability of armour layer units can be a consequence of a number of events.

- Displacements in multilayer armour units around SWL causes underlayer and core to erosion. Subsequently an S-profile develops which will result in wash-down of the crest of the structure. This failure development is rather slow
- A similar mechanism can occur for single layer units. In case a large portion of armour layer units is displaced, the underlayer of core is exposed. Subsequently, erosion in these layers can occur which eventually leads to armour layer erosion.
- Breakage of armour units, due to wave and gravity stresses, can cause exposure to less reinforced lower layers and failure.
- Deterioration due to temperature, abrasion or chemical reactions can cause the same process of failure.
- A premature failure of the toe berm can also cause a failure in the armour layer. since the toe berm serves as a means of support for the armour layer. Failure in starts in the shoulder of the toe and spreads to foot of armour layer. When total failure of toe, the armour layer can start to slide off.
- Similarly, if seabed scour occurs the armour layer can experience sliding and eventual failure.
- Lastly, pore pressure build up in core leads to either lifting of a proportion or entire armour layer, or lifting of single slab units. This exposes the underlayers to erosion (Burchart and Hughes, 2006).

B.2. RELIABILITY ANALYSIS

B.2.1. FORM II ANALYSIS

$$N(\mu_R - \mu_S, \sqrt{\sigma_R^2 + \sigma_S^2}) \tag{B.1}$$

The probability of failure is then defined as shown by equation B.3.

$$p_f = P(Z < 0) = \phi\left[\frac{0 - \mu_R - \mu_S}{\sqrt{\sigma_R^2 + \sigma_S^2}}\right] = \phi(-\beta) \tag{B.2}$$

with,

$$\beta = \frac{\mu_Z}{\sigma_Z} = \frac{\mu_R - \mu_S}{\sqrt{\sigma_R^2 + \sigma_S^2}} \tag{B.3}$$

In case of a non-linear limit state function, then the equation can be linearized with by means of Taylor series approximation. Hence, first order approximation. This is also referred to as Mean Value First order second

moment method (MVFOSM). However, this method has some limitations. Such as, marginal distributions are ignored, truncation errors and errors induced by how the limit state function is formulated (or the invariance problem) (Haldar and Mahadevan, 1995).

B.3. PARAMETRIC APPROACH

(Pezzutto et al., 2012) firstly studied the dissipation capacity for π-type floating breakwaters by conducting a parametric analysis. He defined two non-dimensional parameters, χ and s, which he would then manipulate in order to determine the dissipation coefficient of a floating breakwater. The results and effects of the manipulations are validated and studied by conducting physical tests and not by programmed outcomes. Pezzutto continued his work in a research on the efficiency of floating breakwater based on a 2DV parametric analysis (Pezzutto, 2013).

(Janardhan, 2013) conducted a research on the possibilities for an optimum berm breakwater solution. The structural stability and economy in construction of breakwater were measurements for this predetermined optimum. Therefore, for an optimum solution, the berm breakwater should be constructed with small size armour units. By influencing various sea state and structural parameters on the stability of statically stable reshaped berm breakwater made of concrete cube armour, an optimum was sought. To validate or determine this optimum, physical tests were carried out.

(Booshi and Ketabdari, 2016) also conducted in a parametric analysis, using modified N-S equations and cut-cell method. It touched the topic of wave interaction with porous submerged rubble mound breakwaters. It showed that an increase and decrease in certain parameters, would induce a phase lag between incident and transmitted waves. Subsequently, other parameters were manipulated to gather more intelligence on a proposition for future design criteria. The validity was investigated based on the comparisons with the available experimental data.

C

APPENDIX C

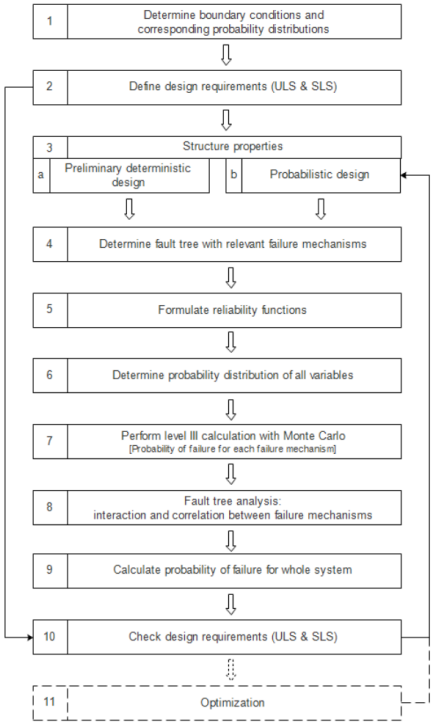

Figure C.1: Full probabilistic design process (Allsop et al., 1999)

Overtopping equation for shallow foreshores

$$\frac{q}{\sqrt{g \cdot H_{m0}^3}} = 0.21 \cdot \exp\left[-\left(1.5 \frac{R_c}{(0.33 + \xi_{m-1,0} 0.022) \cdot H_{m0} \cdot \gamma_f \cdot \gamma_\beta} \right)^{1.3} \right] \tag{C.1}$$

Limit state function overtopping

$$Z_{overtopping} = q_{adm} - \sqrt{g \cdot H_{m0}^3} \cdot \frac{0.023}{\sqrt{\tan \alpha}} \gamma_b \cdot \xi_{m-1,0} \cdot \exp\left[-\left(2.7 \frac{R_c}{\xi_{m-1,0} \cdot H_{m0} \cdot \gamma_b \cdot \gamma_f \cdot \gamma_\beta \cdot \gamma_v} \right)^{1.3} \right] \tag{C.2}$$

Limit state function armour layer stability

$$Z_{armour} = d_{n50} - \frac{H_s}{\Delta \cdot c_{pl,d} \cdot P^{0.18} \cdot \left(\frac{S_d}{\sqrt{N}}\right)^{0.2} \cdot \xi_s^{-0.5}} \quad \text{(Plunging breakers)} \tag{C.3}$$

Limit state function toe stability

$$Z_{toe} = d_{n50} - \frac{H_s}{\Delta\left(2 + 6.2 \cdot \left(\frac{h_t}{h}\right)^{2.7}\right) \cdot N_{OD}^{0.15}} \quad \text{for} \quad 0.4 < \frac{h_t}{h} < 0.9 \tag{C.4}$$

Table 5.24 *Range of validity of parameters in deep water formulae by Van der Meer (1988b)*

Parameter	Symbol	Range
Slope angle	$\tan\alpha$	1:6–1:1.5
Number of waves	N	< 7500
Fictitious wave steepness based on T_m	s_{om}	0.01–0.06
Surf similarity parameter using T_m	ξ_m	0.7–7
Relative buoyant density of armourstone	Δ	1–2.1 [1]
Relative water depth at toe	$h/H_{s\text{-}toe}$	> 3 [2]
Notional permeability parameter	P	0.1–0.6
Armourstone gradation	D_{n85}/D_{n15}	< 2.5
Damage–storm duration ratio	$S_d/\sqrt{N}$	< 0.9
Stability number	$H_s/(\Delta D_{n50})$	1–4
Damage level parameter	S_d	$1 < S_d < 20$

Figure C.2: Range of validity armour layer stability formulae for deep water (CIRIA/CUR, 2007b)

C.1. INPUT FILE / EXCEL GUI

The input file consists of seven input sheets. These are categorised in the following categories:

- Probabilistic input values
- Hydraulic boundary conditions
- Geometric variables
- Restrictional variables
- Fixed and variable parameters
- Costs
- Uncertainty

Table 5.26 *Range of validity of parameters in Van der Meer formulae for shallow water conditions*

Parameter	Symbol	Range
Slope angle	$\tan \alpha$	1:4–1:2
Number of waves	N	< 3000
Fictitious wave steepness based on T_m	s_{om}	0.01–0.06
Surf similarity parameter using T_m	ξ_m	1–5
Surf similarity parameter using $T_{m-1,0}$	$\xi_{s-1,0}$	1.3–6.5
Wave height ratio	$H_{2\%}/H_s$	1.2–1.4
Deep-water wave height over water depth at toe	H_{so}/h	0.25–1.5
Armourstone gradation	D_{n85}/D_{n15}	1.4–2.0
Core material – armour ratio	$D_{n50\text{-}core}/D_{n50}$	0–0.3
Stability number	$H_s/(\Delta D_{n50})$	0.5–4.5
Damage level parameter	S_d	< 30

Note

For further details on the field of application in terms of water depths, see overview in Tables 5.28 and 5.29.

Figure C.3: Range of validity armour layer stability formulae for shallow water (CIRIA/CUR, 2007b)

USER INPUT

In the file the user is required to specify the values for different variables. These are case specific and should be altered accordingly. For instance in the hydraulic boundary conditions variables such as the wave height, period, water levels and bed levels should be specified. In the geometry section, the user is required to specify the lower bound, upper bound and step size of the different geometry parameters. If a single value is desired, this can be done by setting the lower and upper bound to the same value. In the sheet, the cell colour shows which variables are alterable and which are not. Green means alterable and grey means locked. A more thorough analysis and interpretation of the input sheets in given in Appendix D.

DEFAULT VALUES

As mentioned above, some of the sheets contain grey fields. These grey fields are not alterable and contain default values. These default values are for instance standard inputs for different limit state functions. They are portrayed with the intention to clearly and transparently show the input of the model. This way the user can determine whether or not they are satisfied with the input and how they react on this. Furthermore, some assumptions are made, regarding the uncertainties and probability distribution function for example. These can be seen as well.

PYTHON INPUT DIRECTORY

This file contains the following python scripts:

- Input values
- Variable files (for hydraulic boundary conditions, geometric variables, fixed variables, etc.)
- Damage number armour
- Damage number toe
- Rockgradings

The excel input file is subsequently imported into the Python model. The model recognises the indexes specified in the excel file. Thus, it recognises the input values by name, instead of recognition by cell. This is

realised by a simple pandas module function. The main advantage is that in case a value is moved in the excel file, that model still recognises the input value. Once imported the input values are assigned to corresponding names in the variable files for further use.

The damage numbers are a function of the predetermined limit state and alpha value of the slope. Thus the limit state and slope angle which are specified in the excel input file and translated in the python, is now imported in the damage number files. With if statements a function is made to determine the damage number. The function can be called in another file for further use (Simm, 2005).

PYTHON: BOUNDARY CONDITIONS DIRECTORY

This directory contains three scripts which calculate the following:

- A composite Weibull distribution function
- A script which determines if the it is a deep or shallow water case
- A script which determines whether the waves are plunging or surging waves

The latter two scripts are simply function which are callable in a later stadium. However, the Composite Weibull distribution function is a user input option. It determines the significant wave height H_s and the 2% exceedence wave height $H_{2\%}$, based on the mean spectral wave height H_{m0}. Certainly, if these inputs are known prematurely, there is no need for this function. Moreover, if this equation is not desired, a simple conversion ratio can also be applied, to the users desire.

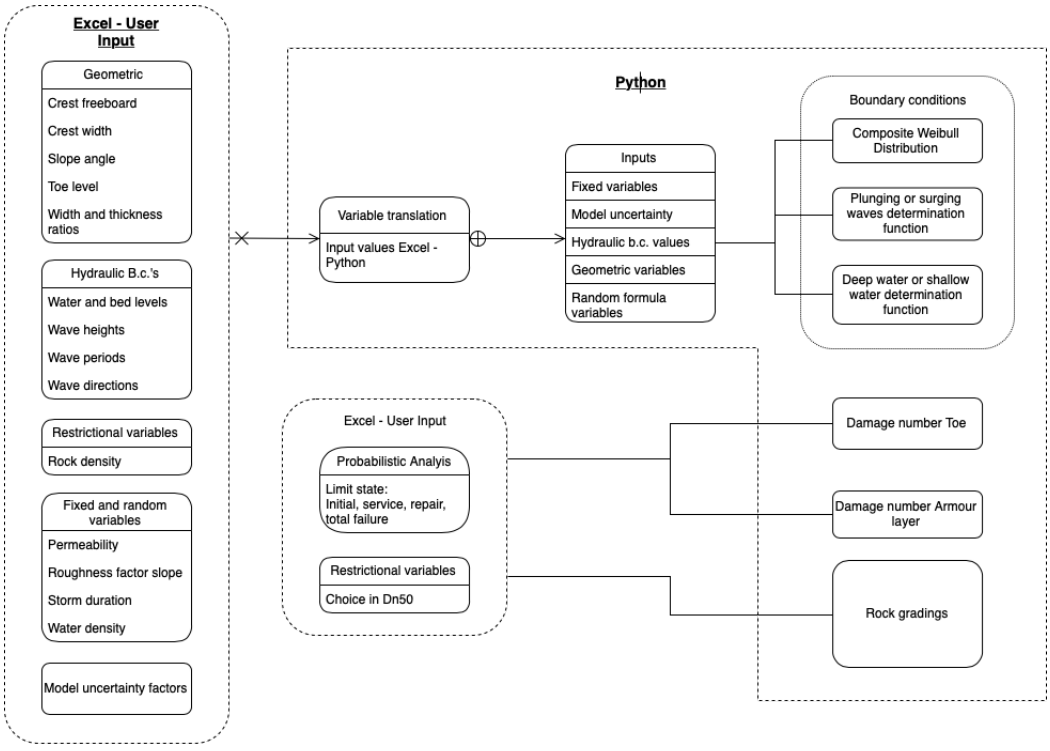

Figure C.4: Model implementation inputs

C.2. PYTHON: FAILURE MECHANISMS AND LIMIT STATE FUNCTION DIRECTORIES

In this directory multiple scripts are composed. Each representing a limit state functions of different failure mechanisms. These are devided in the following scripts:

- Overtopping LSF's

- Armour layer stability - Surging waves SW LSF's
- Armour layer stability - Surging waves DW LSF's
- Armour layer stability - Plunging waves SW LSF's
- Armour layer stability - Plunging waves DW LSF's
- Toe stability LSF's

Each of these scripts contain multiple limit state functions; a deterministic LSF, a probabilistic LSF and a probabilistic LSF containing a model correspondence uncertainty factor.

In the Excel input sheet it can be specified, which approach is desired. If a deterministic approach is desired, the model automatically imports the deterministic LSF of each failure mechanism. Idem for the other options. Note that for the armour layer stability, the boundary conditions scripts need to be read, in order to define the the wave type and water level conditions.

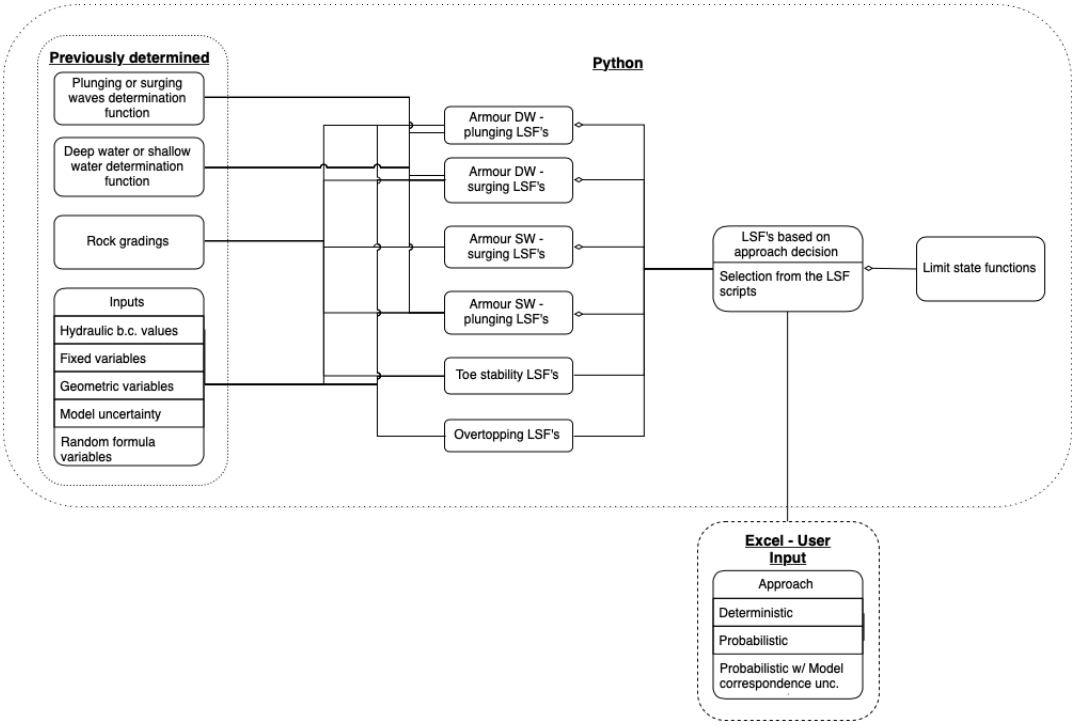

Figure C.5: Model implementation Limit state functions

C.3. PROBABILITY

The probabilistic scripts import the limit state functions. Thus, an equal amount of scripts have been composed. Furthermore, the probabilistic scripts import the probabilitic module, which has been adopted. The exact module is extracted from a GitHub open source page and is called PyRe. It also determines if a Crude Monte Carlo analysis is conducted or a FORM analysis, based on the input and the desires of the user, which are defined in the Excel input file.

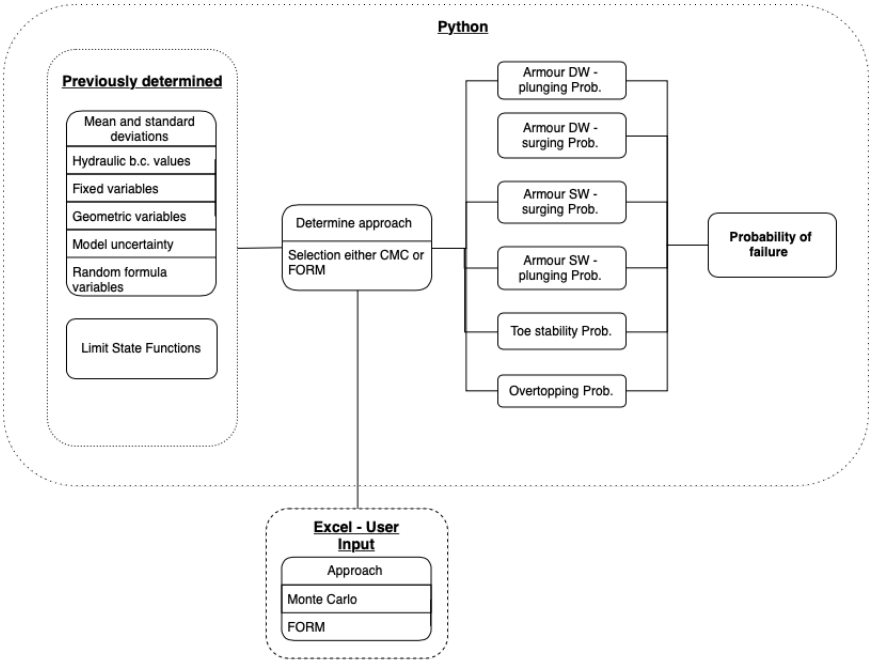

Figure C.6: Model implementation Probability functions

C.4. GEOMETRIES

The section generally determines the geometries per section element, i.e. an armour layer, toe, etc. Some of the dimensions, for instance the armour layer thickness as a ratio of the rocks size, can be determined manually in the Excel input file. Furthermore, the Excel also asks for a core material choice. The volumes are all given in cubic meters per meter length.

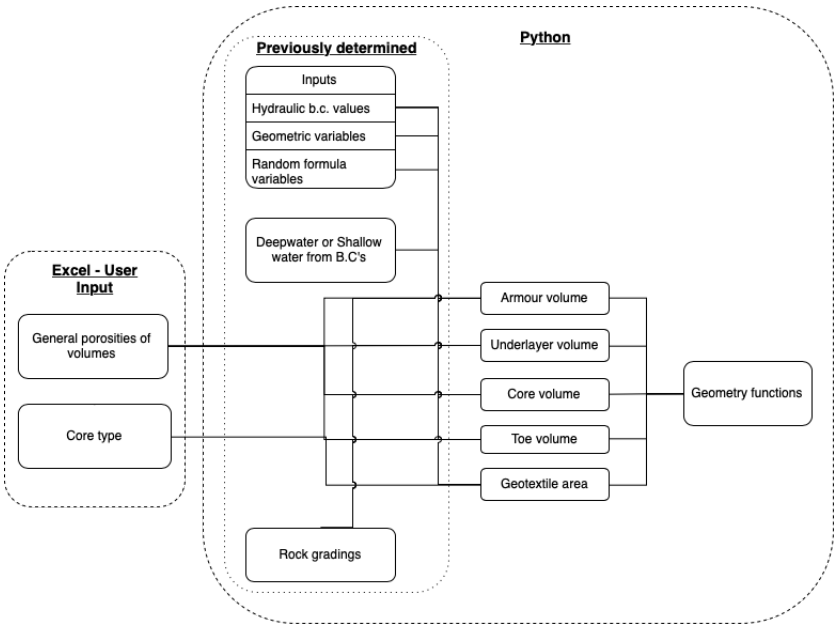

Figure C.7: Model implementation Geometry functions

C.5. COST

The cost functions are defined in Section 3.1.7. They include the initial or construction costs and the maintenance costs. The construction costs are solely based on the volume per unit element, e.g. the armour layer, underlayer or core. The maintenance costs are also a function of the probability of failure and target life time. Furthermore, the user is free to define the unit rates in the Excel GUI. These are also imported in the cost functions. Consequently, the cost functions are coupled to the numerous alternatives.

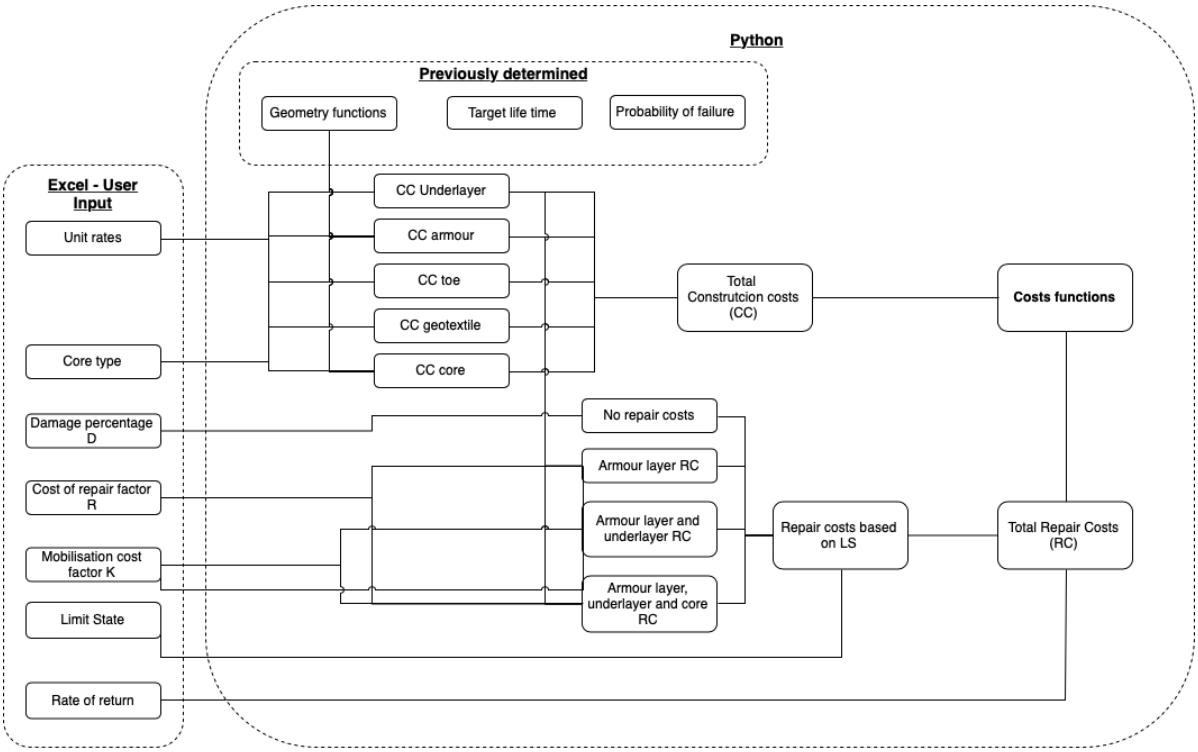

Figure C.8: Model implementation Cost functions

C.6. PARAMETRIC DESIGN AND MAIN INTERFACE MANAGEMENT

This part of the script mainly handles the production of alternatives. Essentially this is the parametric part of the script. The main inputs are the step size, upper and lower bounds of the geometric parameters and the materials. These aspects are responsible for a wide range of alternatives. These alternatives are created in a dataframe. Initially, separately for each failure mechanism. These are later combined in a single dataframe for all failure mechanisms containing all dimensions.

The alternatives are created by a using a Cartesian product of the input geometries. This creates a matrix, or in this case a dataframe, with all possible options. Firstly, the script loops through the dataframes and calculates the limit state functions. If an LSF is already not satisfied, meaning a value smaller than 0, it is deleted. Furthermore, if other boundaries of the LSF are superseded these options are also deleted. Eventually, a deterministic dataframe is realised with all possible options per failure mechanism. If a deterministic outcome is desired the dataframes are combined into a single dataframe. Subsequently, the geometry function and the cost function are looped through the dataframe and added. If costs are not desired this step is skipped. The the next step follows which is explained in Appendix C.7.

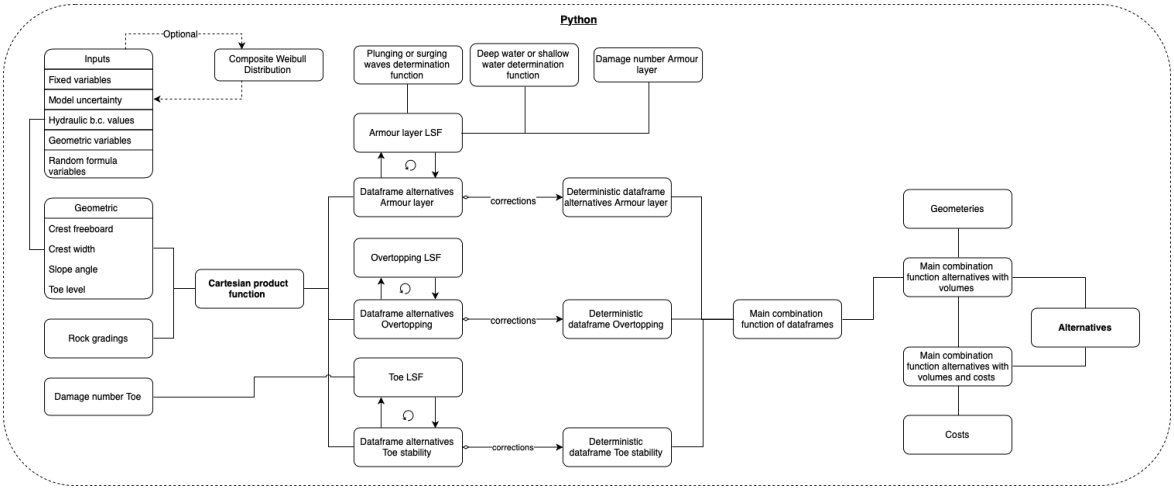

Figure C.9: Model parametric deterministic overview

However, if a probabilistic approach is desired, based on inputs, a different path is taken. The deterministc alternatives are then optimised. The outputs of this optimisation serve as inputs for the probabilistic approach. Again an Cartesian product is made with the inputs. Subsequently, the script loops through the dataframe and performs a probabilistic calculation, as per Appendix C.3, for each alternative. Furthermore, a target probability of failure function is compared to the probability of failure. If the probability of failure of the alternative is larger than the target probability of failure, the the alternative is regarded as unfit and deleted from the dataframe. This is done for all the failure mechanisms seperately and afterwards combined into a single dataframe. Subsequently, the geometry function and the cost function are looped through the dataframe and added. If costs are not desired this step is skipped. The the next step follows which is explained in Appendix C.7.

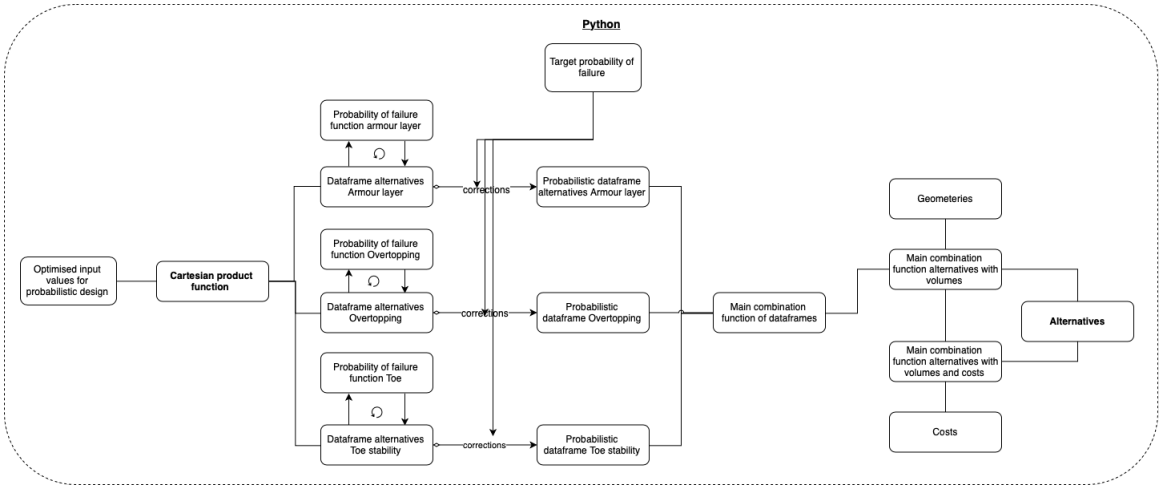

Figure C.10: Model parametric probabilistic overview

C.7. OUTPUT

All the data is collected in the output sheets. A distinction is made between deterministic and probabilistic output sheets. Two different outputs can be asked for. Only the alternatives and the corresponding geometries or the alternatives, the corresponding geometries and the costs. The output scripts make an new excel file, store in there and directly open Excel to show the outcomes.

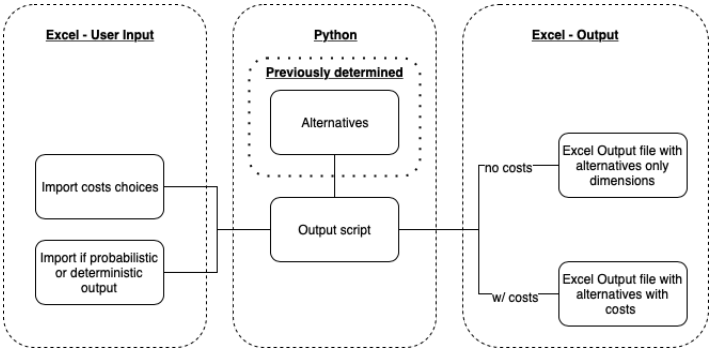

Figure C.11: Model Output overview

D

APPENDIX D

D.1. CASE INFORMATION

Figure D.1: Location of offshore NOAA data point for wave conditions (source: Google Earth)

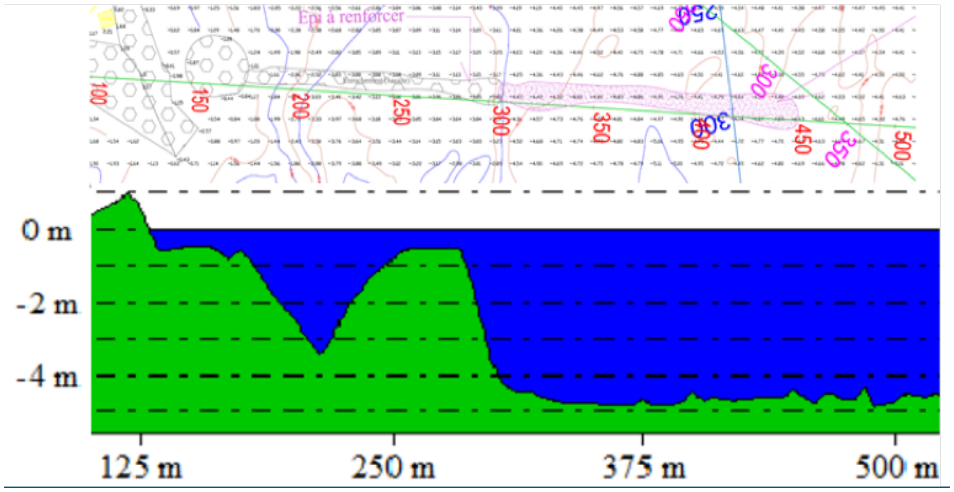

Figure D.2: Bathymetry along the southern breakwater

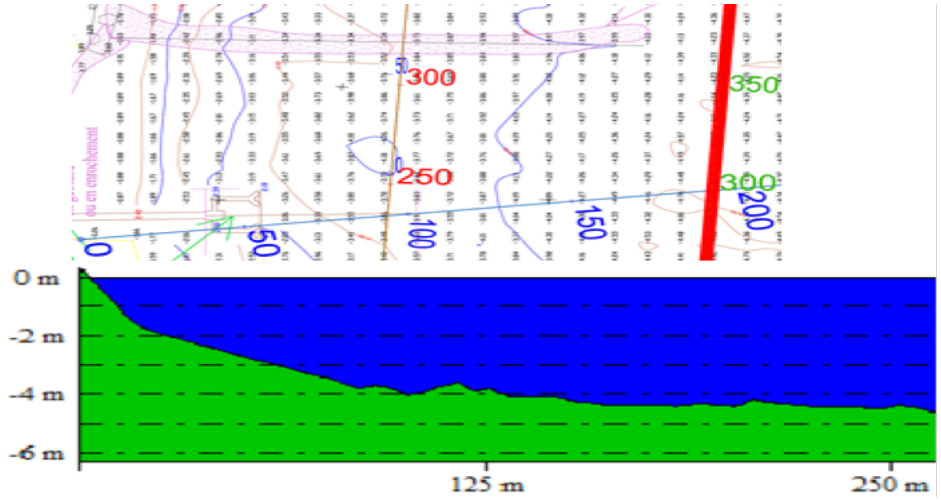

Figure D.3: Bathymetry along the northern breakwater

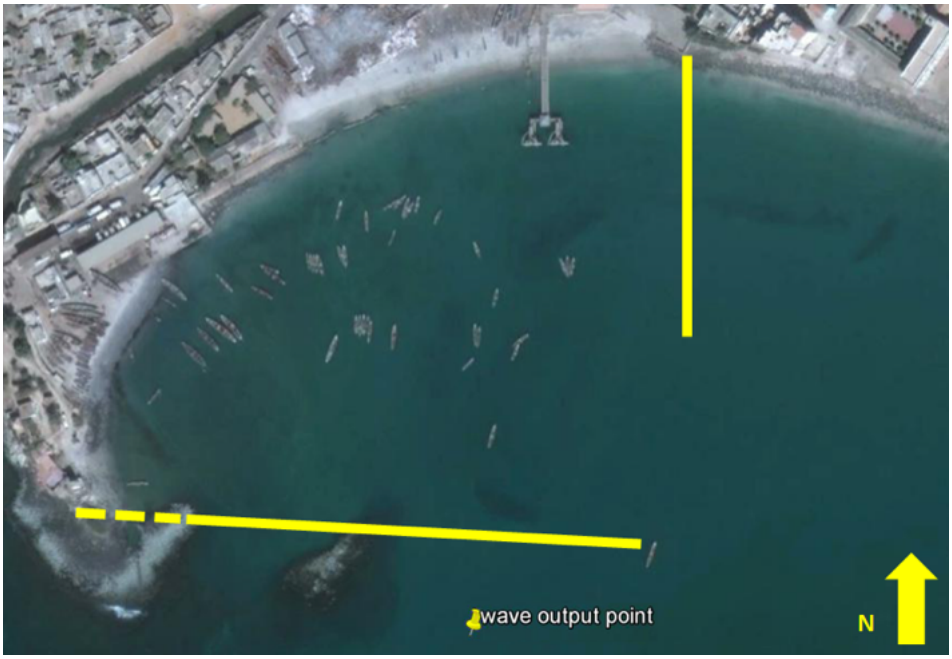

Figure D.4: Locations of southern and northern breakwaters

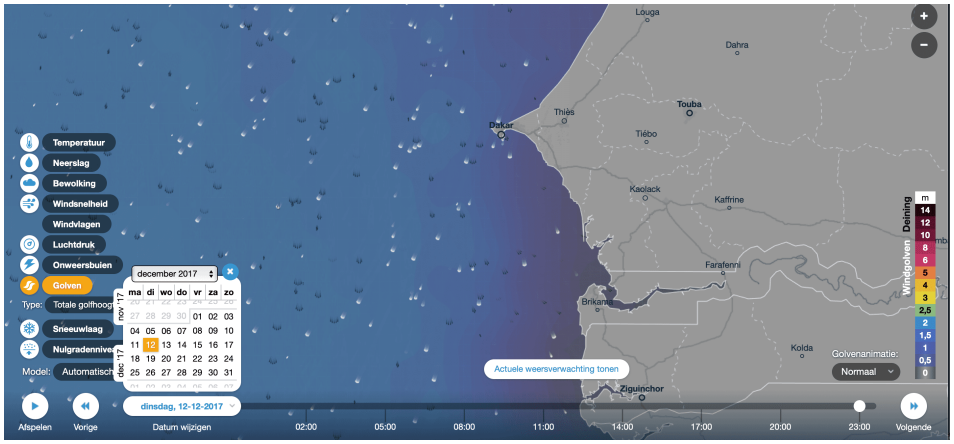

Figure D.5: Wave climate winter

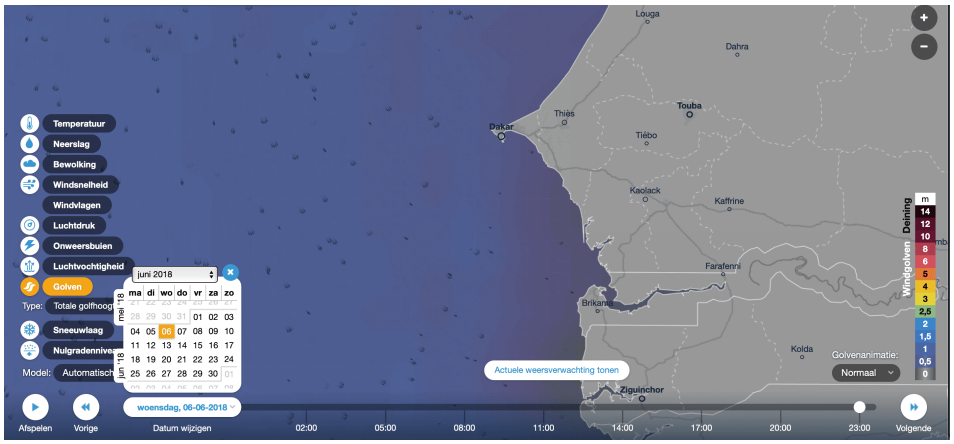

Figure D.6: Wave climate summer

D.2. EXTREME VALUE ANALYSIS

D.2.1. FITTING A MARGINAL DISTRIBUTION

Maximum Likelihood method (ML)

The Maximum Likelihood method uses the function GEV-fit (Generalised extreme value distribution fitting). This function estimates the maximum-likelihood of the "best" fit to the data. It determines the shape parameters of the extreme value distribution, i.e. the shape, location and scale parameters. Subsequently, these paramaters relate best to an asymptotic distribution, e.g. type I, II or III. These are respectively a gumbel, Frechet or a reverse Weibull distributions.

Method Of Moments (MOM)

An alternative method to fit a distribution to a data set is with the Method of Moments. For a distribution with k-parameters, one defines the equations such that it gives the k central moments, i.e. mean, variance,etc., of the distribution in terms of parameters. Subsequently, the moments are filled in with the sampled central moments. The equation is inverted to solve the parameters in terms of the sampled moments (Wicklin, 2017).

Maximum product of spacing estimation (MPS)

The maximum product of spacing estimation or the maximum spacing estimation method, is an estimation method to finding the parameters of a univariate statistical model. It tries to find a distribution function for which the the differences between the values of the cumulative distribution function and neighbouring data points are the same (Singh et al., 2014). This can be achieved by maximizing the geometric mean of spacing between ordered samples (Kumar Singh et al., 2016; inFERENCe, 2015).

GOODNESS OF FIT

Fitting an asymptotic distribution to the empirical distribution is a delicate process. In order to adress whether or not the fitting is reliable or not can be investigated by the goodness of fit. This can be done with several error estimations methods. The two methods used in this research are the residual quantile error and the root mean square error. The results of these errors are shown in Table D.2.

Data set H_{m0}	Fitting method
Dir.1 [168.8 - 191.3]	MPS
Dir.1 [191.3 - 213.8]	MPS
Dir.1 213.8 - 236.3]	MPS
Dir.1 [236.3 - 258.8]	ML
Dir.1 [258.8 - 281.3]	ML
Dir.1 [281.3 - 303.8]	MOM

Table D.1: Fitting methods per extreme data set

Directional data set	Goodness of fit	
	RMSE	RSQ
Dir.1 [168.8 - 191.3]	0.023	0.990
Dir.1 [191.3 - 213.8]	0.015	0.995
Dir.1 213.8 - 236.3]	0.019	0.990
Dir.1 [236.3 - 258.8]	0.024	0.983
Dir.1 [258.8 - 281.3]	0.021	0.992
Dir.1 [281.3 - 303.8]	0.019	0.993

Table D.2: Goodness of fit per directional extreme data set

The value of the RSQ error should approach 1.0 for the results to be ideal. For the RMSE to be ideal, the value should approach 0.0. A brief explanation of the calculation of these errors is given below.

Residual Quantile plot (RSQ)
The residuals are the predicted error values of the model. This is basically the difference in predicted values as opposed to th actual observed values. In principle, one wants the data points to be closely clustered around the regression line. The residual quantile plots show the predicted value on the x axis and the residuals on the y-axis. Essentially, the data points should be randomly distributed along the regression line, ideally closely clustered as well. The least ideal is a clear pattern in the residuals. For instance a linear or non-linear pattern where residuals decrease or increase in line with the predicted values.

Root mean square Error (RMSE)
The root mean square error is one of the methods used to check the how well the fitting corresponds to the empirical distribution. This is error can be translated as a standard deviations on the prediction errors. These errors, or residuals, show how the regression line corresponds to the data. It is simply a means to express how well the data points are concentrated around the best fit. It can be calculated as follows (Holmes, 2000):

1. Square the residuals.

2. Find the average of the residuals.

3. Take the square root of the result

D.2.2. RESULTS

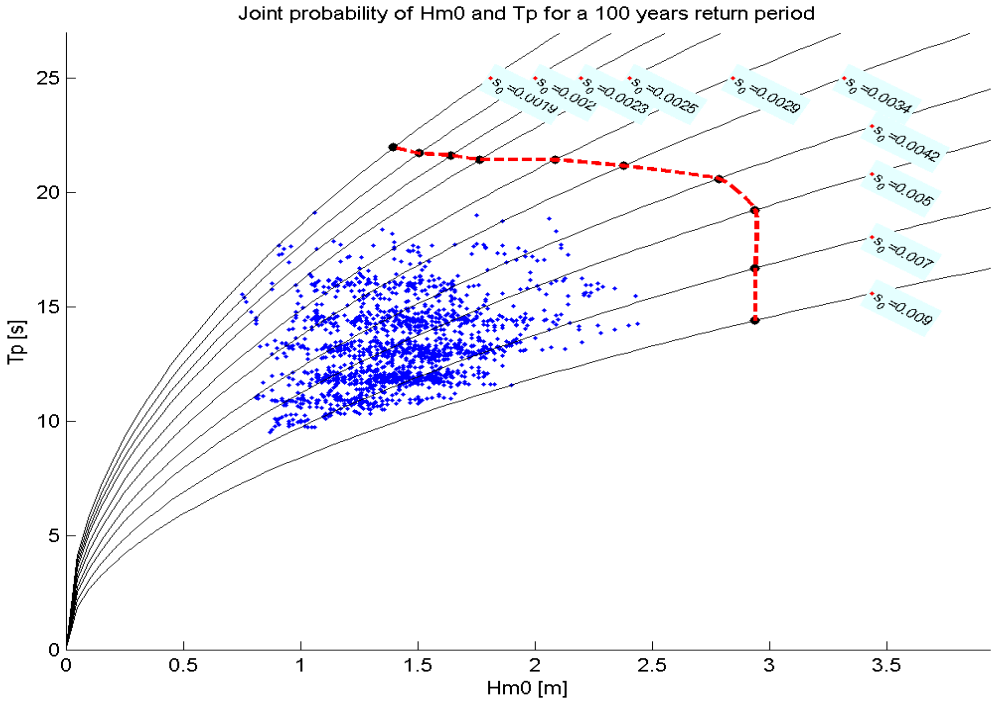

Figure D.7: Joint probability H_{m0} and T_p for 100 years return period

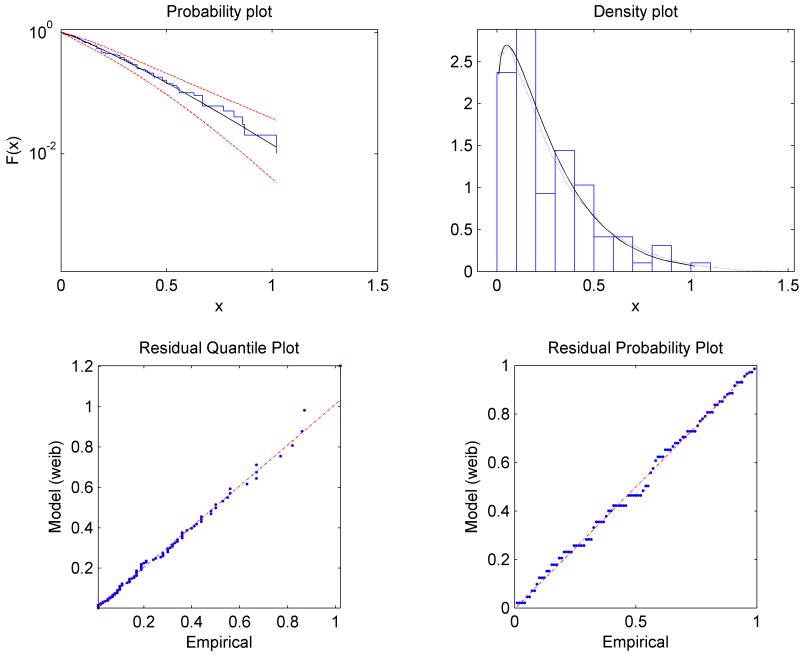

Figure D.8: Fitting summary significant wave height.

A brief explanation of each fitting method is given.

ENVIRONMENTAL PARAMETERS

The incoming wave first encounter the southern breakwater. However, they refract around the end of the breakwater and continue towards the northern breakwater. This diffraction causes wave energy dissipation and results in lower wave heights at the lee breakwater. Royal HaskoningDHV has already determined the diffraction factors for the incoming waves and wave directions. The following diffraction factors have been determined:

- $\theta_{lee} = 0°$ $K_d = 0.7$(applicable for incoming wave directions of about 195°)
- $\theta_{lee} = 12°$ $K_d = 0.6$(applicable for incoming wave directions of about 206°)
- $\theta_{lee} = 23°$ $K_d = 0.5$(applicable for incoming wave directions of about 217°)

The incoming wave lines and their orientation to the breakwaters are shown in Appendix D. Thus, the governing offshore wave direction is 180° (highest waves and least diffraction) are reduced with a diffraction factor of 0.7. The wave heights estimated on the northern breakwater head are shown in table D.3. The waves come perpendicular to the breakwwater head, hence $\beta = 0°$. However, further on the trunk of the breakwater it is assumed that the wave will turn slightly towards the breakwater, hence a $\beta = 80°$.

Water level	H_{m0} [m]	T_m [s]	$T_{m-1,0}$ [s]	θ_w[◦]	H_s [m]	$H_{2\%}$/H_{s}$ [-]	β[◦]
	1.5	7.8	12.5	197	1.6	1.4	0
HW = +1.8m ZH	1.8	7.7	12.3	196	1.9	1.4	0
	1.7	5.7	8.9	195	1.8	1.4	0
MSL = +1.0m ZH	1.5	7.6	12.2	196	1.6	1.4	0
LW = +0.2m ZH	1.3	7.4	12.1	196	1.4	1.4	0

Table D.3: Nearshore 1/100yr wave conditions at offshore direction 180° Northern breakwater

Grading class	W_{50} (range)	W_{50} (average)	D_{n50}
5 - 40 kg	12 - 28 kg	21 kg	0.20 m
10 - 60 kg	27 - 47 kg	37 kg	0.24 m
40 - 200 kg	101 - 152 kg	126.5 kg	0.36 m
60 - 300 kg	149 - 236 kg	192.5 kg	0.42 m
300 - 1000 kg	628 - 802 kg	715 kg	0.65 m
1 - 3 ton	1870 - 2310 kg	2090 kg	0.92 m
3 - 6 ton	4430 - 5060 kg	4745 kg	1.21 m
Grading class	D_{n50}	W_{50} (average)	
45 - 125 mm	85 mm	0.965 kg	
45 - 180 mm	113 mm	2.266 kg	
63 - 180 mm	122 mm	2.852 kg	

Table D.4: Standard quarry rock and gravel gradings

D.3. PROBABILISTIC CALCULATION VALIDATION

D.3.1. FORM ANALYSIS

Armour layer stability

Armour stability (SW-Surging wave)	β	Probability of failure	Percent error
Output Prob2B	0.234800	0.407200	0.027%
Output Secondary FORM module	0.234466	0.407311	0.0002455%
Output Model	0.234467	0.407310	-

Table D.5: FORM calculation output comparison table - Armour layer stability (SW-Surging waves)

Toe stability

Toe armour stability	β	Probability of failure	Percent error
Output Prob2B	1.7760	0.037900	0.0211%
Output Secondary FORM module	1.7755	0.037907	0.002638%
Output Model	1.7754	0.037908	-

Table D.6: FORM calculation output comparison table - Toe stability

OTHERS / ADDITIONS

Armour stability (SW-Plunging wave)	β	Probability of failure
Output Prob2B	3.2	0.0006862
Output Secondary FORM module	3.20031463796627	0.000686388190766718
Output Model	3.2003144199179685	0.0006863887100901356

Table D.7: FORM calculation output comparison table - Armour layer stability (SW-Plunging wave)

Armour stability (DW-Plunging wave)	β	Probability of failure
Output Prob2B	1.251	0.1055
Output Secondary FORM module	1.25089226620660	0.10548689293190971
Output Model	1.2508914815642387	0.10548703608637844

Table D.8: FORM calculation output comparison table - Armour layer stability (DW-Plunging wave)

Armour stability (DW-Surging wave)	β	Probability of failure
Output Prob2B	1.307	0.09555
Output Secondary FORM module	1.30770791750695	0.0954861984243689
Output Model	1.307704894124268	0.09548671135726028

Table D.9: FORM calculation output comparison table - Armour layer stability (DW-Surging wave)

D.3.2. CRUDE MONTE CARLO

Armour layer stability

Armour stability (SW-Surging)	β	Pf (10000 samples)	Coefficient of variation
Output Prob2B	0.2780	0.3905	-
Output Model	0.250759	0.401	0.012221

Table D.10: CMC calculation output comparison table - Armour layer stability (SW-Surging)

Toe stability

Toe armour stability	β	Pf (10000 samples)	Coefficient of variation
Output Prob2B	1.813	0.03490	-
Output Model	1.817	0.034583	0.048231

Table D.11: CMC calculation output comparison table - Toe stability

ADDITIONAL FORM & CMC PROBABILISTIC VALIDATION

Armour stability (SW-Plunging)	β	Pf (10000 samples)	Coefficient of variation
Output Prob2B	3.239	0.0006	-
Output Model	3.1708377805261403	0.00076	0.11466426966078887

Table D.12: CMC calculation output comparison table - Armour layer stability (SW-Plunging wave)

Armour stability (DW-Plunging)	β	Pf (10000 samples)	Coefficient of variation
Output Prob2B	1.265	0.1030	-
Output Model	1.2508204283945634	0.1055	0.046039854978545465

Table D.13: CMC calculation output comparison table - Armour layer stability (DW-Plunging wave)

Armour stability (DW-Surging)	β	Pf (10000 samples)	Coefficient of variation
Output Prob2B	1.297	0.09730	-
Output Model	1.2930319761442421	0.098	0.04796895254394518

Table D.14: CMC calculation output comparison table - Armour layer stability (DW-Surging wave)

D.4. CASE VALIDATION

INPUT

Firstly, the inputs of the case per breakwater are described. For both the northern and the southern breakwater. The difference between a quarry rock core and Geo-container core is slight difference and is described separately, containing a similar explanation for both breakwater sections.

SOUTHERN BREAKWATER

Environmental parameters

The water levels and wave conditions have been introduced in sections 4.1.1 and 4.1.1 respectively. Royal HaskoningDHV has already conducted a nearshore wave transformation by numerical modelling with a software called SWaN. These wave conditions have only been determined for the high water level (+1.8m ZH), in every direction. However, for toe stability a lower water level can be governing (MSL and LW). Only the wave heights from one direction (180°) are considered, since the highest waves during high water are found in this direction. An overview of the governing wave heights to the corresponding water levels is shown in table D.15.

Water level	H_{m0} [m]	T_m [s]	$T_{m-1,0}$ [s]	θ_w [◦]	H_s [m]	$H_{2\%}$/H_{s}$ [-]	β [◦]
	2.2	7.8	12.5	197	2.3	1.272	14
HW = +1.8m ZH	2.5	7.7	12.3	196	2.6	1.224	13
	2.4	5.7	8.9	195	2.5	1.232	12
MSL = +1.0m ZH	2.2	7.6	12.2	196	2.3	1.226	13
LW = +0.2m ZH	1.9	7.4	12.1	196	2.0	1.230	13

Table D.15: Nearshore 1/100yr wave conditions at offshore direction 180°, Southern Breakwater

BOTH BREAKWATERS

For both breakwater the structural and material parameters are similar. Furthermore, some of the hydraulic parameters are also similar, such as the sea water density and the storm duration. The sea water density is $1025 k/m^3$ and the storm duration in this case is 6 hours.

Structural parameters
The structural parameters include the structural parameters for both front and rear slope. In this research the rear slope is not part of the scope and shall therefore be neglected. The parameters which are taken into consideration are shown in table D.16

Structural parameters	Unit	Value
Damage figure (allowed) - front slope	-	2 - 3
Damage figure (allowed) - toe	-	0.75
Average overtopping dischare (allowed)	l/s/m	10
Notional permeability factor	-	0.4 (for permeable core - rock) 0.1 (for impermeable core - sand)
Rock density	kg/m^3	2650
Roughness of quarry rock on front slope (for wave overtopping)	-	0.4

Table D.16: Case structural input parameters

Material properties
The material properties are the main rock gradings which are considered for the the design of the breakwater. This case uses the standard quarry rock and gravel gradings according to the Rock Manual (CIRIA/CUR, 2007c). An overview of these gradings is given in Table D.4.

CASE STUDY SOLUTIONS OUTPUT

An overview of the design summary in presented in Figures D.9 and D.10, for option 1 and 2 respectively.

Breakwater option 1 (rock core):

Southern breakwater:

- Front slope: 1 : 2.5 slope gradient
  1 – 3 tonnes armour rock grading
  Thickness is 1.75 m
- Rear slope: 1 : 2 slope gradient
  1 – 3 tonnes armour rock grading
  Thickness is 1.75 m
- Crest: Crest height = +5 mZH
  Crest width = 5 m
- Toe: 60 – 300 kg armour rock grading
  Total toe thickness = 1.25 m (incl. filter layer)
  Toe (top) width = 3.5m
- Core: Quarry run 1 – 250 kg
- Underlayer: 60 – 300 kg; thickness is 0.80 m
- Filter layer: 45 – 180 mm; thickness is 0.45 m
- Roundhead: 1 : 3.5 slope gradient
  1 – 3 tonnes armour rock grading

Figure D.9: Design summary southern breakwater option 2

Breakwater option 2 (sand core of geo-container):

Southern breakwater:

- Front slope: 1 : 2.5 slope gradient
  3 – 6 tonnes armour rock grading
  Thickness is 2.30m
- Rear slope: 1 : 2.5 slope gradient
  3 – 6 tonnes armour rock grading
  Thickness is 2.30m
- Crest: Crest height = +6mZH
  Crest width = 5m
- Toe: 60 – 300 kg armour rock grading
  Total toe thickness = 1.25m (incl. filter layer)
  Toe (top) width = 3.5m
- Quarry run: 1 – 250 kg
- Underlayer: 40 – 200 kg; thickness is 0.70 m
- Filter layer: 45 – 180 mm; thickness is 0.45 m
- Roundhead: 1 : 3.5 slope gradient
  3 – 6 tonnes armour rock grading

Figure D.10: Design summary southern breakwater option 2

CASE STUDY MODEL OUTPUT

An overview of the design summary in presented in Tables D.17 and D.18, for option 1 and 2 respectively.

Parameter	cot_a	$dn50_{armour}$	Sd	R_c	w_{crest}	h_{crest}	z_{toe}	$dn50_{toe}$	$LSF_{ov,front}$	$LSF_{ov,back}$	LSF_{toe}	LSF_{rock}
Value	2.5	0.92	3	3.2	5	5	-3.25	0.41	3.74	9.05	0.0995	0.0306

Table D.17: Model output: Southern Breakwater option 1 (Quarry run core)

Parameter	cot_a	$dn50_{armour}$	Sd	R_c	w_{crest}	h_{crest}	z_{toe}	$dn50_{toe}$	$LSF_{ov,front}$	$LSF_{ov,back}$	LSF_{toe}	LSF_{rock}
Value	2.5	1.22	3	4.2	5	6	-3.25	0.41	9.30	9.89	0.0995	0.0908

Table D.18: Model output: Southern Breakwater option 2 (Geo-containers)

D.5. INFLUENCE ON THE COST OF THE DESIGN OF EACH VARIABLE

D.5.1. INFLUENCE OF ALL VARIABLES ON COSTS

It should be noted that the step size are the same for all variables and the amount of data points as well. The wave climate is the same as given in Appendix D.4.

Variable	0	1	2	3	4	5	6	7	8	9	10
$Slopeangle$	3.5	3.4	3.3	3.2	3.1	3.0	2.9	2.8	2.7	2.6	2.5
$dn50_{armour}$	1.9	1.8	1.7	1.6	1.5	1.4	1.3	1.2	1.1	1.0	0.9
R_c	3.5	3.4	3.3	3.2	3.1	3.0	2.9	2.8	2.7	2.6	2.5
w_{crest}	4.0	3.9	3.8	3.7	3.6	3.5	3.4	3.3	3.2	3.1	3.0
z_{toe}	-3.0	-3.1	-3.2	-3.3	-3.4	-3.5	-3.6	-3.7	-3.8	-3.9	-4.0
$dn50_{toe}$	1.4	1.3	1.2	1.1	1.0	0.9	0.8	0.7	0.6	0.5	0.4

Table D.19: Combination table for costs and probability of failure sensitivity analysis

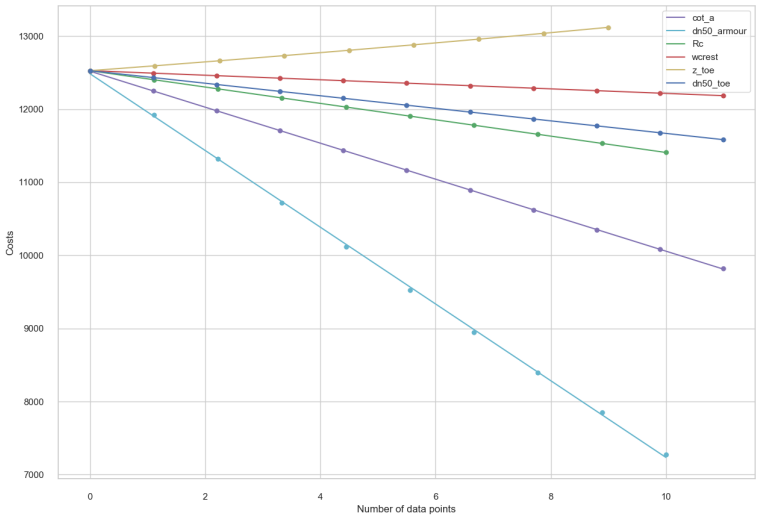

Figure D.11: This figure represent the change in costs per variable, when all other variables are kept constant, each x-axis of the curve is given in table D.19

In Figure D.11 it can be seen that the armour unit size have the largest influence on the total costs of the structure. This can be explained by the fact that the costs function is based on volumes of the structure. The volume of the armour layer is mainly determined by the thickness, which is a function of the armour size. This is similarly the same explanation for the under layer and the core. The second most influential parameter is the slope angle. The toe height increase the costs of the structure mildly as the toe height becomes larger, thus a larger toe volume. Furthermore, it is seen that the crest width has a smaller influence on the difference in costs, than the crest height.

From Figure D.11 only conclusions can be drawn from visual observations. However, in order to quantify the influence of the different parameters, the gradients can be computed. The gradients can tell us something about the rate of change in costs as a variable is changed with 10 cm. Table D.20 shows the gradients per variable, with a variable being denoted as v_i.

Variable v_i	Gradient $dE[cost]/dv_i \vert v_i \vert [euro]$
cot_α	-270.585
$dn50_{armour}$	-580.878
R_c	-124.351
w_{crest}	-34.200
z_{toe}	75.131
$dn50_{toe}$	-94.400

Table D.20: Sensitivities of each variable to the total costs of the structure for the serviceability limit state

D.5.2. SENSITIVITY OF MOST INFLUENTIAL VARIABLES ON COSTS

This section further zooms in on the impact of the most influential parameters. Previous section shows that the armour unit size is the most influential parameter. However, since this parameter follows a predetermined set of options, i.e. the standard rock gradings. This parameter is not further investigated regarding its influence. The slope angle on the other hand is further investigated as to what its influence is.

As in the previous section, all of the other variables are kept constant as the slope angle is varied.

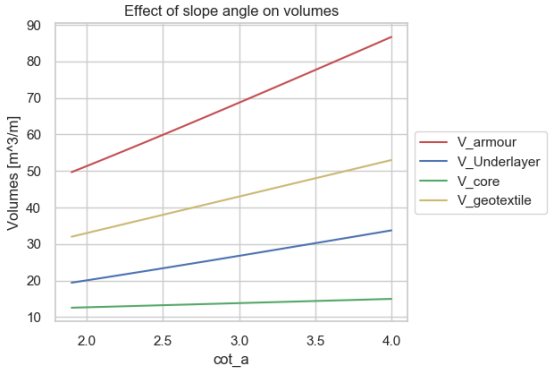

Figure D.12: Change in different volumes for a change in slope angle

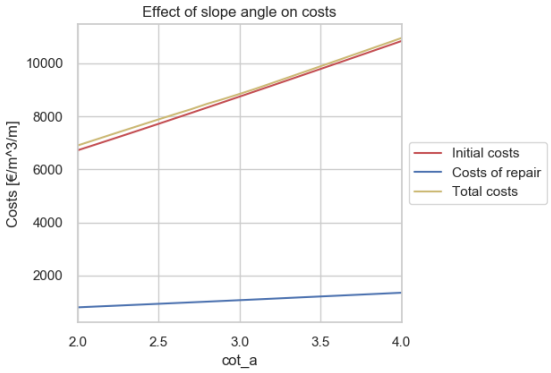

Figure D.13: Change in different costs for a change in slope angle

From Figure D.12 it can be concluded that the main reason that the slope angle has such a large influence to the difference in costs, is due to the large volume change in in armour layer.

It shows that the geotextile, which is proportional to the footprint of the slope, is second most influential. Thus the increase in footprint is noticed as the slope angle increases. However, the costs of the geotextle are much cheaper, compared to the costs of the armour layer. Thus, this not considered a larger impact. The under layer does changes less than the geotextile, but is more costly, which impacts the change in costs with more gravity. The change in volume of the core is barely noticeable, thus shall not impact the total cost much.

The influence of the sole increase in slope angle with all of the other variables kept constant is shown in Figure D.13. This is done for the serviceability limit state. Only a minor portion of the total costs is for the costs of repair. In Figure D.14 the distribution of the volumes over the total dike volume is shown in percentages to the total volume. It is seen that the constribution to the total volume, thus inherently to the total costs, is mainly due to the armour layer volume. Additionally, by changing the slope angle the total distribution does not differentiate much.

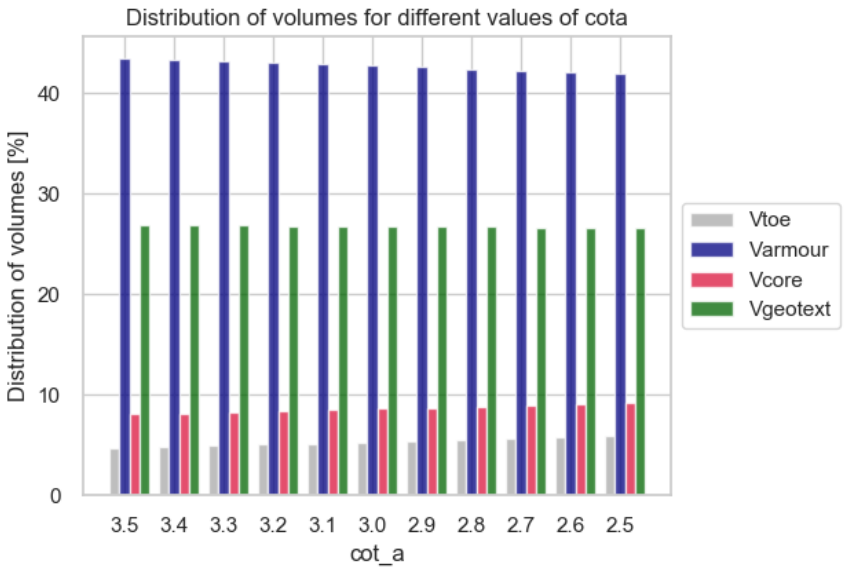

Figure D.14: Change in volume distribution for a change in slope angle

E

APPENDIX E

E.0.1. DETERMINE INPUT RANGE FOR ALL METHODS

To specify an applicable variable input range, within the proximity of the case study input, first a coarse input range is chosen. In this sense, coarse is defined as specifying wide boundaries and large step sizes to the parametric input variables. Subsequently, a finer input range is chosen. A finer range entails narrower boundaries, provided that they enclose the case input, and smaller step size. Notably, a smaller step size, should be within the range of buildable step sizes, i.e. a step size for a crest height should not be 1 mm, since this is relatively not a realistic order of magnitude. Subsequently, the probabilistic calculations are set to be deterministic. Eventually, the model runs the earlier mentioned options; the southern breakwater for quarry run core. The other options are not considered, for conciseness reasons. The initial coarser range and step size, are shown in Table E.1a for deterministic and probabilistic approaches respectively.

The lower and upper bounds are altered accordingly. The step sizes are refined to achieve a more accurate crest height, free board and toe height. The model inputs after specification are shown in Table E.1b, for the deterministic approach and the deterministic approach with uncertainty respectively.

Input	Range	Step size
Crest freeboard (R_c)	1 - 10 [m]	0.5 [m]
Crest width (B)	1 - 7.5 [m]	0.5 [m]
Slope angle (cot_α)	1.5 - 4.5	0.5
Toe height (z_{toe})	-4.5 - 0 [m]	0.5 [m]
Permeability	0.4	
$dn_{50,toe}$	Std. rock grading	
$dn_{50,armour}$	Std. rock grading	
Core	Quarry run	

(a) Southern breakwater option 1, coarse estimates

Input	Range	Step size
Crest freeboard (R_c)	1 - 5.5 [m]	0.1 [m]
Crest width (B)	1 - 5.5 [m]	0.5 [m]
Slope angle (cot_α)	1,5 - 4.5	0.5
Toe height (z_{toe})	-3.5 - -1 [m]	0.25 [m]
Permeability	0.4	
$dn_{50,toe}$	Std. rock grading	
$dn_{50,armour}$	Std. rock grading	
Core	Quarry run	

(b) Southern breakwater option 1, fine estimates

E.1. MODEL OUTPUT GRAPHS

OUTPUTS DETERMINISTIC APPROACH

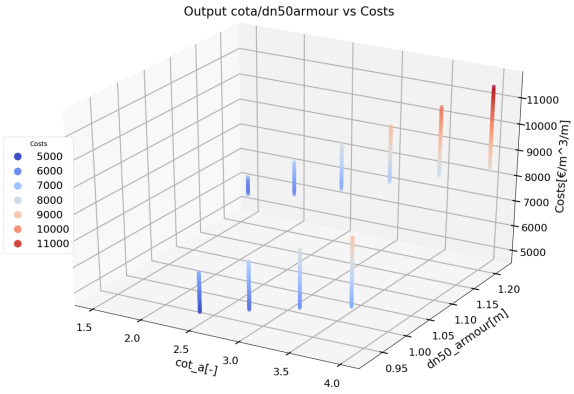

Figure E.1: Deterministic output cota / dn50 / Costs

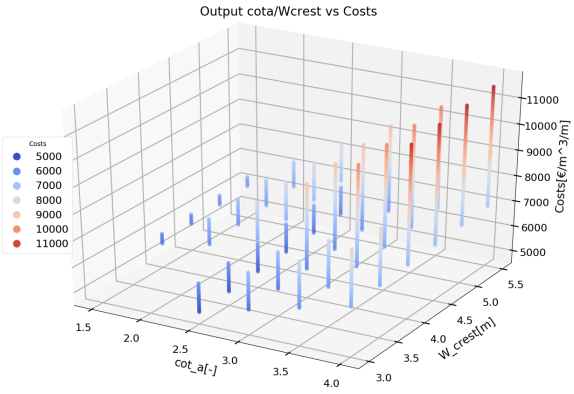

Figure E.2: Deterministic output cota / B / Costs

OUTPUTS AFTER THE LOCAL OPTIMA SELECTION

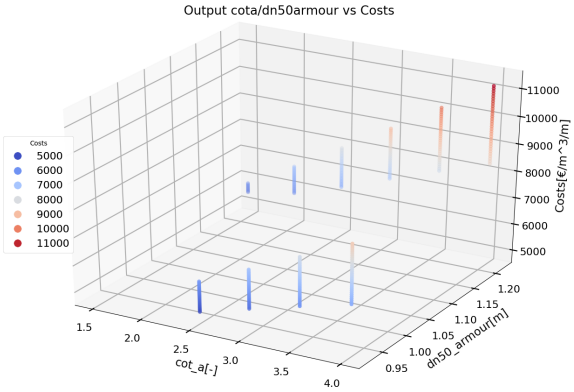

Figure E.3: Det. Local optimisation cota / dn50 / Costs

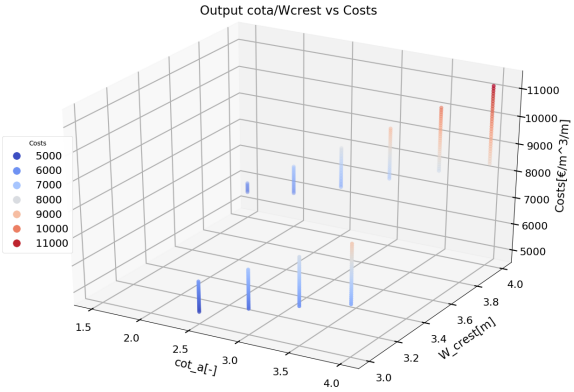

Figure E.4: Det. Local optimisation cota / B / Costs

OUTPUTS OF THE OPTIMISATION SCHEME

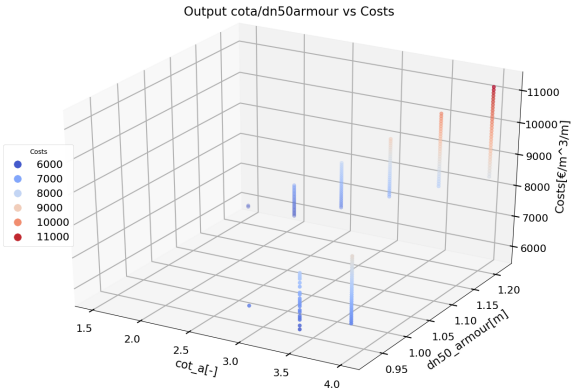

Figure E.5: Det. Optimised output cota / dn50 / Costs

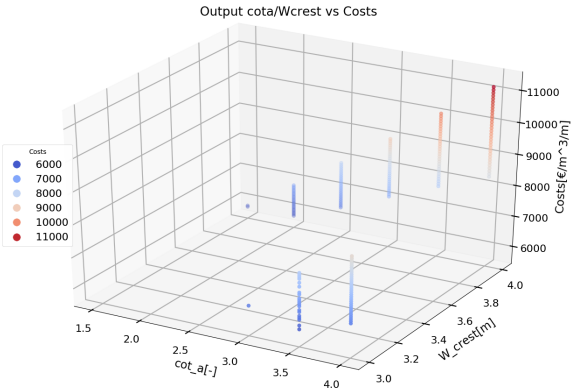

Figure E.6: Det. Optimised output cota / B / C

MODEL OUTPUT FORM ANALYSIS

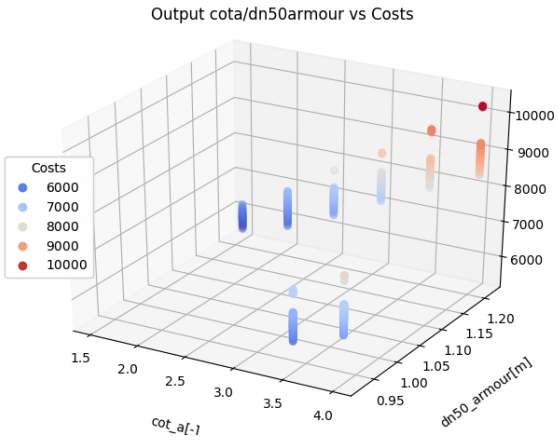

Figure E.7: FORM cota / dn50 / C

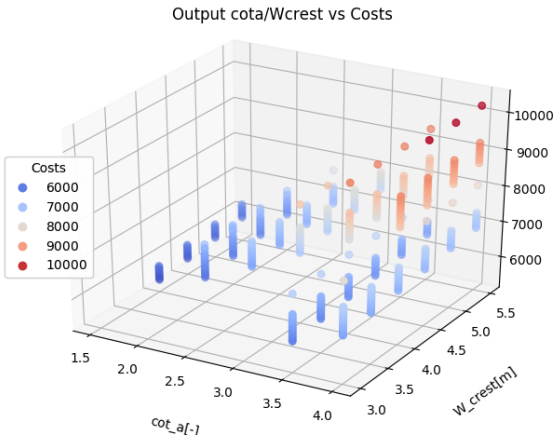

Figure E.8: FORM cota / B / Costs

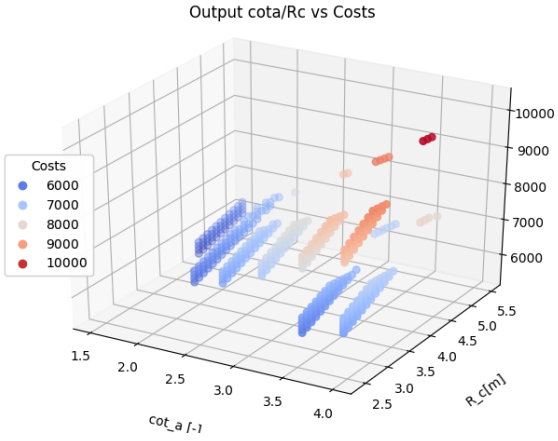

Figure E.9: FORM Rc / B / Costs

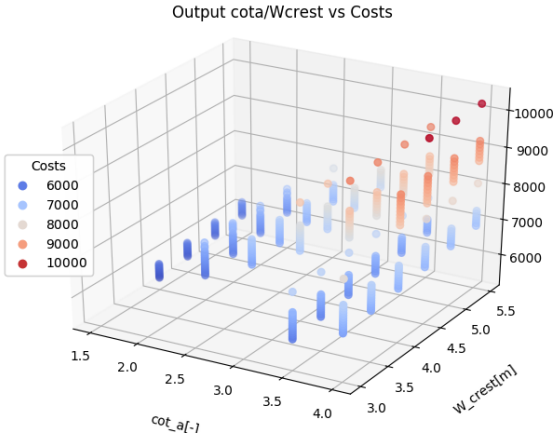

Figure E.10: FORM cota / Rc / C

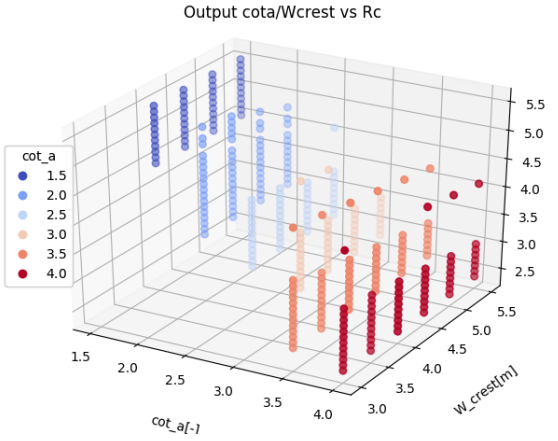

Figure E.11: FORM cota / B / Rc

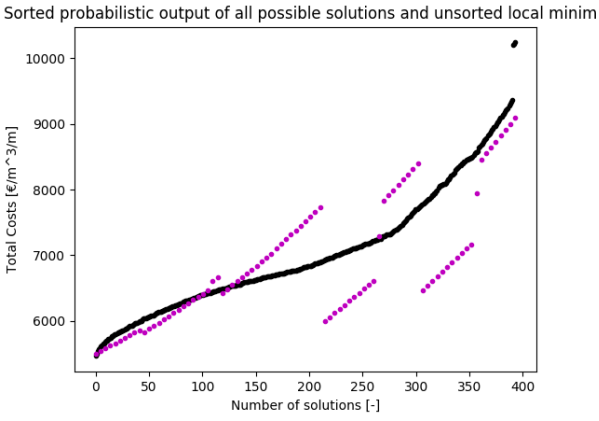

Figure E.12: FORM all options 2D

MODEL OUTPUT CMC APPROACH

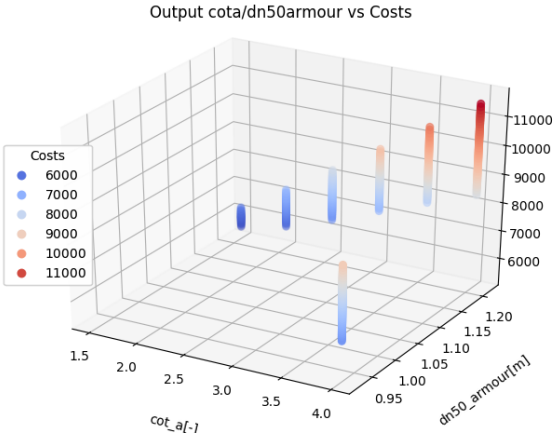

Figure E.13: CMC cota / dn50 / Costs

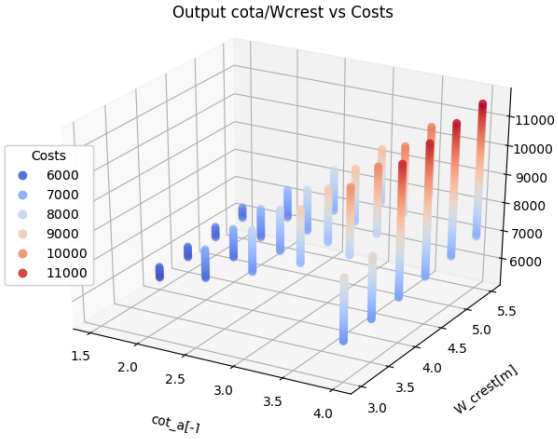

Figure E.14: CMC cota / B / Costs

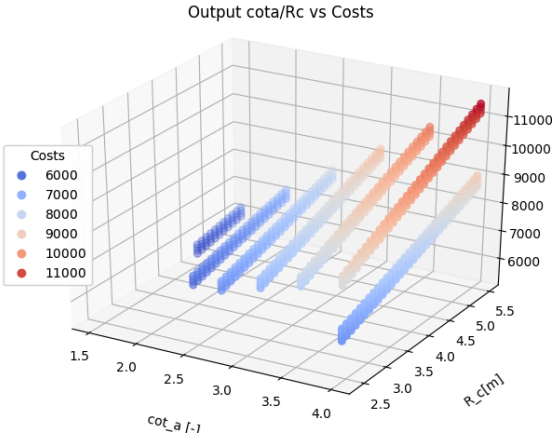

Figure E.15: CMC rc-B-C

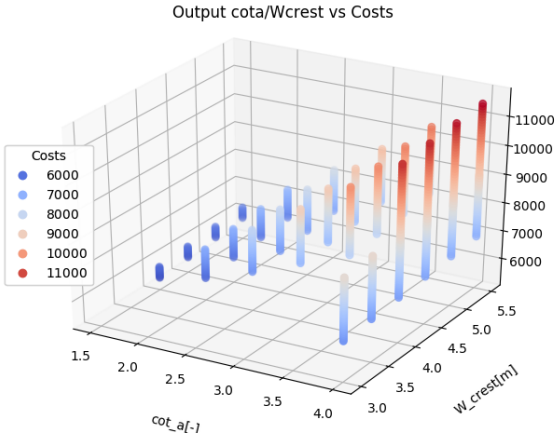

Figure E.16: CMC cota / Rc / Costs

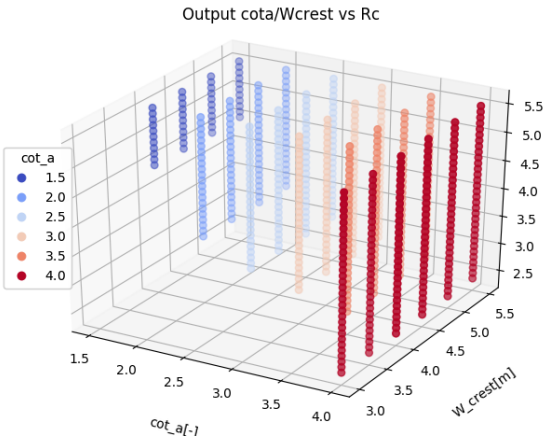

Figure E.17: CMC cota / B / Rc

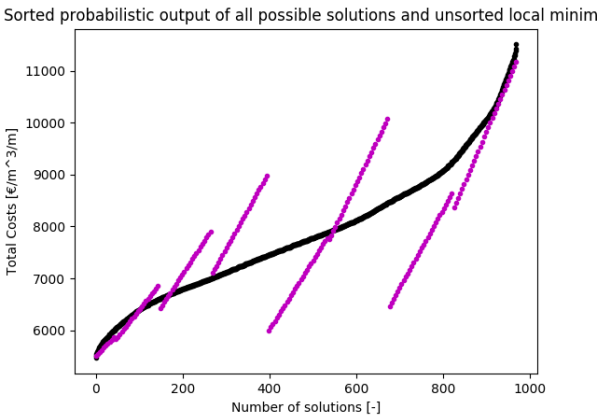

Figure E.18: CMC all options 2D

MODEL OUTPUT DETERMINISTIC APPROACH WITH UNCERTAINTY

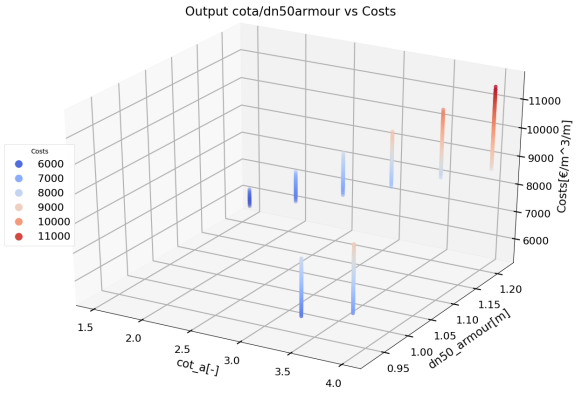

Figure E.19: Deterministic w/ uncertainty cota / dn50 / Costs

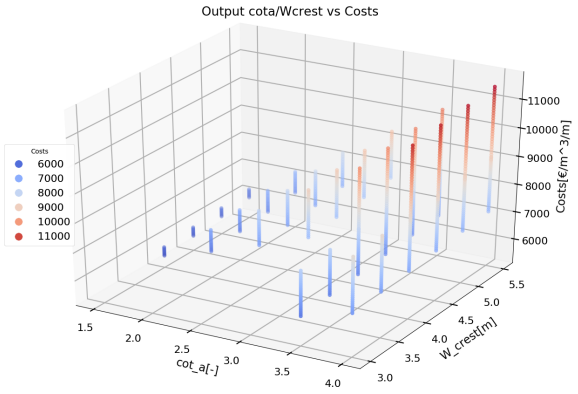

Figure E.20: Deterministic w/ uncertainty cota / B / Costs

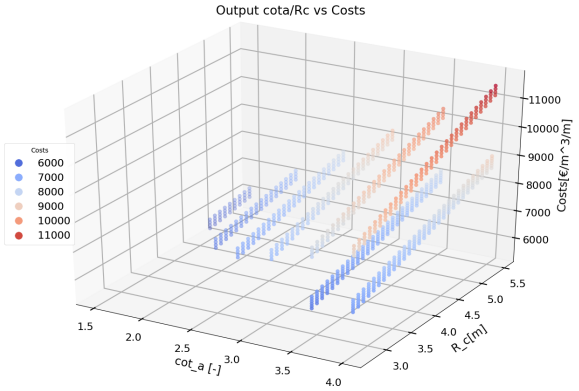

Figure E.21: Deterministic w/ uncertainty Rc / B / Costs

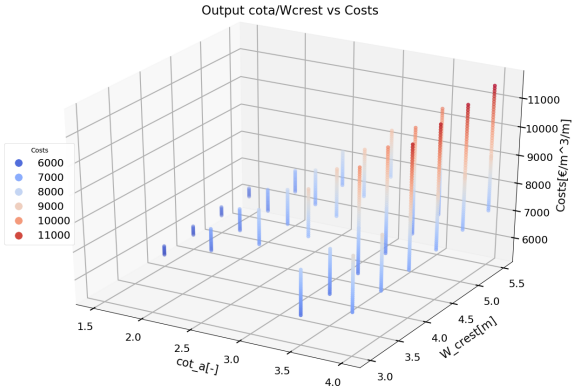

Figure E.22: Deterministic w/ uncertainty cota / Rc / Costs

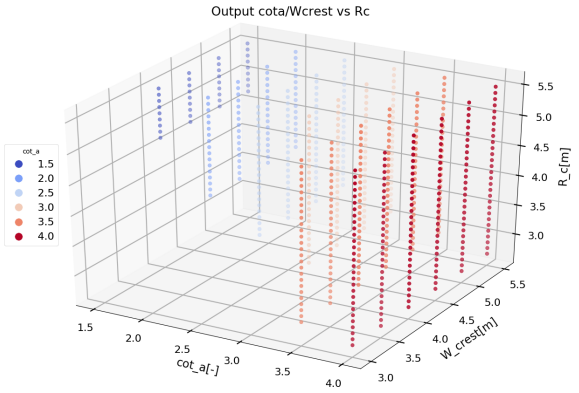

Figure E.23: Deterministic w/ uncertainty cota / B / Rc

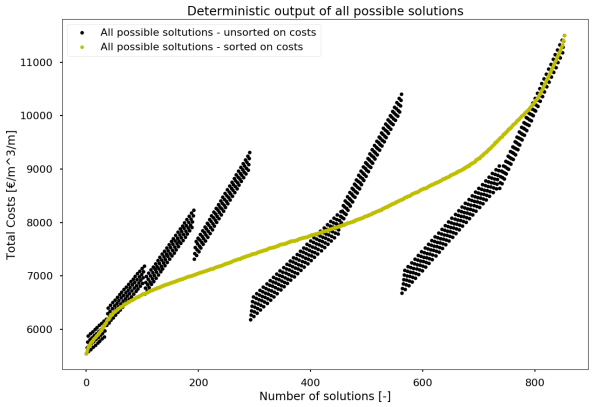

Figure E.24: Deterministic w/ uncertainty all option 2D